

**A ROLE FOR COLONY STIMULATING FACTOR 1 RECEPTOR
SIGNALING AND MICROGLIOSIS DURING EPILEPTOGENESIS**

by

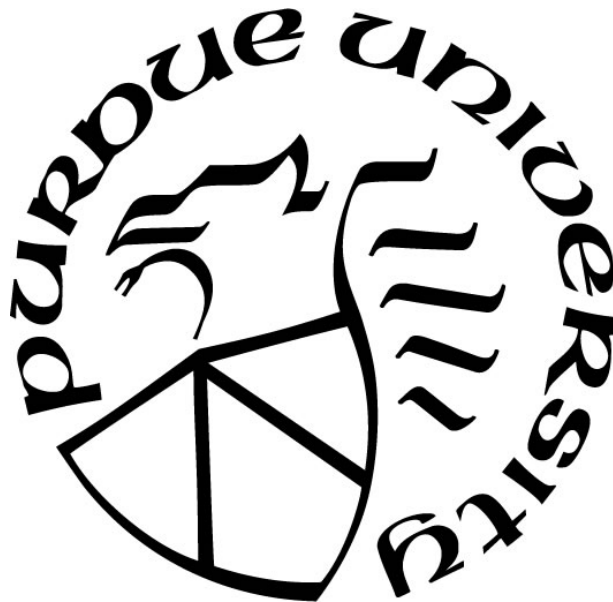
Season Kealyn Johnson

A Dissertation

Submitted to the Faculty of Purdue University

In Partial Fulfillment of the Requirements for the degree of

Doctor of Philosophy



Department of Psychological Sciences

West Lafayette, Indiana

May 2020

**THE PURDUE UNIVERSITY GRADUATE SCHOOL
STATEMENT OF COMMITTEE APPROVAL**

Dr. Amy L. Brewster, Chair

Department of Psychological Sciences

Dr. Julia A. Chester

Department of Psychological Sciences

Dr. Susan E. Swithers

Department of Psychological Sciences

Dr. Yang Yang

Department of Medicinal Chemistry and Molecular Pharmacology

Approved by:

Dr. David Rollock

ACKNOWLEDGMENTS

The author of this dissertation would like to express and recognize the individuals whose help and guidance contributed to its conclusion. To my advisor, Dr. Amy L. Brewster, thank you for the meaningful guidance throughout the completion of this dissertation. To Dr. Nicole Schartz, thank you for being my partner throughout graduate school and allowing me to learn from you throughout our time together. To Alex Sommer, M.S., thank you for your endless help with weekend behavior, copying all those heat maps into individual files, providing technical and emotional support, and for being another engineer in the laboratory. To Kevin Shim, thank you for your hours of watching behavior videos, your technical assistance, and for helping me become a better mentor throughout this experience. To Steph Lam, thank you for walking through the snow every weekend that you had to help me with behavior. To Catherine Nagy, thank you for your hours of watching videos and your positivity you bring every day to the laboratory. I would also like to acknowledge my financial support provided by Purdue University Research Foundation Grant.

Finally, I would like to recognize those who did not provide direct research support but who provided the emotional support needed to complete this dissertation. To my mom, Darlene Wyatt, thank you for always asking how my day was and always being interested as I explained my research to you. To my dad, Larry Wyatt, who is no longer with me but who helped inspire me throughout my graduate studies. To my brother, Dr. Noel Ratliff, thank you for your memes and words of encouragement and for inspiring me to want to get a higher degree when I watched you graduate when I was in third grade. To my sister-in-law, Catina Ratliff, M.S., thank you for always understanding and offering solutions to my problems, for being my role model, and for showing me that women can do anything. To my brother and sister-in-law, Nicholas and Megan Ratliff, thank you for always being interested in my work. To my Leo, thank you for your support when I was at a breaking point and for making me take breaks to play with you. Finally, to my husband, Jake Johnson, thank you for reading the endless drafts of my dissertation, for giving me your honest opinion, for supporting me through this endeavor every single day, and for making me realize happiness is the most important goal in my life. I could not have done this without you.

TABLE OF CONTENTS

LIST OF TABLES	6
LIST OF FIGURES	7
ABSTRACT	9
INTRODUCTION	11
Epilepsy Pathology	11
Temporal Lobe Epilepsy and Status Epilepticus Pathology	13
Animal Model of SE and TLE	14
Hippocampal Dendritic Alterations in SE	16
Gliosis and Inflammation Alterations Following SE	19
Neuro-Immune Interactions in SE	22
Phagocytic Microglia and Neuronal Crosstalk	22
Microglia Motility and Response to Neuronal Cues	27
Inhibition of Microgliosis in SE	28
Hypothesis	32
Specific Aims	33
METHODS	35
Animals	35
Pilocarpine Induced SE	35
Chow With PLX3397	36
Open Field (OF)	37
Novel Object Recognition (NOR)	37
Barnes Maze (BM)	38
Perfusion Through the Heart	40
Cryoprotection for Histology	40
Immunohistochemistry (IHC)	41
Microglia Counts	42
Semi-Quantitative IHC Densitometry Analysis	43
PLX3397 Non-Responder Cutoff	44
Western Blot (WB)	44

Densitometry Analysis for Western Blot.....	45
Statistical Analysis.....	45
RESULTS	48
Group Assignment was Randomly Distributed After SE Induction.....	48
Inhibition of CSF1R Signaling does not Attenuate SE-Induced Weight Loss	51
Treatment with PLX3397 and the Induction of SE does not Alter Locomotion	51
Inhibition of CSF1R Signaling does not Recover the SE-Induced Recognition Memory Deficits	56
Inhibition of CSF1R Signaling does not Recover the SE-Induced Spatial Memory Deficits ...	63
Inhibition of CSF1R Signaling Attenuated the SE-Induced Microgliosis.....	66
Inhibition of CSF1R Signaling Attenuated the SE-Induced Astrocytic Protein Levels	70
Inhibition of CSF1R Signaling Attenuated the SE-Induced Dendritic Microtubule Decrease .	74
Inhibition of CSF1R Produced a Group of Non-Responders that had no Variation in Weight Change	78
Inhibition of PLX3397 Produced a Group of Non-Responders that had Increased Microgliosis	83
Inhibition of PLX3397 Produced a Group of Non-Responders that had no Recovered GFAP or Map2 Levels.....	85
DISCUSSION.....	87
LIST OF REFERENCES	95

LIST OF TABLES

Table 1. Modified Racine Level Seizure Scale (Racine, 1972).....	36
Table 2. The Rat Specific Antibodies Used for IHC and WB Experiments.....	42
Table 3. The Guidelines for Morphological Classification of IBA1-Positive Cells.....	43
Table 4. Multiple Comparison Analysis of Weight Change Across Each Day	53
Table 5. Dunn’s Multiple Comparison Test for Microglial Morphology for Each Group	71
Table 6. Microglial Morphological Breakdown of Each Group.....	71
Table 7. Microglial Morphological Breakdown of the PLX3397 Non-Responders.....	85

LIST OF FIGURES

Figure 1. Experimental timeline of the induction of status epilepticus (SE) and treatment with PLX3397.	49
Figure 2. Rats were randomly distributed after the induction of status epilepticus (SE) into vehicle (Veh) or PLX3397 (PLX) treatment.	50
Figure 3. Status epilepticus (SE) triggers acute weight loss that is not attenuated with PLX3397 (PLX) treatment.	52
Figure 4. Status epilepticus (SE) or treatment with PLX3397 (PLX) does not alter locomotion during open field (OF) test.	54
Figure 5. Status epilepticus (SE) results in a deficit in recognition memory which is not recovered by PLX3397 (PLX) treatment.	57
Figure 6. Status epilepticus (SE) triggers a decline in hippocampal-dependent spatial learning in Barnes maze (BM) that is not recovered by PLX3397 (PLX).	58
Figure 7. Status epilepticus (SE) triggers a decline in time spent in target quadrant in Barnes maze (BM) that is not recovered by PLX3397 (PLX).	59
Figure 8. Status epilepticus (SE) does not alter locomotion during Barnes maze (BM) and this is not affected by PLX3397 (PLX) treatment.	60
Figure 9. Status epilepticus (SE) triggers a decline in hippocampal-dependent spatial memory in Barnes maze (BM) that is not recovered by PLX3397 (PLX) treatment.	61
Figure 10. Status epilepticus (SE) induced hippocampal microgliosis is attenuated by PLX3397 (PLX) treatment.	67
Figure 11. Status epilepticus (SE) induced hippocampal microglial morphology is altered by PLX3397 (PLX) treatment.	69
Figure 12. Status epilepticus (SE) induced astrogliosis is attenuated with PLX3397 (PLX) treatment.	72
Figure 13. Status epilepticus (SE) triggers decline in hippocampal Map2 signal that is recovered by PLX3397 (PLX) treatment.	75
Figure 14. Status epilepticus (SE) triggers decline in dendritic markers in the CA1 region of the hippocampus that is not altered by PLX3397 (PLX) treatment.	76
Figure 15. Status epilepticus (SE) induced rats treated with PLX3397 (PLX) that did not have a 60% reduction microgliosis displayed no changes in Racine scale level.	79
Figure 16. Status epilepticus (SE) induced rats treated with PLX3397 (PLX) that did not have a 60% reduction microgliosis displayed no changes in weight.	80

Figure 17. Status epilepticus (SE) induced rats treated with PLX3397 (PLX) that did not have a 60% reduction in the hippocampal microgliosis displayed increased IBA1 levels and altered morphology..... 81

Figure 18. Status epilepticus (SE) induced rats treated with PLX3397 (PLX) that did not have a 60% reduction microgliosis still had a reduction in astrocytic protein level GFAP in the CA1 region of the hippocampus..... 82

ABSTRACT

Evidence from experimental models of epilepsy support that prolonged seizures (status epilepticus, SE) promote pathological hippocampal synaptodendritic remodeling which contributes to the development of seizures and cognitive decline. One potential mechanism underlying the SE-induced sequelae is microgliosis.

Evidence from models of experimental epilepsy supports a significant spatiotemporal correlation between SE-induced decreases in the microtubule associated protein 2 (Map2) loss and microgliosis in the hippocampus. In addition, pharmacological suppression of microgliosis after SE with the drug rapamycin attenuated the losses of Map2 and the dendritic ion channels Kv.4.2 and HCN1 in the hippocampus. This microglia suppression paralleled a recovery of the SE-induced recognition and spatial memory deficits. Based on these studies, we hypothesized that the inhibition of microgliosis during epileptogenesis will attenuate the SE-induced hippocampal dendritic and cognitive pathology. To further investigate the role of microgliosis in the SE-induced dendritic pathology, we tested the efficacy of a more selective inhibitor of the survival and proliferation of microglia, PLX3397, using the pilocarpine model of SE and acquired epilepsy. PLX3397 binds to colony stimulating factor 1 receptor (CSF1R) on microglia and inhibits the downstream signaling responsible for survival and proliferation of these cells.

To test this hypothesis, we induced SE in male rats with pilocarpine (280-300mg/kg) while and controls (Ctrl) received saline. Rats were randomly assigned to a diet of either chow alone (vehicle; Veh) or chow with PLX3397 (50mg/kg) for 20 days post-SE. At two weeks post-SE, rats were subjected to novel object recognition (NOR) and Barnes maze (BM) to evaluate hippocampal-dependent recognition memory, and spatial learning and memory, respectively. Following the behavioral assessments, rats were sacrificed for brain analysis at 20 days post-SE. We used histological analysis to determine the amount of microgliosis with IBA1 and dendritic stability with Map2. We used western blotting to measure the protein levels of molecules involved in the crosstalk between microglia and astrocytes: GFAP, IL-6, C3, and iC3b. We also measured the protein levels of the dendritic ion channels Kv4.2 and HCN1, and the synaptic marker PSD95.

NOR showed that the Ctrl+Veh and Ctrl+PLX3397 groups spent significantly more time exploring the novel object ($p < .05$), while the SE+Veh and SE+PLX3397 did not. Similar results were observed in the BM test, Ctrl+Veh and Ctrl+PLX3397 groups had a faster latency to find the

target compared to the SE+Veh and SE+PLX3397 groups ($p < .05$). These data suggest that recognition and spatial memory deficits induced by SE were not attenuated by treatment with PLX3397. We found that the PLX3397 treatment significantly decreased microgliosis in Ctrl+PLX3397 rats compared to Ctrl+Veh rats ($p < .05$). As expected, we found a significant increase in the number of microglial cells in hippocampi of SE+Veh rats compared to Ctrl+Veh rats ($p < .05$). Interestingly, in the PLX3397-treated SE group, we observed two distinctive groups which we categorized as responders and non-responders when compared to the SE+Veh group. The SE+PLX responders had significantly decreased microgliosis compared to the SE+Veh group ($p < .05$). The SE+PLX non-responders had higher levels of microgliosis compared to the SE+Veh group ($p < .05$). We found levels of GFAP were increased in the SE+Veh group compared to the Ctrl+Veh group ($p < .05$). Treatment with PLX3397 in the SE group reduced these levels compared to the vehicle treated SE group ($p < .05$). We also found increases in C3 and iC3b following the induction of SE compared to Ctrl+Veh group ($p < .05$), and these levels remained similar in the SE+PLX3397 group compared to the SE+Veh group ($p > .05$). There was a reduction in Map2 immunoreactivity as well as the protein levels of Kv4.2 and PSD95 in the SE+Veh group compared to the Ctrl+Veh group ($p < .05$). We found that treatment with PLX3397 recovered the SE-induced loss of Map2 labeled dendrites compared to SE+Veh group ($p < .05$). However, treatment with PLX3397 did not recover the SE-induced reduction Kv4.2 and PSD95 ($p > .05$). In parallel, we found that a group of SE+PLX3397 animals did not have reduced microgliosis compared to the SE+Veh group ($p < .05$), and therefore was categorized as a non-responder group.

Our findings are the first to show that blocking CSF1R signaling with PLX3397 suppressed microgliosis in the hippocampus, partially recovered the SE-induced decline of Map2 immunoreactivity in the hippocampal CA1 region but had no effect in the recognition or spatial memory deficits. These data suggest that while hippocampal microgliosis may play a role in the disruption of dendritic structural stability in the hippocampus it does not seem to critically contribute to the memory decline that occurs during epileptogenesis.

INTRODUCTION

Epilepsy Pathology

Approximately 50-70 million people worldwide currently have epilepsy (Saxena & Li, 2017; Thijs et al., 2019). In a global comparison analyzing disease and injury in terms of overall disability referring to years of life lost and time spent in reduced health, severe epilepsy ranked fourth out of 220 diseases and injuries after schizophrenia, severe multiple sclerosis, and spinal cord lesion (Salomon et al., 2012; Saxena & Li, 2017). In the United States, approximately 3 million people have active epilepsy, meaning they have experienced at least 1 spontaneous seizure in the past year (Greenlund et al., 2017; Tian et al., 2018). The diagnosis of epilepsy is received after having at least two spontaneous seizures. Seizures are abnormal bursts of electrical activity in the brain that occur abruptly and unprovoked. Typically during a seizure, disruptions in behavior, movements, and level of consciousness occur (Cole et al., 2002). Epilepsy itself is not one disease, but it is the encompassing word for a spectrum of different types of epilepsies. The type of epilepsy is determined by seizure origination/propagation and, if possible, the underlying cause (Panayiotopoulos, 2005). The origination and propagation of seizures is broken down by either the seizure starting at a focal point and propagating throughout the brain or the seizure generalizing to one or both hemispheres with no focal point. Generally, epilepsy is divided into three basic categories: focal epilepsy, generalized epilepsy, and unknown if generalized or focal epilepsy (Pack, 2019). Focal epilepsy is one of the more common types of epilepsy, roughly 50% of patients are diagnosed in this category, while 30% of patients have generalized epilepsy, and the rest are unknown (Blume, 2010; Pack, 2019). Furthermore, epilepsy can be divided into more categories based on the location of the seizures and how the development of epilepsy occurred, genetic or acquired (Cole et al., 2002; Greenlund et al., 2017; Thijs et al., 2019). Each category is subdivided into either the production of motor or non-motor seizures. During motor seizures, altered levels of consciousness occur along with physical movements including atonic (loss of muscle strength), tonic (stiff and tensing of muscles), clonic (jerking movements), tonic-clonic (combination of stiff and tensing with jerks), and myoclonic (shock-like jerks). Non-motor seizures, also referred to as absence seizures, lack the physical characteristics and only alter the level of consciousness. Based on the different categories and subcategories, there are a plethora of different types of seizure

disorders, but treatment options tend to over generalize to all the types of epilepsy. This is why we are focusing on the most common type of epilepsy focal epilepsy most commonly associated with mesial temporal lobe epilepsy. A majority of the currently available anti-seizure medications (ASMs) only inhibit seizures and their propagation, and do not alter the pathology of the disease (Panayiotopoulos, 2005; Talati et al., 2011). Importantly, only 43-50% of patients on ASMs are determined to be seizure free (Xia et al., 2017). Of the patients who respond to ASMs, about 34-40% will have seizures again within five years, 20-26% will have seizures after five years, and only 40% will remain seizure-free (Schiller, 2009; Schmidt, 2011). Even after the successful suppression of seizures with ASMs, many patients must remain on the drugs for their lifetime, as withdrawal from ASMs results in the relapse of seizures in 27% of people with epilepsy (Lossius et al., 2008; Schmidt, 2011). In addition, ASMs have been shown to have unintended side effects due to the non-specificity of the treatment, meaning that the ASMs are not just altering the location of the seizures, but the entire brain is affected by the treatment (Du et al., 2019; Park & Kwon, 2008; Wang et al., 2012). The side effects include impairments with learning and memory possibly caused by over suppressing neuronal excitability (Brodie et al., 2016; Du et al., 2019; Meador et al., 2007; Park & Kwon, 2008). This means that people with epilepsy that are seizure-free with ASMs can still be plagued by the side effects resulting from the ASMs (Schmidt, 2011). The 30-40% of people with epilepsy who do not have suppressed seizure activity with ASMs are considered to be drug-resistant (refractory) (Schiller, 2009). A treatment option for people with refractory epilepsy after they have failed to respond to at least two ASMs is surgical resection of the seizure focal point. Surgery can only be an option if the focal point can be determined and the location of the focal point does not interfere with the ability of the person to communicate (Bianchin et al., 2013; Memarian et al., 2013; Wiebe, Blume, et al., 2001). Of those who are candidates for surgical resection, only 50% will be seizure free for their lifetime (Langfitt & Wiebe, 2002; Ozanne et al., 2016; Wiebe, Blume, et al., 2001). This indicates a great need for new treatment options for individuals with epilepsy.

Epilepsy is not solely a disorder of seizures; it persists on a spectrum, with the focus on seizures. Epilepsy has other harmful effects that most people do not focus on, and these include the numerous co-morbid conditions. Roughly 26-84% of people with epilepsy have at least one co-morbid condition including depression and Alzheimer's disease (AD) (Naydenov et al., 2019; Seidenberg et al., 2009). People with epilepsy have a higher likelihood, about 25%, of suicidal

ideation and they are also at a 21% increased likelihood of mortality from falling, drowning, car accidents, and sudden unexplained deaths (Alonso-Vanegas et al., 2013; Beghi, 2019; Shackleton et al., 1999; Vergeer et al., 2019; Wiebe, Eliasziw, et al., 2001). Increased cognitive deficits have been observed in people who have epilepsy with 6-64% having deficits in processing information, attention, and learning and memory (Seidenberg et al., 2009). These comorbidities, particularly deficits in learning and memory, remain untreated with current ASMs. Roughly 75% of people who develop epilepsy start having seizures during their childhood (Beghi, 2019; Lopes et al., 2014). In children with epilepsy, depending on their age, the seizures can have significant impacts on their cognitive development (Alonso-Vanegas et al., 2013; Giovagnoli & Avanzini, 1999; Lopes et al., 2014; Vergeer et al., 2019), making treatment that also attenuates the cognitive deficits critical. Individuals who have refractory epilepsy or who are not seizure free after ASMs or surgical resection are the reason new treatment options that alter the underlying pathology of epilepsy are necessary.

Temporal Lobe Epilepsy and Status Epilepticus Pathology

The most common type of focal epilepsy is temporal lobe epilepsy (TLE), which has the highest percentage of epileptic individuals with drug resistant (refractory) seizures, about 40-89% (Asadi-Pooya et al., 2017; Pack, 2019; Semah et al., 1998). There are two main reasons for this large variation in the statistics associated with TLE (Bell et al., 2014; Kwan et al., 2010; Saxena & Li, 2017; Thijs et al., 2019). First is the inconsistent definition of refractory, which varies by physician and region. In some cases, the diagnosis of refractory is received only if the seizures are fully uncontrolled, and in other cases, the diagnosis is received if the seizures are partially uncontrolled. Secondly, the rates of reporting in developing countries are low, as individuals with epilepsy typically do not have the same access to physicians as those in developed countries (Bell et al., 2014). This makes it difficult to determine the exact prevalence of refractory epilepsy, although it has been estimated to be up to 80% (Bell et al., 2014; Kwan et al., 2010; Saxena & Li, 2017; Thijs et al., 2019). TLE is the most common type of focal epilepsy, with about 6 in every 10 people with a focal form of epilepsy having TLE (Kwan et al., 2010; Wiebe, 2000). TLE is characterized by injury to the temporal lobe. Approximately 80% of TLE cases have injuries to the internal structures of the temporal lobe, including the hippocampal region, compared to the neocortical or lateral temporal lobe regions (Tatum, 2012). The initial injury of TLE can be

acquired by severe head trauma, stroke, infections, or can be from the result of status epilepticus (SE), a sustained seizure that lasts at least 5 minutes and is classified as a medical emergency (England et al., 2012; Manno et al., 2011; Wylie et al., 2020). SE can occur in people with epilepsy, but it occurs 50% more often in individuals who do not have epilepsy. The causes of an episode of SE have been determined to be from infection at rates of 12-40%, change in medication at rates of 18%, stroke at rates of 25%, trauma at rates of 5%, drugs/alcohol at rates of 13%, and unknown at rates of 9% (Cherian & Thomas, 2009). There are roughly 150,000 new cases of SE in the United States every year and in those cases, 40% of people with epilepsy will go on to develop TLE (Pichler & Hocker, 2017; Santamarina et al., 2015). These data make it important to focus on people who have TLE and those who develop TLE from an episode of SE.

TLE and SE are often most detrimental to the hippocampus, as it often sustains seizure-induced damage. The hippocampus is highly susceptible to seizures and is linked to drug resistant seizures (Chatzikonstantinou, 2014; Dupont & Vercueil, 2015). This could be due to the high density of excitatory ion channels and receptors (Wolfart & Laker, 2015) and the numerous connections the hippocampus has to other brain regions, allowing for propagation of seizure pathology (Chatzikonstantinou, 2014). Due to the involvement of the hippocampus in memory, the cognitive deficits—particularly the deficits in learning and memory—are severely affected after SE and in epilepsy (Dupont & Vercueil, 2015). Individuals with TLE are at an increased risk for cognitive deficits with 50% having memory impairments (Hocker, 2015; Nouha et al., 2018; Pichler & Hocker, 2017; Silva-Alves et al., 2017; Steiger & Jokeit, 2017). Individuals that have TLE with co-morbid learning and memory deficits self-report decreases in quality of life due to the stigmas associated with epilepsy and impairments in their ability to learn and remember (Alonso-Vanegas et al., 2013). There is a critical need for treatments that aim to alter the seizure pathology and alleviate comorbidities, specifically those in learning and memory. A potential candidate mechanism for these cognitive deficits and epileptic pathology may be from the interaction between neuronal and immune signaling in the brain.

Animal Model of SE and TLE

The animal models of epilepsy can be broken down into two major categories: genetic and injury acquired through either physical, chemical, or electrical methods (Kandratavicius et al., 2014; Löscher, 2011). Genetic models work to mimic the genetic mutations that have been

observed in human epilepsy, but typically, both humans and animals are born with these mutations. Modeling these types of epilepsy can be challenging due to the genetic differences between humans and animals and the interference of other variants and environmental factors (Becker, 2018; Frankel, 2009). The injury models of acquired epilepsy focus on mimicking the neuropathology of epilepsy (Löscher, 2011). Most frequently, these animal models focus on replicating TLE because it is the most common type of epilepsy in humans (36% of the epileptic population) (Lévesque et al., 2016). TLE has four main features that are used to appraise the validity of animal models that replicate TLE. These include (1) seizure focal point localized in the limbic structures including the hippocampus; (2) the initial injury that is typically observed; (3) a period of time following the injury in which no seizures occur called the latent period; (4) neuropathology of sclerosis or lesion caused by neuronal loss and gliosis predominately observed in the Cornu Ammonis 1 region (CA1) in the hippocampus (Curia et al., 2008). The validity of TLE animal models is determined based on how well they replicate all four aspects of TLE. The animal model that has been extensively validated and fits all of these requirements is the rat model of pilocarpine induced SE (Morimoto et al., 2004).

Rat studies support that a single episode of SE, lasting at least 45 minutes, is sufficient to cause an initial injury to the hippocampus and that leads to the development of TLE and the associated cognitive comorbidities in more than 90% of male juvenile rats (Lévesque et al., 2016; Löscher, 2011; Nirwan et al., 2018; Serrano-Castro et al., 2012). The use of the chemoconvulsant pilocarpine to induce SE has shown to be more advantageous over other methods. Pilocarpine leads to a more rapid induction of SE with an intraperitoneal (i.p.) injection compared to that of another chemoconvulsant, kainic acid (Covolan & Mello, 2000; Curia et al., 2008). The average latent period for the development of unprovoked seizures is 14 days for pilocarpine and 3-30 days for kainic acid, though both models can result in 100% spontaneous seizures in animals that reached SE. This is compared to the traumatic brain injury model, where only 11% go on to develop spontaneous seizures (Curia et al., 2008; Glushakov et al., 2016). The presence of lesions in the hippocampus are apparent following pilocarpine induced SE (Curia et al., 2008; Lévesque et al., 2016; Nirwan et al., 2018). Finally, the pilocarpine model also shows a similar ASMs response when compared to humans with TLE (Chakir et al., 2006; Glien et al., 2002). In cultured neurons, pilocarpine has been shown to produce an imbalance between the transmission of excitatory and inhibitory neurons which results in seizure activity (Priel & Albuquerque, 2002).

The pilocarpine model of SE and TLE has consistent pathological and behavioral data with human TLE (Becker, 2018; Nirwan et al., 2018; Seinfeld et al., 2016). During the latent, seizure-free period also described as the epileptogenic period, animals display neuronal loss and spine density reductions, and this is linked to network reorganization similar to what is observed in human TLE (Dachet et al., 2015; Lehmann et al., 2001; Pearson et al., 2014; Ravizza & Vezzani, 2006; Schartz et al., 2016; Wong et al., 2009). Epileptogenesis is also hallmarked by gliosis. There is an increase in astrocytic levels and number of microglia following the induction of SE and this mimics what is observed in human TLE brain samples (Dachet et al., 2015; Ravizza & Vezzani, 2006; Schartz et al., 2016; Shapiro et al., 2008; Vargas-Sánchez et al., 2018). Animals treated with ASMs following pilocarpine induced SE respond at reduced levels similar to humans. Treatment with the ASM, diazepam, is able to reduce seizure severity but can take up to three hours to stop electrographic seizures (Curia et al., 2008; Goffin et al., 2007). The cognitive deficits that are commonly associated with individuals who have TLE are also observed in the pilocarpine model of SE and acquired TLE (Jessberger & Parent, 2015; Lévesque et al., 2016; A. K. Sharma et al., 2007). We and others have found memory deficits starting 2-3 weeks post-SE in tests that include novel object recognition (NOR), Barnes maze (BM), and Morris water maze (MWM) which measure hippocampal-dependent recognition and spatial learning and memory (Brewster et al., 2013; Grayson et al., 2015; Rojas et al., 2016; Schartz et al., 2018). These behavioral deficits in learning and memory are long-lasting similar to humans with TLE (Cilio et al., 2003; Wu et al., 2001; Zhang et al., 2010). Taken together, this evidence supports the use of the pilocarpine model of SE and TLE as the most appropriate model to study the underlying mechanisms of TLE.

Hippocampal Dendritic Alterations in SE

Epilepsy is a disorder of seizures characterized by neuronal and dendritic alterations in both human and animal models of SE and epilepsy (Scharfman, 2007). SE and TLE are characterized by network remodeling, decreased spine density, neuronal loss, and dendritic instability (Casanova et al., 2012; Dachet et al., 2015; Wong & Guo, 2013). In human and animal models, these alterations parallel neuroinflammation, microgliosis, and astrogliosis (Brewster et al., 2013; Dachet et al., 2015; Ravizza & Vezzani, 2006; Wyatt et al., 2017). It is likely that the correlation between dendritic changes and glial alterations may play a role in epileptogenesis and the development of spontaneous seizures (Dachet et al., 2015; Eyo et al., 2017; Schartz et al., 2016).

The hippocampus is particularly susceptible to neuronal injury induced by SE due to the high density of excitatory ion channels and receptors, as well as the numerous connections to other brain regions (Abdelmalik et al., 2005; Golarai et al., 2001; Hasegawa et al., 2007; Morimoto et al., 2004). These factors may contribute to the intensity and propagation of seizure activity. This may occur by aiding in the activity of excitable neurons and inactivity of inhibitory neurons, which could promote the seizure activity to propagate through the brain (Faria et al., 2017; McEwen, 1994; Shen et al., 2016). Decreased levels of the microtubule associated proteins 2 (Map2) and spine density have been observed in human epilepsy (Dachet et al., 2015; M. Wong & Guo, 2013; Ying et al., 2004). Evidence from animal models support that SE provokes dendritic structural instability through transient loss of Map2 and reduced spine density (Ballough et al., 1995; Brewster et al., 2013; Schartz et al., 2016; Swann et al., 2000; Wong, 2008). These changes occur most drastically within the CA1 area of the hippocampus (Medvedeva et al., 2017) and are associated with synaptic circuitry remodeling and neuronal hyperexcitability (Feng et al., 2017; Hong et al., 2018; Hwang et al., 2013). Together, the evidence from these studies support that SE alters dendritic elements in experimental models of epilepsy similar to that in human epilepsy.

In TLE and SE, numerous dendritic ion channel alterations occur throughout the brain. The two major ion channels specifically localized to the CA1 pyramidal dendrites are the voltage-gated potassium channel, Kv4.2, and hyperpolarization-activated cyclic nucleotide-gated channel subunit 1 (HCN1). Both Kv4.2 and HCN1 have been found to be decreased in human epilepsy and animal models of SE (Bernard et al., 2004; Brewster et al., 2013; D'Adamo et al., 2013; Greene et al., 2018; Gross et al., 2016; Jung et al., 2007; Lerche et al., 2013; Poolos & Johnston, 2012; Tang & Thompson, 2012; Wolfart & Laker, 2015). Decreases in Kv4.2 protein levels and mRNA levels have been observed following SE (Birnbaum et al., 2004; Gross et al., 2016). In Kv4.2 knockout mice, it has been shown that the mice have deficits in spatial learning with the MWM and Lashley maze (Lugo et al., 2012; Smith et al., 2017). These mice also develop SE and spontaneous seizures at an increased rate compared to wild type mice (Smith et al., 2017). These data indicate the involvement of Kv4.2 in memory and seizure threshold (Barnwell et al., 2009). HCN1 channel is also mainly localized to the hippocampal CA1 distal dendrites where it works to dampen neuronal excitability under physiological conditions (Frigerio et al., 2018; Marcelin et al., 2012). Loss of function of the HCN1 gene is highly correlated with epilepsy development and increased seizure susceptibility (Marini et al., 2018). Thus, the SE-induced downregulation of

Kv4.2 and HCN1 during epileptogenesis is thought to increase the excitability of neurons and may be associated with the later development and reoccurrence of seizures (Bernard et al., 2004; Brewster et al., 2002, 2005; Brewster et al., 2013; Jung et al., 2007).

In addition to loss of dendritic ion channels, seizures can provoke a reduction in the levels of synaptic proteins such as the postsynaptic density protein 95 (PSD95), a major scaffolding protein on excitatory synapses that is highly concentrated in CA1 dendrites (Chen et al., 2006; Vincent & Mulle, 2009; Ying et al., 2004). PSD95 has been found to have major roles in the modulation of ion channels and signaling molecules at postsynaptic sites (Keith & El-Husseini, 2008). Reductions in PSD95 can decrease the retention of receptors at the synapse producing either decreased excitation or increased inhibition (Chen et al., 2011; Keith & El-Husseini, 2008). These reductions can also indicate loss of synapses, as correlational studies support stronger synapses have higher levels of PSD95 (Chen et al., 2011; Sheng & Kim, 2011). In contrast, overexpression of PSD95 increases excitation and decreases inhibition. Following recognition memory tasks including NOR and spatial memory tasks including MWM, high levels of PSD95 were found (Soulé et al., 2008). PSD95 knockout mice showed impaired spatial memory in the MWM (Delint-Ramírez et al., 2008). In human epilepsy, both increases and decreases have been found in PSD95, but these observations have been from different brain regions (Wyneken et al., 2003; Ying et al., 2004). In the hippocampus, PSD95 was found to be reduced (Wyneken et al., 2003) while in the occipital and frontal cortex, PSD95 was found to be increased (Keith & El-Husseini, 2008; Ying et al., 2004). In animal models of SE, decreased levels of PSD95 have been observed at one day post-SE and continued to decrease for up to six weeks post-SE (Sun et al., 2009; Wyneken et al., 2003). These decreases were correlated to decreased behavioral performance in MWM (Sun et al., 2009). This body of evidence supports the idea that a reduction in the levels of PSD95 may be an adaptive mechanism to decrease the hyperexcitability, but this decrease may contribute to the memory deficits following SE. Although dendritic instability and its potential role in cognitive deficits is a considerable issue in SE and epilepsy, the current ASMs do not help with this pathology or the comorbidities. We sought to investigate the role of gliosis as a potential underlying cause in the synaptodendritic pathology of SE and TLE.

Gliosis and Inflammation Alterations Following SE

In human TLE, another pathological hallmark is the activation and accumulation of glial cells, also noted as gliotic scarring. Glial cells are the most abundant type of cells in the brain and provide support to neurons (Jäkel & Dimou, 2017; Purves et al., 2001). The two key glial cells most widely reported as altered in epilepsy are astrocytes and microglia (Patel et al., 2019). Microglia have been simply known as the immune cells of the brain, thought of as the “macrophages of the brain”, but their job includes much more i.e. surveilling, responding, maintaining, and phagocytosing (Eyo & Wu, 2019; Gomes-Leal, 2019; Kettenmann et al., 2011; Low & Ginhoux, 2018). The origination of microglia has been extensively studied (Eyo & Wu, 2019). It is known that they originate outside of the central nervous system (CNS) and migrate into the brain during the embryonic period. In the brain, microglia can proliferate from previous microglia or can be derived from precursor c-kit cells (Kierdorf et al., 2013). Microglia constantly survey their microenvironments for disturbances. Upon receiving signals from pathological events, microglia respond and release anti-/pro- inflammatory cytokines and chemokines aiding in the attraction of other immune cells (Feng et al., 2019; Ménard et al., 2017). The pro-inflammatory cytokines produced by microglia lead to similar results as their release by astrocytes (Fernández-Arjona et al., 2017; Xie et al., 2014). It has been observed that the release of cytokines including, interleukin (IL)-1 β , IL-6, tumor necrosis factor alpha (TNF- α), along with complement C3 aid in the interaction between astrocytes and microglia, also known as crosstalk (Sheridan & Murphy, 2013). In vitro, the production of IL-6 was shown to induce the proliferation and accumulation of microglia (Batlle et al., 2015; Streit et al., 2000). This crosstalk can induce neuroprotective roles in astrocytes and regulate microglial motility and aid in microglial accumulation and phagocytosis (Batlle et al., 2015; Jha et al., 2019; Lian et al., 2016).

Proliferation and accumulation of microglia, microgliosis, in the hippocampus is found in both human and experimental models of epilepsy (Abiega et al., 2016; Dachet et al., 2015; Loewen et al., 2016; Shapiro et al., 2008; Sierra et al., 2010, 2013; Torres-Platas et al., 2014; Zhao et al., 2018). In the pilocarpine model of SE, densitometry analysis of microgliosis following SE showed alterations in microglia starting at four hours post-SE and the highest peak of accumulation at two to three weeks post-SE (Schartz et al., 2016; Wyatt-Johnson et al., 2017). In the kainic acid model of SE, similar patterns are observed with the peak accumulation occurring at three days post-SE (Feng et al., 2019). Using genetic labeling to selectively tag microglia and macrophages, Feng et

al., (2019) showed that the SE-induced accumulation of microglia paralleled an increase in macrophage infiltration (Feng et al., 2019). Labeling microglia with Brdu and Ki-67, both known proliferation markers, showed a significant increase in the proliferation of microglia cells (>70%) compared to the migration of other microglia and macrophages (Feng et al., 2019) This indicates that proliferating microglia are a major contributor to microgliosis and the epileptic pathology. Together, this supports that microglia are highly involved in epilepsy.

Along with microglia, astrocytes have been found to play a role in brain function. Astrocytes are involved in the homeostasis and survival of neurons by performing a multitude of tasks including controlling the blood brain barrier and regulating synapses (Blackburn et al., 2009). Astrocytes have been implicated in memory function, as they can regulate synaptic transmission and plasticity which are both important in memory formation. They also have been shown to be important in the buildup of neuroinflammation and recruitment of microglia and macrophages (Aronica et al., 2012). In both human epilepsy and animal models, astrocytic expression of glial fibrillary acidic protein (GFAP) is upregulated and astrocytes undergo significant physiological changes, including production and release of proinflammatory molecules (Aronica et al., 2012; Vasile et al., 2017). Astrocytes are observed as swollen and increased in cell volume. The swollen phenotype of astrocytes has been shown to indirectly enhance network excitability through increased release of neurotransmitters (Aronica et al., 2012; Losi et al., 2012; Shapiro et al., 2008). In vitro work has also shown that astrocytes contribute to the production of IL-1 β , IL-6, TNF- α , and complement C3 (Aronica et al., 2012; Blackburn et al., 2009; Codeluppi et al., 2014; Leal et al., 2013; Lian et al., 2016).

The production of IL-1 β and TNF- α can increase blood brain barrier permeability by recruiting peripheral macrophages into the brain as well as having indirect toxic effects on neurons (Neniskyte et al., 2014). These inflammatory cytokines can be beneficial by attracting microglia and allowing for aid in dealing with pathological events, but high amounts of inflammation can produce detrimental effects (Wilcox & Vezzani, 2014). In high quantities, it has been observed that both IL-1 β and TNF- α can induce neuronal death (Kaur et al., 2014). In human and experimental epilepsy, increases in IL-1 β , TNF- α , and IL-6 are increased following seizure activity (Paudel et al., 2018; Rana & Musto, 2018; Scharz et al., 2016; Wilcox & Vezzani, 2014; Xie et al., 2014). IL-6 has more recently been shown to be a key contributor in disease. The combination of IL-6 and astrocytes has been shown to have diminishing effects on the survival of hippocampal

neurons (Vallières et al., 2002). IL-6 also has emerged as having a potential role in epilepsy (Battle et al., 2015; Baune et al., 2012; Codeluppi et al., 2014; Erta et al., 2012). People with epilepsy have increased IL-6 levels in their cerebral spinal fluid following a seizure, indicating a neuroprotective factor (De Luca et al., 2004; De Sarro et al., 2004; Erta et al., 2012; Minami et al., 1991). While IL-6 knockout mice are more susceptible to chemoconvulsants and increased damage to the hippocampus (De Luca et al., 2004; De Sarro et al., 2004; Erta et al., 2012; Minami et al., 1991), suggesting that IL-6 release may be a neuroprotective response to seizures. We and others have shown transient increases in inflammation occurring immediately following SE and remaining elevated for up to three days (Schartz et al., 2016; Shapiro et al., 2008; Wilcox & Vezzani, 2014). Although inflammation and astrocytes do have a part in epilepsy as stated, the release of complement 3 (C3) and the accumulation of microgliosis may play a larger role.

The production of C3 by astrocytes has been shown to be important for the microglial response to changes in neural homeostasis (Aronica et al., 2007; Lévi-Strauss & Mallat, 1987; Lian et al., 2016). During the development of synapses, C3 has been found to play an important role in the ability of microglial elimination of weak synapses (Paolicelli et al., 2011; Schafer et al., 2012; Stevens et al., 2007; Tremblay et al., 2010). While C3 knockout mice display defects in synapse elimination in the developing retinal system (Stevens et al., 2007), these knockouts also displayed increased spatial memory in the water T-maze (WTM) compared to wild type controls (Shi et al., 2015). Elevated levels of C3 occur in human refractory epilepsies, and in animal models. High levels of C3 correlate with seizure severity (Aronica et al., 2007; Chu et al., 2010; S. D. Reddy et al., 2019; Schartz et al., 2018; Wyatt et al., 2017). In human focal cortical dysplasia (FCD), a genetic epilepsy where the cerebral cortex has malformations, we found increases in the protein levels of both C3 and iC3b, the cleavage product of C3 that acts as an opsonin for microglia engulfment (Wyatt et al., 2017). We have shown similar increases in C3 and iC3b following pilocarpine induced SE at 2-3 weeks that correlate with behavioral deficits in recognition and spatial memory (Schartz et al., 2018). Taken together, this evidence supports the idea that the role of C3 in microglial function may play an important part in the pathology of epilepsy. Altogether, this evidence supports the importance of the maintenance of neuronal communication with glial cells, particularly microglia.

Neuro-Immune Interactions in SE

Physical neuro-immune interactions involve the microglial processes in close proximity to dendritic elements and have been reported under physiological conditions (Eyo & Wu, 2013; Hong et al., 2016). Live imaging studies support that microglia-dendritic contacts are increased during the addition of glutamate to brain slices, which mimics the increased neuronal excitation that is observed during seizures (Eyo et al., 2016). In human and experimental models of epilepsy, we and others have found interactions between microglia and dendrites (Brewster et al., 2013; Chugh & Ekdahl, 2016; Eyo et al., 2016; Hasegawa et al., 2007; Wyatt et al., 2017). In human refractory epilepsy, the accumulation of CD68-positive microglia co-occurs in consecutive sections with dendritic Map2 loss (Dachet et al., 2015). Interestingly, the spatial and temporal profile of SE-induced microgliosis significantly correlates with the peak in decline of both the immunoreactivity of Map2 and density of spines (Brewster et al., 2013; Scharz et al., 2016, 2018). Importantly, we previously reported that acute treatment with rapamycin attenuated SE-induced hippocampal microgliosis and loss of Map2, Kv4.2 and HCN1. Treatment with rapamycin also recovered recognition and spatial memory deficits following SE-induction (Brewster et al., 2013). In other models of acquired and genetic epilepsy, a similar recovery of the neuropathology and cognitive deficits has been described (Crino, 2019). Because rapamycin treatment works on multiple subsets of brain cells including both neurons and microglia (Crino, 2011; Siman et al., 2015; Zeng et al., 2009), this study suggested the possibility that one or both cell types may contribute to the SE-induced dendritic changes. We seek to investigate if microgliosis is a contributing factor to the loss of dendritic Map2, Kv4.2, and HCN1, as well as the accompanying cognitive deficits in recognition and spatial memory.

Phagocytic Microglia and Neuronal Crosstalk

Most neurological disorders, including epilepsy, are highly focused on the inflammation and the inflammatory actions of microglia, and little has been done on the other major aspect of microglia, phagocytosis. Phagocytic microglia are recognized as the janitors of the brain; they clean up dead and dying cells, as well as any leftover debris, but they play a more essential role in healthy and disease states (Sierra et al., 2013). Phagocytosis is the process in which microglia ingest and remove unwanted elements. This process occurs through a series of steps orchestrated

by a variety of molecules and receptors which regulate chemoattraction and engulfment—known as “find-me” and “eat-me” signals (Diagram 1) (Brown & Neher, 2014; Sierra et al., 2013; Wyatt-Johnson & Brewster, 2019). The “find me” signals include fractalkine receptor CX3CR1 and its

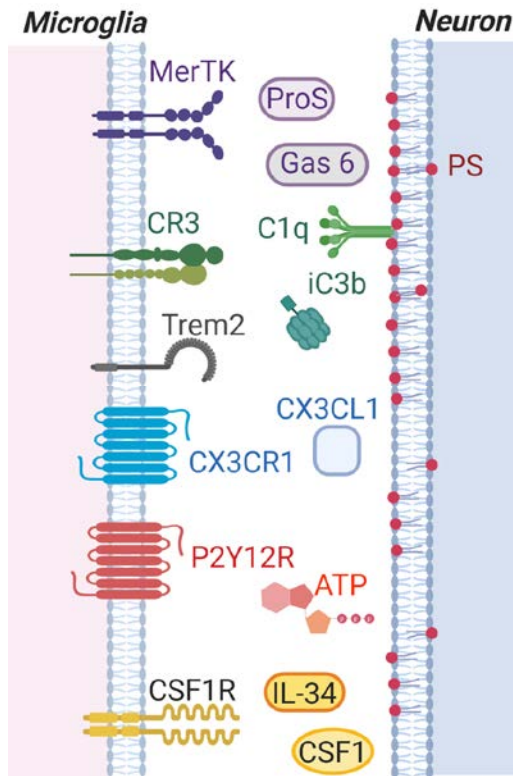


Diagram 1: Receptors and ligands that aid in the interaction between microglia and neurons. Microglia phagocytic activity is mediated by “eat-me” signals Gas6/ProS/MerTK, PS, C1q/C3b/CR3, and Trem2. The “find-me” signals CX3CL1/CX3CR1 and ATP/P2Y12 that are associated with increased neuroimmune interactions during seizures. CSF1R signaling activated by CSF1/Interleukin-34 (IL-34), that regulate microglial survival, proliferation, and phagocytic microglial properties.

ligand CX3CL1 (Brown & Neher, 2012, 2014; Sheridan & Murphy, 2013). CX3CL1 is a major ligand involved in the crosstalk between neurons and microglia. It is located in highest quantities in hippocampal neurons (Harrison et al., 1998; Sheridan & Murphy, 2013). The production of CX3CL1 by neurons aids in the removal of weak synapses during development and during brain injury (Brown & Neher, 2014). CX3CL1 is thought to be released in high quantities to guide microglia through its receptor, CX3CR1, to the neurons (Brown & Neher, 2014; Meucci et al., 2000; Sheridan & Murphy, 2013). This crosstalk reduces the production of pro-inflammatory cytokines, indicating this as a potential neuroprotective role (Mattison et al., 2013). Mice with a knockout of CX3CR1 have reduced density of spines in the hippocampus and displayed reduced neuronal loss (Bolós et al., 2018; Fuhrmann et al., 2010). Interestingly, CX3CR1 knockout mice also displayed increased severity during induction with a chemoconvulsant (Eyo et al., 2014, 2016, 2017).

Together, this suggests that microglial cells communicate with neurons via a myriad of “eat me” and “find me” signals. The “eat me” signals that aid in phagocytosis of the target include the opsonins Gas 6 and Protein S, as well as their receptor Mer Tyrosine Kinase (MerTK), C3b and its receptor complement receptor 3 (CR3), and opsonin C1q—the initiating molecule for C3 cleavage. Another receptor that mediates the rearrangement of the microglial cytoskeleton to allow engulfment of the target is the Triggering

receptor expressed in myeloid cells 2 (Trem2) (Brown & Neher, 2014; Sierra et al., 2013). Microglia from Trem2 knockout mice had less PSD95 content than microglia from wild type mice suggesting reduced engulfment of this synaptic protein (Filipello et al., 2018). Cells undergoing apoptosis typically externalize phosphatidylserine (PS), an “eat-me” signal to the outer plasma membrane. PS is recognized by Gas 6, Protein S, and MerTK, that initiate the remodeling of the cytoskeleton to allow microglia to engulf and phagocytose the cell (Brown & Neher, 2012).

Under physiological conditions microglia remain in a resting morphology, termed as ramified. When microglia remodel their cytoskeleton, they alter their phenotype from ramified to other distinct morphologies that include, hypertrophied, bushy, amoeboid, and rod-shaped (Wyatt-Johnson et al., 2017). Each morphology is speculated to have certain biochemical properties, but this has largely been up for debate (Fernández-Arjona et al., 2017). Based on the environments surrounding each morphology, it has been speculated that each morphology serves a different biochemical property of microglia to allow microglia to best respond to changes in their microenvironments (Cengiz et al., 2019; Fernández-Arjona et al., 2017; Heindl et al., 2018; Kettenmann et al., 2011). Ramified microglia are generally observed in homeostatic environments. Microglia in this morphology have a small cell body and numerous, highly branched processes (Glenn et al., 1991; Sadasivan et al., 2015; Wyatt-Johnson et al., 2017). The hypertrophied morphology displays increased diameter in microglial processes and a larger cell body; its morphology has also been widely observed with the release of inflammatory cytokines (Guadagno et al., 2013; Timmerman et al., 2018). The rod morphology has been more recently investigated. This shape is characterized by the appearance of elongated cell bodies and processes. They are also most frequently observed with their bodies parallel to dendrites (Taylor et al., 2014). Little is known about the function of the rod morphology, but it has been shown in culture to promote the proliferation and recruitment of other microglial cells (Tam & Ma, 2014; Taylor et al., 2014). Although each morphology has been observed under different conditions, it is not yet known what the morphologies may indicate in pathological conditions.

Bushy and amoeboid morphologies of microglia have been mostly observed in association with phagocytic markers in microglia. Studies have shown that increase in CD68, a lysosomal marker that indicates breakdown and degradation of recently engulfed matter, in microglia with bushy and amoeboid morphologies (Dachet et al., 2015; Fernández-Arjona et al., 2017;

Morin-Brureau et al., 2018; Perez-Pouchoulen et al., 2015). Animals that had a selective knockout of tuberous sclerosis 1 (TSC1) gene, which enhances the downstream mTOR pathway, in microglia showed altered morphologies of microglia. These microglia displayed a bushy and amoeboid morphology more frequently than ramified and they also contained higher levels of CD68 (X. Zhao et al., 2018). Furthermore, there was a decrease in the production of inflammatory cytokines and chemokines (X. Zhao et al., 2018). The TSC1 knockout mice also had increased seizure activity and frequent spontaneous seizures with up to six per day starting at post-natal day 20 (H. Zhao et al., 2018). In genetic mouse models of focal cortical dysplasia with epilepsy, there was an increase shown in ionized calcium binding adaptor molecule 1 (IBA1) positive cells occurring in the periods of frequent and spontaneous seizures (Curatolo, 2015). When treated with an inhibitor of mechanistic target of rapamycin (mTOR), a protein involved in the proliferation pathway in microglia (Bockaert & Marin, 2015), this decreased microgliosis and epileptic activity (Curatolo, 2015; Nguyen et al., 2015). This indicates that mTOR hyperactivation results in an enhanced phagocytic phenotype of microglia (H. Zhao et al., 2018; X. Zhao et al., 2018). In comparison to human tissue samples of people with refractory epilepsy, the regions of cortical tissue that had high interictal spiking before surgery showed an increase in CD68 positive microgliosis with bushy and amoeboid morphology (Dachet et al., 2015). Increased IBA1 positive cells, major histocompatibility complex (MHC) II positive cells, and CD68 positive cells were observed in temporal lobe tissue resected from people with refractory epilepsy (Morin-Brureau et al., 2018). Taken together, these data indicate the contribution of neuron-immune crosstalk and phagocytic microgliosis to SE and the development of epilepsy.

Recent evidence indicates that the “eat me” phagocytic signaling molecules are crucial for the establishment and maintenance of synaptic connectivity by coordinating the microglial removal of apoptotic neurons and unwanted synapses from early postnatal development to adulthood in the healthy brain (Hong et al., 2016; Hong & Stevens, 2016). During the development of synapses in the healthy brain, microglia utilize their phagocytic function by engulfing and eliminating weak synapses in an activity-dependent manner to allow for stronger synapses to form functional connections (Paolicelli et al., 2011; Schafer et al., 2012; Stevens et al., 2007; Tremblay et al., 2010). Insufficient synaptic elimination has been observed in association with increases in spine density, synaptic connectivity, and excitability in the somatosensory cortex (Chu et al., 2010; Ma et al., 2013). The functional implications of microglia failing to eliminate synapses during

development include altered memory function, as synapses/spines have been shown to be involved in modulation and consolidation of memory (Giovagnoli & Avanzini, 1999; Hong & Stevens, 2016; Vasek et al., 2016). The evidence supports that microglial failed synaptic elimination contributes to neuronal hyperexcitability and an increase in seizure susceptibility (Chu et al., 2010; Hong et al., 2016; Schafer et al., 2012; Shi et al., 2015; Stevens et al., 2007; Vasek et al., 2016). Interestingly, emerging data support that phagocytic microglial signals can become dysregulated and can contribute to the alterations of neural circuits in neurological disorders, including epilepsy (Bachiller et al., 2018; Brewster, 2019). Recent microglia profiling using histological and transcriptomic analysis from individuals with refractory seizures showed that microglia are highly abundant in CR3, Trem2, and MerTK (Böttcher et al., 2019; Dchet et al., 2015; Gosselin et al., 2017; Morin-Brureau et al., 2018; Wyatt et al., 2017). In human FCD, we also found that the protein levels of Protein S were decreased, and that paralleled an increase in MerTK (Wyatt et al., 2017). These data suggest a robust phagocytic phenotype in human epilepsy.

The phagocytic properties of microglia allow them to “eat” not only dead cells but also healthy yet stressed cells if they are in proximity to the neurons (Brown & Neher, 2014). The secretion of inflammatory molecules and the phagocytosis of stressed, healthy cells by microglia have led to the hypothesis that microglia have an important role in many diseases (Wolf et al., 2017). Transcriptome studies have shown a link between microglial mutations in phagocytosis, increase in inflammation release, and the pathology of AD (Holtman et al., 2015; Bin Zhang et al., 2013). Similar findings have been replicated in the mouse model of AD (Dong et al., 2019; Hickman et al., 2008; Wolf et al., 2017). Studies in rodent models of AD describe that the acute initial microglial response may be neuroprotective but a continued long-lasting response or overresponse may potentially contribute to disease progression (Dong et al., 2019; Hickman et al., 2008; Wolf et al., 2017). Similarly, in Parkinson’s disease and amyotrophic lateral sclerosis, microglial response was first determined to be neuroprotective, but throughout the progression of the disease microglial prolonged activation contributes to the loss of motor neurons (Brites & Vaz, 2014; Schapansky et al., 2015; Wolf et al., 2017). These studies support the idea that microglia are not the issue in disease, only reacting to the situations (Gomes-Leal, 2019; Lalancette-Hébert et al., 2007). The reactions of microglia to pathological events, including secretions of cytokines and their response to neuronal cues, are critical but these actions can result in the priming of microglia, potentially leading to their overreaction later on (Gomes-Leal, 2019; Neher & Cunningham, 2019).

This is one of the theories behind why inhibition of microgliosis can be simultaneously detrimental and beneficial and requires additional research. Another important aspect of microglia is their heterogeneity throughout the brain. In different brain regions, microglia portray different molecular signals and are thought to be responding to the same pathology differently (Brewster, 2019; Li et al., 2019; Ohgomori & Jinno, 2019; Stratoulis et al., 2019). These data and ideas make it critical to understand microglial inhibition during disease pathology and particularly in epilepsy.

Microglia Motility and Response to Neuronal Cues

Microglia respond to their local microenvironment and levels of neuronal activity through their purinergic receptors. In a normal healthy brain, microglia move in a function of re-arrangement, with cells translocating, proliferating, and dying in small amounts. These functions are regulated by the purinergic receptor, P2Y₁₂R. P2Y₁₂R on microglia aid in the ability of microglia to sense neuronal activity and respond to adenosine triphosphate (ATP) release (Beamer et al., 2019). Under normal conditions, active neurons and astrocytes typically release ATP, but this is disrupted by insults to the brain that include seizures, which trigger higher releases of ATP (Beamer et al., 2019). In knockout P2Y₁₂ mice, microglia have a significantly reduced ability to re-arrange, meaning there are less cells gained through either proliferation, translocation, or lost through cell death (Eyo et al. 2018). Consequently, microglial processes rapidly move to these areas and structures in an activity-dependent manner (Abiega et al., 2016; Eyo et al., 2014; Tremblay, 2011). Sepulveda-Roderiquez et al., (2019) used acute slice recordings to analyze microglia motility and purinergic activity in the hippocampus following pilocarpine induced-SE and electroconvulsive induced seizure (ECS). They found that the motility of microglial processes to move in close proximity to dendrites was ATP-directed in both SE and ECS, and they found that the ECS were enough to alter purinergic receptor function in microglia (Sepulveda-Rodriguez et al. 2019). These data indicate that seizure activity is enough to alter microglia motility and for microglial processes to move into close proximity to dendrites. Although the physiological impact of microglial process in close proximity to dendrites is not definitively known, two-photon imaging of living microglia in cortical and hippocampal networks demonstrated activity-dependent microglia synaptic contacts were followed by the disappearance of spines (Weinhard et al., 2018). These data suggest that the microglial contacts with dendrites may be playing a role in controlling neuronal excitability. Therefore, it is not surprising that physical neuro-immune

interactions have been observed in both human and experimental epilepsy. In human refractory epilepsy, microglial processes were found in close proximity to dendrites (Wirenfeldt et al., 2009; Wyatt et al., 2017). In experimental models, pronounced microglial interactions with hippocampal CA1 dendrites were observed during and after SE (Brewster et al., 2013; Eyo et al., 2014; Hasegawa et al., 2007).

Studies using two-photon live imaging of in vivo and ex vivo systems demonstrated that microglial processes move rapidly towards dendrites and axons in response to seizures, a process that is dependent on microglial P2Y₁₂R and CX3CR1-CX3CL1 signaling (Eyo et al., 2014, 2016, 2017). These studies reported that mice with a knockout of P2Y₁₂R displayed higher Racine seizure scores during induction with a chemoconvulsant similar to CX3CR1 knockout mice (Eyo et al., 2014, 2016, 2017). In animals who have a knockout of CX3CR1, microglia have no physical changes in morphology, however, the movement of microglial processes was decreased (Liang et al., 2009). CX3CR1 knockout mice do not have any reduction in proliferation of microglia, indicating that CX3CR1 is not critical in proliferation but in activity response (Eyo et al. 2018). The question remains how the accumulation and proliferation of microglial cells alters the dendritic pathology observed after SE.

Inhibition of Microgliosis in SE

Currently, more focus has been on determining how to reduce microgliosis in epilepsy. The more recent focus has been on the mTOR inhibitor, rapamycin. The pathway of mTOR is found ubiquitously throughout the brain but plays a diverse role in different cells types, including microglia (Bockaert & Marin, 2015; Crino, 2011). In microglia, it is thought to modulate inflammation and proliferation (Xie et al., 2014). In epilepsy, mTOR hyperactivation has been observed in animal models as well as human refractory epilepsy (Brewster et al., 2013; Crino, 2011; Curatolo, 2015; Nguyen et al., 2015, 2019; X. Zhao et al., 2018). Several studies have shown that the hyperactivation of mTOR in neurons and microglia has been shown to correlate with seizure severity (Brewster et al., 2013; Nguyen et al., 2019; X. Zhao et al., 2018). In these studies, treatment with rapamycin showed a reduction in seizure severity, recovery of learning and memory deficits, and reduced microgliosis in the hippocampus in both rat and mouse models of epilepsy (Brewster et al., 2013; Nguyen et al., 2015; Zhang et al., 2018; H. Zhao et al., 2018).

While there is some controversy over this treatment, as studies have shown both improvements (Brewster et al., 2013; Nguyen et al., 2015) and no changes (Buckmaster & Lew, 2011; Zeng et al., 2010) with rapamycin, the key to these differences is time and length of treatment. The length of treatment with rapamycin is extremely important, as long treatment (1-3 months) with rapamycin does not alter seizure severity in mice (Buckmaster & Lew, 2011; Zeng et al., 2010), while short treatment (1-2 weeks) has shown reduction in severity of seizures and microgliosis (Brewster et al., 2013; Nguyen et al., 2015). These differences could be potentially due to the toxic effect of rapamycin that has been observed after long treatment (Fischer et al., 2015; Tyler et al., 2011). These studies indicate the need for a more critical analysis of microglial treatments. A pathway that has become more common as a mechanism of specifically altering microgliosis is the colony stimulating factor 1 receptor (CSF1R) (El-Gamal et al., 2018; Erlich

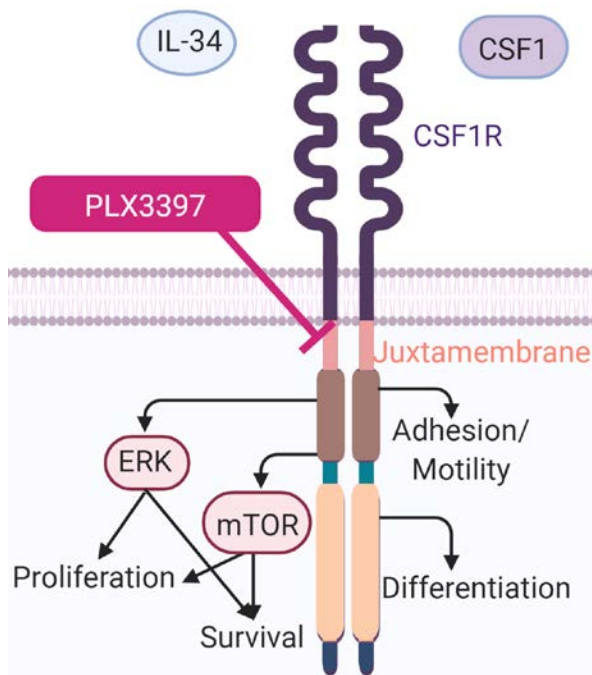


Diagram 2: Colony stimulating factor 1 receptor (CSF1R) pathway activation through ligands IL-34 and CSF1 leading to the downstream activation of signaling pathways involved in proliferation, survival, adhesion/motility, and differentiation. Inhibition of CSF1R with the drug PLX3397, inhibits at the juxtamembrane to block the ability of the receptor to exit its autoinhibited state.

et al., 2011). With the use of computational casual reasoning analytical framework for target discovery, researchers were able to identify CSF1R as a potential anti-epileptic target. To perform this computational analysis, Srivastava et al., (2018) studied RNA expression of 100 epileptic mice and 122 epileptic human samples and they were able to find CSF1R as a module target gene for treatment (Srivastava et al., 2018). This data indicates that the CSF1R pathway could be a potential beneficial therapeutic target for epilepsy. The CSF1R pathway is part of a family of receptors that are responsible for regulating the pathway that is known to control microglial proliferation, survival, differentiation, and motility/adhesion (Diagram 2) (Stanley & Chitu, 2014). CSF1R

activation is done through the binding of either CSF1 ligand or interleukin 34 (IL-34) depending on the location of microglia and period of time during development, with CSF1 involved in

prenatal development (Easley-Neal et al., 2019; Griffiths et al., 2007; Imai & Kohsaka, 2002). CSF1R in microglia leads to the direct downstream activation of the extracellular signal regulated kinases (ERK) and mTOR signaling cascades which in turn promote microglial survival and proliferation through enhancing mRNA translation (Ulland et al., 2015). Blocking CSF1R specifically inhibits microglial proliferation, leading to a decrease in the amount of microglia in normal brains (Elmore et al., 2014, 2015; Han et al., 2017). A homozygous knockout of CSF1R in mice has been used as a tool for understanding microglia during development, but does not allow for long term studies as these mice live for less than three postnatal weeks (Jia Li et al., 2006). In these mice, early development continues until the post-natal period when there are higher numbers of neurons, enlarged ventricles are evident, and an increased number of astrocytes with almost 99% mortality during these stages (El-Gamal et al., 2018; Erblich et al., 2011). Evidence from mice with a CSF1R knockout indicates the importance of microglial CSF1R in the survival of newborn animals. Recently, a homozygous CSF1R mutation was found in two humans. One child presented with ablation of microglia cells and structural malformations in the brain including the corpus callosum which failed to develop; this led to a short life ending before 1 year of age. The other individual, age 24, has other brain malformations and build up in calcifications in the periventricular regions, as well as severe cognitive deficits and epilepsy (Oosterhof et al., 2019). These data indicate the CSF1R receptor as a crucial receptor for the function and survival of microglia in both human and experimental models.

In order to block CSF1R without permanent genetic changes, several drugs have been developed. These drugs include BLZ945, GW2580, PLX647, PLX3397, and PLX5622. Out of the current selection of inhibitory drugs, PLX3397 has the most positive responses with the least modification of other brain cells (Butowski et al., 2016; Elmore et al., 2014). BLZ945 has been shown to reduce microgliosis in multiple sclerosis, but caused increases in oligodendrocytes and astrocytes (Beckmann et al., 2018) and GW2580 treatment took longer, 10 weeks, to show decreases in microglia (Gerber et al. 2018). PLX3397 is an orally active and more potent inhibitor that also blocks the precursor cells of microglia, c-kit. It was developed based on the original PLX647 but is more specific to CSF1R receptor and inhibits the precursor cells to microglia unlike PLX5622. PLX3397 has been further tested through clinical trials for breast cancer and glioblastoma, compared to both PLX family drugs (Butowski et al., 2016; Dagher et al., 2015). PLX3397 works by altering and enhancing its polarity to bind to the juxtamembrane of CSF1R.

This ATP-binding site, which is normally bound in the autoinhibited state of the receptor, is targeted and the drug interacts with the inhibitory loop residues, 546 (Tyr546) and 550 (Trp550), through hydrogen bonds to prevent the ability of the receptor from exiting the inhibited state. This interference inhibits ATP and substrate binding affecting the phosphorylation of the receptor needed to activate the survival and proliferation signaling pathways (Diagram 2) (Butowski et al., 2016; Tap et al., 2015). In phase I and II clinical trials for glioblastoma, it was found that PLX3397 is well tolerated in humans with a maximum serum concentration of 7760 ng/mL after 1000 mg/kg dose. After seven days, levels of CSF1R were depleted, determined by IBA1 density (Butowski et al., 2016). In animal models, rats have a maximum serum concentration of 10200 ng/mL after a dose of 30mg/kg, while mice have a maximum serum concentration of 449000 ng/mL after a 30 mg/kg dose, indicating that rats may have a more similar bioavailability of the drug to humans compared to mice (Butowski et al., 2016; El-Gamal et al., 2018; Tap et al., 2015; Wesolowski et al., 2019).

Under physiological conditions, the CSF1R inhibitor, PLX3397, has been shown to reduce the population of microglial cells as well as improve behavioral test performance in BM and contextual fear conditioning of naïve animals both young and aged (Elmore et al., 2014, 2018; Han et al., 2017). In these conditions, PLX3397 depleted microglial cells within seven days of treatment, and after discontinuing PLX3397, microglial cells repopulated the brain in three days (Elmore et al., 2014; Najafi et al., 2018). Importantly, inhibiting CSF1R activity with PLX3397 also prevents LPS (lipopolysaccharide)-induced activation and proliferation of microglia (Elmore et al., 2014). Under pathological conditions, a 21-day treatment with PLX3397 reduced the volume of the brain lesion due to intracerebral hemorrhage (M. Li et al., 2017) and reduced the loss of dendritic spines in models of AD (Spangenberg et al., 2016), but led to exacerbated inflammation in models of brain ischemia and stroke (Han et al., 2017; Jin et al., 2017; Szalay et al., 2016). This suggests that PLX3397 works to deplete microglia under both physiological and pathological conditions.

In epilepsy, recent studies have been done to test PLX3397 and its family of drugs. One study tested the CSF1R target with a high dose of 30 mg/kg and low dose of 3 mg/kg of PLX3397 and found a reduction in seizure frequency with the use of the high dose and a decrease in IBA1 labeled cells in both doses (Srivastava et al., 2018). When Theiler's murine encephalomyelitis virus is administered to mice, the mice develop brain infection and high inflammation leading to the subsequent development of spontaneous seizures and epilepsy. In these mice, microglia were

blocked with PLX5622 in chow prior to virus administration and the mice developed paralysis, increased seizures, and died by 10 days post infection (Sanchez et al., 2019). Taken together, these data support that inhibition of microgliosis is important in the epileptic pathology, but how microglia inhibition affects the epileptic pathology in TLE remains largely unknown. Therefore, to specifically test the role of microglia in SE-induced CA1 Map2 and dendritic ion channel alterations and the associated cognitive deficits, we used PLX3397 to inhibit microglial CSF1R signaling and prevent microgliosis in the rat model of SE and acquired TLE.

Hypothesis

TLE is the most common type of focal epilepsy and it affects the amygdalo-hippocampal network. TLE can be acquired following brain injury, including events of SE. Current anti-epileptic pharmaceutical treatments only focus on the symptoms (i.e. seizures) and are not disease modifying. Because roughly 40-89% of people with TLE have refractory seizures, there is a critical need for novel treatments that target the underlying mechanisms of epilepsy and its comorbidities such as memory deficits (Hocker, 2015; Pichler & Hocker, 2017; Serrano-Castro et al., 2012; Silva-Alves et al., 2017; Voltzenlogel et al., 2015). SE provokes dendritic structural instability through losses of Map2, dendritic branching, and spine density, which can promote pathological synaptic network remodeling, neuronal hyperexcitability in the hippocampus, and deficits in learning and memory (Brewster et al., 2013; Schartz et al., 2016, 2018; Shapiro et al., 2008). We have shown a significant spatial and temporal correlation between SE-induced Map2 loss and microgliosis in the hippocampus (Brewster et al., 2013; Schartz et al., 2016, 2018). In addition, pharmacological suppression of microgliosis after SE with the drug rapamycin attenuated the loss of Map2 and numerous dendritic ion channels in the hippocampus. This suppression improved recognition and spatial memory (Brewster et al., 2013). Based on these studies, we hypothesized that the inhibition of microgliosis during epileptogenesis would attenuate the SE-induced hippocampal dendritic and cognitive pathology. To test this hypothesis, we blocked microglial activation and proliferation during the period of epileptogenesis (Schartz et al., 2016; Wyatt-Johnson et al., 2017). Activation of CSF1R in microglia leads to the direct downstream activation of signaling cascades that promote microglial survival and proliferation. The drug PLX3397 inhibits activation of CSF1R and stops microglial proliferation (Elmore et al., 2014). Our *rationale* was targeting the SE-induced microgliosis by inhibiting CSF—which is exclusively found in

microglia/macrophages unlike mTOR/rapamycin (Bockaert & Marin, 2015)—would provide evidence that microglial cells may underlie the hippocampal dendritic alterations and memory deficits that develop after an episode of SE. Our approach for this project was to use the pilocarpine model of SE in rats. Immediately after the induction of SE (post-SE day 0), the rats were given the CSF1R inhibitor, PLX3397, at an average dose of 50mg/kg body weight per day in their food, ad lib, for 3 consecutive weeks to prevent microglial activation and proliferation (Elmore et al., 2014; Han et al., 2017). Rats were randomly assigned into one of four groups: control (Ctrl)+vehicle (Veh), Ctrl+PLX3397, SE+Veh, or SE+PLX3397. These groups were blinded to the investigator during behavioral tests and analyses as well as biochemical and histological analysis.

Specific Aims

Specific Aim #1: To determine the role of microgliosis in SE-induced hippocampal-dependent learning and memory deficits. People with epilepsy with TLE and SE often have comorbidities that include learning and memory deficits, which have been shown to be a factor in reducing their quality of life (Alonso-Vanegas et al., 2013). Similar findings are observed in the rodent models of acquired TLE (Jessberger & Parent, 2015; Lévesque et al., 2016; A. K. Sharma et al., 2007). We and others have found memory deficits starting two to three weeks post-SE in tests that include novel object recognition (NOR), Barnes maze (BM), and Morris water maze (MWM) in the pilocarpine model of SE and acquired TLE (Brewster et al., 2013; Grayson et al., 2015; Rojas et al., 2016; Schartz et al., 2018). Our working hypothesis is if SE-induced microgliosis contributes to the hippocampal-dependent learning and memory deficits, then inhibiting microglial proliferation will attenuate this pathophysiology. Our approach was to use NOR to test recognition memory and BM to test hippocampal-dependent spatial learning and memory. OF was performed to test for any potential locomotor confounds. We performed behavioral testing starting 13 days post-SE.

Specific Aim #2. To determine the role of microgliosis in the dendritic structural pathology of SE. We and others have found increases in microgliosis and morphological changes of microglia alongside decreases in the dendritic stability marker, Map2, in human and experimental models of epilepsy (Brewster et al., 2013; Dachet et al., 2015; Schartz et al., 2016; Shapiro et al., 2008; Wyatt et al., 2017; Wyatt-Johnson et al., 2017). After epileptogenesis, it has been shown that Kv4.2 and HCN1 in dendrites are decreased. These channels are particularly important as they have been

shown to play a role in neuronal excitability and learning and memory under physiological conditions (Bernard et al., 2004; Brewster et al., 2013; Hall et al., 2015; Lugo et al., 2012; Nolan et al., 2004). Microglia have been shown to make direct contacts with synapses, based on synaptic activity, and prune synapses under physiological and pathological conditions (Hong et al., 2016; Hong & Stevens, 2016; Tremblay, 2011). However, in SE, the contacts and correlation between microglia and dendrites has yet to be classified as beneficial or detrimental. Our *working hypothesis* is if SE-induced microgliosis contributes to hippocampal-dendritic structural instability, then inhibiting microglial proliferation will attenuate the synaptodendritic pathology. Our approach was to sacrifice the rats from Aim 1 after the behavioral assessments. Rats were perfused and brains were removed. Brains were dissected sagittal, alternating right and left hemispheres. One hemisphere was used for immunohistochemistry (IHC) (Expt.1) and the other for biochemical analysis (Expt.2). IHC was used to analyze the number of microglial cells and dendritic stability in consecutive sections. We investigated dendritic instability by measuring protein levels of Kv4.2, HCN1, and PSD95 with western blots.

At the conclusion of this research, our *expectation* is to have identified PLX3397 as a mechanism of inhibiting microgliosis to recover dendritic instability and cognitive deficits following the induction of SE. We also expect to gain more information about the relationship between microglia and dendrites and whether microgliosis is detrimental in this relationship. This work will have a *positive impact* by identifying a novel epilepsy modifying treatment that may prevent the comorbid memory deficits after SE.

METHODS

Animals

Male Sprague Dawley rats (150-200grams) (Envigo) and single housed in cages (19 x 10.5 x 8 inches) upon arrival to our facilities. Rats were single housed before and during the experiment to account for any cage mate deaths that might occur following the induction of SE. Rats were handled for 2-3 minutes per day by the same experimenter starting the day after arrival until they were sacrificed. The rats were housed at ambient temperature, 22 °C, with diurnal cycles of a 12-hour light and 12-hour dark (0700 to 1900). All rats had access to unlimited food and water. Male rats were chosen due to their comprehensively mapped microglial, dendritic, and cognitive profiles following pilocarpine induced-SE (Brewster et al., 2013; Eyo et al., 2017; Marcelin et al., 2012; Scharz et al., 2016). Female rats have yet to be fully characterized and studies focused on this characterization have shown protective effects of estrogen during SE induction (Iacobas et al., 2018; Tan & Tan, 2001). This effect could greatly impact this study due to the length of treatment, as it would be likely that the estrous cycle will affect seizure progression and activity (J Li et al., 2016, 2018).

Pilocarpine Induced SE

The induction of SE started with an i.p. injection of scopolamine methyl bromide (1mg/kg; Cat# S8501-1G, Sigma-Aldrich, St. Louis, MO) to prevent systemic effects of pilocarpine on the cholinergic system (Renner et al., 2005) (Figure 1). Thirty minutes later pilocarpine hydrochloride (280-300mg/kg; Cat# P6503-10G, Sigma-Aldrich) was given as an i.p. injection ($n = 46$). Behavioral observations of rats were recorded based on the Racine seizure severity scale (1-6) (Table 1) for each rat (Racine, 1972). Rats that reached a 5-6 meet the criteria for severe SE ($n = 28$; 61%). Any rats that failed to reach a Racine level of 5-6 were marked as non-SE ($n = 16$; 35%) or did not survive SE were removed from the study ($n = 2$; 4%). Forty-five minutes after the rat reached the threshold for severe SE an i.p. injection of diazepam (10mg/kg; Hospira, Inc., Lake Forest, IL) was given to stop SE. Due to the side effects of diazepam including, decreased heart rate and hypothermic effects, all rats were placed onto heating pads for warmth (Carpenter et al., 1977). Control rats were given scopolamine (1mg/kg) followed by an i.p. injection of 0.9% saline

(Hudson RCI, Morrisville, NC) 30 minutes later and at about the same time as the SE rats control rats were given an i.p. injection of diazepam (10mg/kg). All rats were continuously monitored. Four hours following diazepam injection rats received an i.p. injection of 1.5mL of 0.9% saline for hydration. Ensure, fruit loops, and subcutaneous (s.c.) injections of 1.5mL of 0.9% saline were administered, as needed, during recovery (post-SE days 1-3) to help facilitate weight gain. Rats were weighed daily between 0800-1000 throughout the entire experiment to monitor weight gain (Ctrl+Veh, $n = 13$; Ctrl+PLX3397, $n = 13$; SE+Veh, $n = 14$; SE+PLX3397, $n = 9$; SE+PLX3397 non, $n = 5$; power = .997).

Table 1. Modified Racine Level Seizure Scale (Racine, 1972)

Racine Scale	
1	Rigid posture and mouth moving
2	Tail clonus
3	Partial body clonus and head bobbing
4	Rearing
4.5	Whole body clonic seizures while retaining posture
5	Rearing and falling
6	Tonic-clonic seizure with loss of posture

Chow With PLX3397

After induction, post-SE day 0, control and SE rats were randomly distributed into either standard rodent chow (T.2018) alone (Vehicle, Veh) or standard rodent chow with PLX3397 groups (Pexidartinib; Purity: 99.56%; Selleckchem, Pittsburgh, PA). PLX3397 was shipped overnight to be mixed in chow at Envigo (Madison, WI). According to Envigo, PLX3397 was mixed with chow at approximately 50mg/kg body weight per day for this study (455mg PLX3397/kg of diet) (National Research Council (US) Subcommittee on Laboratory Animal Nutrition, 1995). The rodent chow T.2018, from Envigo, has a diet make up of 18.6% protein, 6.2% fat, and 3.1 kcal/g of metabolizable energy. To add the PLX3397 to the chow, the chow was first

processed into a fine powder then the PLX3397 was mixed into the chow with ~22% water which acted as a pelleting agent. Next, the chow was pressed into pellets and dried at 50°C for 8–10 hours (T. Herfel, personal communication, July 10, 2018). Based on our preliminary findings and confirmation from Envigo, PLX3397 is generally stable during this process. PLX3397 chow was stored at -20°C and allowed to warm to room temperature (RT) before fed to rats each day. Food was available ad lib and was continuously added to keep the rodent chow as fresh as possible. Thirteen controls and 14 SE animals were placed on the diet containing PLX3397 for a total of 27 rats.

Open Field (OF)

On post-SE day 13, rats were placed into training cages (11.5 x 5.75 x 6 inches) and allowed to acclimate to the dark with a single red light for 30 minutes before the test began at 0830. The test followed previously described protocols (Brewster et al. 2013; Schartz et al. 2018). Rats were placed into the testing box (40 x 40 x 30 cm) for ten minutes under red light conditions. Red light condition was used as it allowed for the of behavior to be recorded and mimics the dark cycle in which rats are most active. The apparatus was divided into an inner zone (20 x 20 cm) in the center 20 centimeters from all sides and outer zone defined as the area touching the edge to the inner zone. The test was video recorded from above and tracked with Any-maze video tracking system V4.99 (Wood Dale, IL). The parameters set for Any-maze to track include total distance travelled, average speed, time spent motionless, and time spent in the outer and inner portion of the chamber. OF doubled as habituation for NOR (Ctrl+Veh, $n = 10$; Ctrl+PLX3397, $n = 10$; SE+Veh, $n = 10$; SE+PLX3397, $n = 7$; power = .831).

Novel Object Recognition (NOR)

NOR testing began 24 hours after OF/habituation in the same testing box and followed a previously described protocol (Schartz et al., 2018). On day 14, similar to OF, rats were placed into training cages and acclimated to the dark for 30 minutes before trial 1 started. Trial 1 consist of the familiarization phase of NOR test. Under red light condition, rats were placed into the apparatus and were given five minutes to explore two identical objects, yellow rubber ducks, on opposite sides of the box equal distance. Rats were then placed back into their training cages. After

a two-hour wait in the dark trial 2 began. During trial 2, one of the objects was replaced with a novel object, a brown rubber hamburger. The side the novel object was placed on was alternated to counterbalance for any side preference the rats had. At the start of trial 2, rats were placed into the box and given five minutes to explore. Videos recorded from above and saved with Any-maze video tracking system. These videos were then analyzed by two blinded investigators for time spent exploring each object, determined by the rat's nose coming within two centimeters of the object. The results from both investigators were averaged. The recognition index was determined by time spent with the familiar object in trial 2 (FT2) subtracted by the time spent with the same object, in the left or right position, in trial 1 (FT1), divide by total time spent exploring these two objects $[(FT1 - FT2)/(FT1 + FT2)]$. NOR testing was completed in four cohorts of 9-12 rats per cohort for a total of 40 rats tested with 10 rats per condition (Ctrl+Veh, $n = 10$; Ctrl+PLX3397, $n = 10$; SE+Veh, $n = 10$; SE+PLX3397, $n = 7$; power = .923).

Barnes Maze (BM)

BM training days took place the day after NOR was completed. The BM apparatus was a circular platform that measured at a diameter of 1.22m and elevation of 1.68m. The platform contained 18 circular holes (diameter of 9.5cm) at an equal distance around the apparatus with one hole having a removable escape box placed under it. Three different cues (square, triangle, and cross) were placed on the three walls surrounding the platform, roughly 51 cm away from platform edge, to aid in spatial navigation to the escape box (Gawel et al., 2019). The trials were video recorded from above and tracked with Any-maze tracking system. Before each training/testing day, rats were placed into training cages and brought into an adjacent dark room for 30 minutes and acclimated to the dark. The first day of BM was habituation. During this stage rats were trained to enter the escape box through three separate methods, separated by 15 minutes under red light condition: (1) rats were placed directly into the escape box; (2) rats were placed next to the escape box and gently nudged into the box; (3) rats were placed in center of platform and gently guided to the escape box through an open tunnel. Rats remained in the escape box for two minutes, then were moved back to their training cages until all rats had completed the training. Twenty-four hours later the escape box was rotated 180 degrees from the habituation location. On training days 1-4, rats were tested each day for four trials/blocks, separated by 15-18 minutes, with a total of 16 blocks. The use of bright lights and an open elevated platform acted as a motivator for the rats to

find the escape box, as these conditions are aversive to rats (Gawel et al., 2019; Pitts, 2018). Training started with the rats placed in the center of the platform covered by an opaque start box (10 x 5 x 7 inches) in the dark. Bright lights were turned on and the box was removed after a ten second delay. In each trial, on days 1-4, the rats were given three minutes to find the escape box. If the rats did not find or go into the escape box after three minutes the rats were gently guided into the box. Rats remained in the escape box for one-minute, bright lights were turned off, and rats were then placed back into their training cages and moved back into the adjacent dark room. The time it took for the rats to find the escape box, the average speed, total distanced travelled, and time spent in the escape box quadrant was recorded through Any-maze and confirmed by two investigators blinded to groups. The results were averaged across Any-maze and the two investigators. Any rat that did not find the escape box was recorded as maximum time for that trial (three minutes). After each trial, the platform was cleaned with 70% ethanol, rotated 90 degrees, and the escape box was positioned under the new hole. This was done to prevent any potential smell confounds that could have led the rats to the escape hole (Gawel et al., 2019). On testing day 5, the escape box was removed, and all holes were covered. Rats were placed into the center of the platform covered by an opaque start box; the box was removed after a 10 second delay under bright light condition. Rats were allowed 90 seconds to explore. The time to the escape hole location and time spent over the location of the escape box hole was measured through Any-maze and confirmed by two investigators blinded to groups. The results were averaged across Any-maze and the two investigators. Any rat that did not find the escape box was recorded as maximum time for that trial (90 seconds). Rats were expected to spend a majority of time on top of the escape hole, less than that would indicate decreased spatial memory. Heat maps were generated from Any-maze software and analyzed with MATLAB R2018a (Natick, MA). Generated heat maps were converted to a range of 0-100 with 0 indicating no time spent in location and 100 indicating most time spent in location. The heat maps were then weighted by the number of animals in each group and added together to generate the average heat map for each group. BM testing was completed in four cohorts with 9-12 rats per cohort for a total of 40 rats tested with 10 rats per group (Ctrl+Veh, $n = 10$; Ctrl+PLX3397, $n = 10$; SE+Veh, $n = 10$; SE+PLX3397, $n = 7$; power = .871).

Perfusion Through the Heart

Ice cold 1X phosphate buffered saline (PBS; 137 mM NaCl, 2.7 mM KCl, 4.3 mM Na₂HPO₄, 1.47 mM KH₂PO₄, pH 7.4) was pumped through tubing connected to a needle before the experiment began to remove any residue from the tubing. Rats were anesthetized with a lethal dose of Beuthanasia-D (200mg/kg; active ingredients: 390mg pentobarbital sodium and 50mg phenytoin sodium; NADA #119-807, Merck & Co. Inc, Madison, NJ). Rats were determined to be unconscious and unresponsive with use of the pinch-response method. The pinch-response method used a painful stimulus, the pinch, to confirm unresponsiveness of the rats (Boivin et al., 2017). When rats were unresponsive, the rats were opened with an incision through the abdomen and widened to the length of the diaphragm. The diaphragm was cut to allow for access to cut the rib cage on the right and left of the midline. The rib cage was removed, and the heart was exposed. A needle (20g) was placed into the protrusion of the left ventricle of the heart. When placed the pump was turned on at a rate of 20ml/min, the right atrium was cut, and the rats were perfused with cold 1XPBS. This continued until liver was clear of any blood, approximately 5 minutes. After it was cleared, the head was decapitated with a guillotine, and the brain was removed. One hemisphere was placed into 4% paraformaldehyde (PFA) for immunohistochemistry and the other hemisphere was sub-dissected for the hippocampus and frozen at -80°C for western blot.

Cryoprotection for Histology

After the brain was removed, one hemisphere was placed into 4% PFA for 24 hours at 4°C for fixation, then transferred into 30% sucrose (Thermo Fisher Scientific, Rockville, IL) (diluted in 1X PBS) at 4°C. When the brain hemisphere sank, approximately three days later, the solution was replaced with fresh 30% sucrose. Once the brain hemisphere sank, approximately three more days, they were cryoprotected. Brain hemispheres were removed from sucrose and dabbed with a paper towel to remove excess sucrose from the surface of the brain hemisphere. They were placed in dry ice for five minutes then wrapped in foil and stored at -80°C until cut. Sections were sliced on a Leica CM1860 cryostat at 20µm along the dorsoventral axis at bregma coordinates: -3.00mm, -3.48 mm, -4.08 mm, -4.36 mm, -4.92 mm, and -5.28 mm. Sections were stored in 1XPBS+0.1% sodium azide at 4°C for immunohistochemistry.

Immunohistochemistry (IHC)

IHC was done in free floating sections as previously described (Schartz et al., 2016; Wyatt-Johnson et al., 2017). All sections were placed in 1XPBS for five minutes, 3% H₂O₂ for 30 minutes, and 1XPBS+3% Triton (Tx) for 20 minutes. Next, sections were incubated for one hour in immuno buffer [5% goat serum, 0.3% bovine serum albumin (BSA), 1XPBS+0.3%Tx] at RT. Then, sections were incubated at 4°C for 48 hours on a rotating platform with the primary antibodies listed in Table 2. This was followed by three washes in 1XPBS+0.1%Tx. Next, sections were incubated for one hour in biotinylated goat anti-rabbit secondary antibody (1:1000; BA-1000, Vector Laboratories, Burlingame, CA) at RT. This was again followed by three washes in 1XPBS+0.1%Tx. Sections were placed in ABC Avidin/Biotin complex solution for 30 minutes, washed in 1XPBS+0.1%Tx (3x5minutes), and developed using the DAB Peroxidase (HRP) Substrate Kit, 3,3'-diaminobenzidine (SK-4100, Vector Laboratories) for two minutes. Sections were mounted on gelatin-coated slides which acts as an adhesive to keep the sections bounded to the slide. Once dried sections were either Nissl stained or put directly into the dehydration step. Sections were dehydrated in alcohol at a gradient of 50%, 70%, 95%, 100% and any remaining fat in the tissue was removed with two immersions in Xylene (X5-500, ThermoFisher Scientific) each for three minutes. Finally, sections were cover slipped with glass covers (Global Scientific, Mahwah, NJ) and Permount mounting media (SP15, ThermoFisher Scientific). Immunostaining was visualized using a Leica DM500 microscope and images were captured with high a resolution digital camera (Leica MC120 HD) with 4X, 20X, and 40X objectives using the LAS4.4 software.

Table 2. The Rat Specific Antibodies Used for IHC and WB Experiments

Method	Antibody	Host	Company	Catalog Number	Dilution
IHC	IBA1	Rabbit	Wako	19-19741	1:1mL
	Map2	Rabbit	Cell Signaling	#8707	1:1mL
WB	β -Actin	Mouse	Cell Signaling	#3700S	1:5mL
	C3	Goat	MP Biomedical	855730	1:500 μ L
	GFAP	Mouse	Cell Signaling	#3670	1:50mL
	HCN-1	Mouse	NeuroMab	75-110	1:500 μ L
	IL-6	Rabbit	Abcam	ab6672	1:250 μ L
	Kv4.2	Mouse	NeuroMab	75-016	1:500 μ L
	PSD95	Mouse	NeuroMab	75-028	1:15mL

Microglia Counts

Cells were counted as previously described (Long, Kalehua, Muth, Calhoun, et al., 1998; Long, Kalehua, Muth, Hengemihle, et al., 1998; Wyatt-Johnson et al., 2017). Ionized calcium-binding adapter molecule 1 (IBA1) was used as a marker for microglia cells but due to localization of IBA1 on monocytes, any infiltrating macrophage was also counted (Ohsawa et al., 2004). Counts were taken from the hippocampal CA1 region and all IBA1-positive cells within the entire 40X image were counted. The inclusion guidelines were set as 75% or more of the cell had to be located inside the 40X image and the tissue must be intact throughout the CA1 region. If clusters of IBA1-positive cells were present and single cell bodies could not be distinguished that cluster was counted as one cell. After counting the cells, the morphology of each cell counted was determined. The IBA1-positive morphologies were divided into 5 categories: (1) ramified; (2) hypertrophic; (3) bushy; (4) amoeboid; (5) rod. The guidelines for classification of each morphological category, Table 3, was adopted based on previously published literature (Kettenmann et al., 2011; Kosonowska et al., 2015; Long, Kalehua, Muth, Calhoun, et al., 1998;

Long, Kalehua, Muth, Hengemihle, et al., 1998; Taylor et al., 2014; Torres-Platas et al., 2014; Wyatt-Johnson et al., 2017; Ziebell et al., 2012). Three distinct, non-overlapping images in the CA1 region of the hippocampus were averaged and then average over three to six sections per rat. Cell counts were performed bilaterally. Counts were performed by a single investigator blinded to experimental groups (Ctrl+Veh, $n = 13$; Ctrl+PLX3397, $n = 13$; SE+Veh, $n = 14$; SE+PLX3397, $n = 9$; SE+PLX3397 non, $n = 5$; power = .990).

Table 3. The Guidelines for Morphological Classification of IBA1-Positive Cells

Category	Cell Body Size	Processes Physical Features
Ramified	Diameter: > 50 μm	Fine and highly branched
Hypertrophic	Diameter: 40-50 μm	Thick and highly branched
Bushy	Diameter: 20-25 μm	Thick, dense, and short
Amoeboid	Diameter: 10-15 μm	Retracted
Rod	Length: 10-20 μm Width: 4-8 μm	Fine and short

Semi-Quantitative IHC Densitometry Analysis

The relative mean pixel intensity of the immunostaining signal was acquired using the Image J software V1.49 (NIH) as previously described (Schartz et al., 2016). Images were inverted and the entire image density was measured. The background—determined by any area where signal was not located—was measured and subtracted from the image density. Any sections that had damage in the hippocampal region were excluded. Three distinct, non-overlapping images in the CA1 region of the hippocampus were averaged and then average over three to six sections per rat. Densitometry analyses was performed bilaterally over the CA1 region of the hippocampus (IBA1: Ctrl+Veh, $n = 13$; Ctrl+PLX3397, $n = 13$; SE+Veh, $n = 14$; SE+PLX3397, $n = 9$; SE+PLX3397 non, $n = 5$; power = .998; Map2: Ctrl+Veh, $n = 10$; Ctrl+PLX3397, $n = 10$; SE+Veh, $n = 10$; SE+PLX3397, $n = 7$; SE+PLX3397 non, $n = 3$; power = .956).

PLX3397 Non-Responder Cutoff

Non-responders to PLX3397 were determined by the rats that did not have reduced microgliosis (numbers of IBA1-positive cells). This cutoff was determined by the separation between the averages of the Ctrl+Veh and Ctrl+PLX3397 groups. The Ctrl+Veh average was 171.35 and the Ctrl+PLX3397 was 98.95 the ratio out of 100 was determined by dividing the Ctrl+PLX3397 over the Ctrl+Veh indicating a 60% reduction. The 60% was then applied to the average of the SE+Veh group (702.32) creating the cutoff for the SE+PLX3397 group at 421.39. The group was then subdivided into SE+PLX3397 responders with any rats that had microglia count below 421.39 and another group SE+PLX3397 non-responders with any rat over 421.39. SE+PLX3397 non-responders were removed completely from the SE+PLX3397 group for all analysis. The SE+PLX3397 non-responders were then analyzed separately in Figures 15-18.

Western Blot (WB)

The hippocampi were removed and stored at -80°C until homogenization. Ice cold 1XPBS was added to each hippocampus and they were homogenized with syringes. Samples were handled for immunoblotting according to previously published protocols (Brewster et al., 2013; Schartz et al., 2016). First the protein concentration of each sample was determined with the Bradford Protein Assay (Bio-Rad Laboratories, Hercules, CA). The absorbance was measured with Chromate manager (Awareness Technology, Inc., Palm City, FL) at a wavelength of 595nm. Hippocampal protein samples were diluted to 1 µg/µl with 1XPBS and 4X laemmli buffer (0.25 M Tris, pH 6.8, 6% sodium dodecyl sulfate (SDS), 40% sucrose, 0.04% Bromophenol Blue, 200mM Dithiothreitol). Samples were loaded in 10% Tris-glycine gels (buffer, 30% acrylamide, 10% SDS, 10% ammonium persulfate, 10 µl TEMED) and run through sodium dodecyl sulphate-polyacrylamide gel electrophoresis (SDS-PAGE) in mini protean 3 cell (Cat# 525BR 010890, Bio-Rad Laboratories). After electrophoresis, the gels containing the separated proteins were transferred with mini trans-blot cell (Cat# 153 BR102550, Bio-Rad Laboratories) onto polyvinylidene fluoride membranes (Cat# 88518, GE Healthcare, Chicago, IL) that act as a support matrix for the proteins. After the transfer membranes were blocked with 5% non-fat milk or 5% BSA diluted in 1XPBS+ 0.1%Tx at RT for one hour on a rocking platform to prevent nonspecific binding. Membranes were incubated with primary antibodies listed in Table 2 overnight.

Membranes were washed in 1XPBS with 0.1% Tween (3x5minutes) and incubated in HRP-linked secondary antibodies (anti-rabbit, ab205718, or anti-mouse, ab205719, 1:2000; Abcam, Cambridge, United Kingdom) for one hour at RT. Membranes were again washed in 1XPBS with 0.1% Tween (3x5minutes) and incubated in enhanced chemiluminescence prime detection reagent (GE Healthcare) for five minutes to visualize the immunoreactive bands. These bands were captured on double emulsion blue autoradiography film (BX57, MIDSCI, St. Louis, MO) and the film was developed by hand. Films were exposed to the developer (NC9956374, Thermo Fisher Scientific) until bands were visualizable then films were moved to fixer for two minutes and washed in water. Films were hung to dry before analyzing. Membranes were stripped to remove primary antibodies with stripping buffer (25 mM glycine, pH 2.0, 10% SDS) for two hours at RT then washed in 1XPBS with 0.1% Tween. The membranes were then able to be re-blotted with primary antibody as described above.

Densitometry Analysis for Western Blot

Each film was analyzed with ImageJ software by measuring the relative pixel density of each immunoreactive band (Brewster et al., 2013; Schartz et al., 2018; Wyatt et al., 2017). Background signal from each film was recorded and subtracted from each immunoreactive band. The relative pixel density from each protein of interest was normalized to the relative pixel density of the loading control (beta-actin) for each lane/sample. Samples were normalized within film to the vehicle treated control samples to control for exposure differences (GFAP: Ctrl+Veh, $n = 13$; Ctrl+PLX3397, $n = 11$; SE+Veh, $n = 14$; SE+PLX3397, $n = 9$; SE+PLX3397 non, $n = 5$; power = .851; C3/iC3b: Ctrl+Veh, $n = 9$; Ctrl+PLX3397, $n = 7$; SE+Veh, $n = 8$; SE+PLX3397, $n = 8$; power = .96; IL-6/PSD95/Kv4.2/HCN1: Ctrl+Veh, $n = 13$; Ctrl+PLX3397, $n = 13$; SE+Veh, $n = 14$; SE+PLX3397, $n = 9$; power = .80).

Statistical Analysis

All analyses were completed using GraphPad Prism Software version 8.3. Power calculations with G*Power was used for a priori analysis to determine sample sizes with previously collected data based on a power of 80%. A post-hoc power analysis was performed for each set of experiments with G*Power, in order to ensure that this study was sufficiently powered. Outliers

were determined with ROUT with the maximum desired false recovery rate set to 1%, if an outlier was removed in one test, it was removed in all other dependent tests. All Analysis of Variance (ANOVA) tests were chosen if the data met the conditions for the ANOVA assumptions including normality. ANOVA test were analyzed as condition (control vs SE) and treatment (vehicle vs PLX3397). Tukey's multiple comparison test was chosen for all two and three-way ANOVAs since every mean was being compared with every other mean. One-way ANOVA with Dunnett's multiple comparison test was chosen for the SE+PLX3397 compared to the SE+Veh and SE+PLX3397 responders to compare the SE+Veh group and SE+PLX3397 to the non-responders, since the SE+Veh and SE+PLX3397 had already previously been compared. Kolmogorov-Smirnov test and Kruskal-Willis tests with Dunn's multiple comparison were used for non-normal data distributions. Statistical significance was set at $\alpha < .05$. The appropriate statistical analysis tests were used for each experiment and listed below. (1) Racine scale: To compare the behavioral response of each group to pilocarpine induction of status epilepticus with the Kolmogorov-Smirnov test to determine the distance between both distributions of non-normal data. Student's t-test was used when analyzing seizure threshold levels (3 and 6) of the two groups. Non-responders: We used Kruskal-Willis test with Dunn's multiple comparison to determine whether the samples originated from the same distribution for non-normal data. One-way ANOVA with Dunnett's multiple comparison test was used when analyzing seizure threshold levels (3 and 6) of the SE+PLX3397 non to both the SE+Veh and SE+PLX3397 groups. (2) Weight: To compare the weight changes across the 20 days a three-way mixed effects model (days/time vs condition vs treatment) with Tukey's multiple comparison test was used with the four experimental groups. (3) OF: The behaviors recorded during OF were compared using a two-way ANOVA (condition vs treatment) with Tukey's multiple comparison test to determine effects of the treatment and of their condition. The behaviors that were analyzed: average speed, total distanced travelled, time spent motionless, and percentage of time spent in the inner zone. (4) NOR: The rat's preference of objects (left vs right; familiar vs novel) was compared using student's paired t-tests. The recognition index and time spent exploring both objects in trial 1 and trial 2 was determined using a two-way ANOVA (condition vs treatment) with Tukey's multiple comparison test. (5) BM: The latency to first reach the hole, average speed, total distanced travelled, and time spent in target hole quadrant during the 16 blocks were analyzed by a three-way ANOVA (condition vs treatment vs training block) with Tukey's multiple comparison test. To compare the latency to reach the target

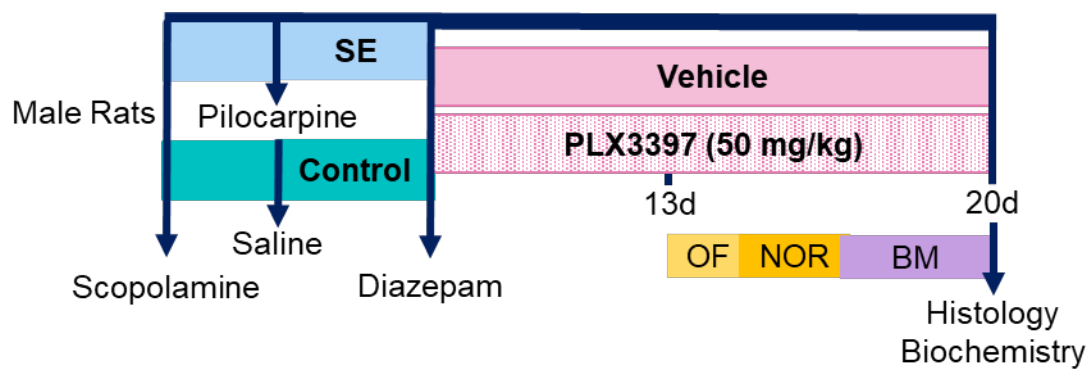
location and percent of time spent over the target during the probe trial, a two-way ANOVA (condition vs treatment) was used with Tukey's multiple comparison test. (6) IHC: For IHC experiments, densitometry and cell counts were analyzed using a two-way ANOVA (condition vs treatment) with Tukey's multiple comparison test with the four experimental groups. Non-responders: One-way ANOVA with Dunnett's multiple comparison test was used when IHC of the SE+PLX3397 non to both the SE+Veh and SE+PLX3397 groups. (7) Microglia morphology: For the microglial morphological analysis, non-parametric statistics was used as the assumption of normality was violated for an ANOVA. The Kruskal-Wallis test was chosen because it ranks the means of the groups and does not assume normality across the groups. (8) WB: WB densitometry was analyzed using two-way ANOVA with Tukey's multiple comparison test with the four experimental groups. Non-responders: One-way ANOVA with Dunnett's multiple comparison test was used when IHC of the SE+PLX3397 non to both the SE+Veh and SE+PLX3397 groups. (9) Correlations: Correlational analysis were analyzed by a linear regression. Data reported in figures were reported as means (m) \pm standard error of the mean (SEM). Figures were generated using Adobe Photoshop (CS6) and Biorender.com.

RESULTS

Group Assignment was Randomly Distributed After SE Induction

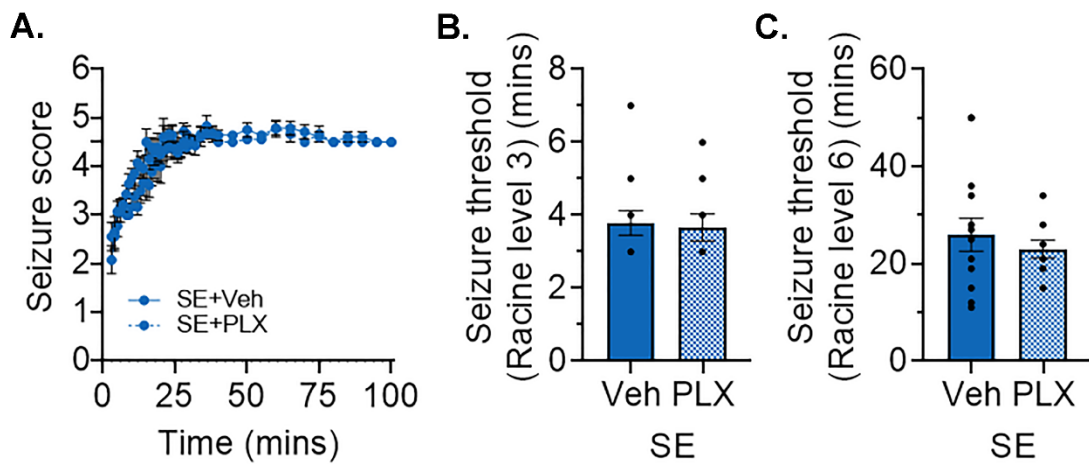
To determine the potential role of microgliosis in dendritic instability and cognitive deficits observed after SE, we used the CSF1R inhibitor, PLX3397, to disrupt microglial survival and proliferation. We induced SE using the chemoconvulsant, pilocarpine, and stopped the seizure with the anticonvulsant, diazepam. Following the induction, SE animals were randomly assigned to either standard rodent chow (Veh) or the chow with PLX3397 groups at a dose of 50mg/kg for 20 days. Ctrl animals were also randomly distributed. We tested four groups of rats: i) Ctrl+Veh, ii) Ctrl+ PLX3397, iii) SE+Veh, and iv) SE+ PLX3397. Starting at 13 days post-SE, we performed a series of behavioral tests including OF, NOR, and BM. Twenty days post-SE, rats were sacrificed for analysis of microgliosis and dendritic alterations (Figure 1).

To confirm that rats were randomly and evenly distributed across both groups, we analyzed their development of SE with a modified Racine scale listed in Table 1 (Figure 2) (Racine, 1972). We compared the Racine scale curves during the induction of SE to confirm that the SE groups were randomly distributed after induction into the two treatment groups, Veh and PLX3397. Due to the non-normality of the data we used Kolmogorov-Smirnov test to determine the distribution between each groups' induction level. We found that there was no significant difference in Racine scale between the SE+Veh and SE+PLX3397 [$D = 0.1556$, $p = .6476$] (Figure 2A). To further quantify any potential difference in the development of SE, both time to Racine level 3, indicating the beginning of seizure activity electrographically, and time to Racine level 6, indicating severe behavioral seizure had been achieved, were analyzed with a one-way ANOVA (Sharma et al., 2018). Time to reach a level 3 seizure was not significantly different between the SE+Veh and SE+PLX3397 groups [$t(21) = 0.2318$, $p = .8190$] (Figure 2B), indicating all rats started seizure activity at a similar time. We also analyzed time to reach a Racine scale level 6 severe seizure which was the criteria for rats in this study to be determined as SE. Time to reach a Racine level 6 was not significantly different between either SE+Veh or SE+PLX3397 groups [$t(21) = 0.6675$, $p = .5117$] (Figure 2C). Together, these data indicate that the potential effects observed by the inhibition of CSF1R signaling was not due to severity of SE of either Veh or PLX3397 group.



Note. A, Timeline of experiment starting with the induction of SE at 0 days followed by treatment with PLX in chow (50 mg/kg per day) or chow alone starting immediately after SE induction, day 0 to 20 days post-SE, with behavior [open field (OF), novel object recognition (NOR), and Barnes maze (BM)] performed starting at day 13 to day 20.

Figure 1. Experimental timeline of the induction of status epilepticus (SE) and treatment with PLX3397.



Note. A, Behavioral observation during the induction of SE were recorded and monitored with the Modified Racine scale. B-C, Time to reach a Racine scale level 3 (B) and 6 (C). Analyzed by (A) Kolmogorov-Smirnov test and (B-C) student's t-test. Data shown as mean \pm SEM, SE+Veh, $n = 14$; SE+PLX, $n = 9$.

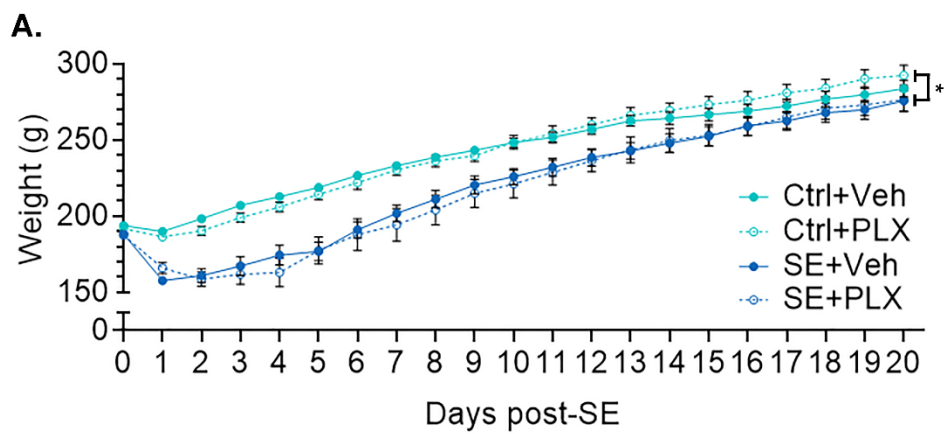
Figure 2. Rats were randomly distributed after the induction of status epilepticus (SE) into vehicle (Veh) or PLX3397 (PLX) treatment.

Inhibition of CSF1R Signaling does not Attenuate SE-Induced Weight Loss

In order to monitor recovery after the induction of SE, all rats were weighed daily starting on the day of induction (Figure 3). The initial weights of all the rats before they were randomly assigned to each group were not significantly different from one another [$F(1, 45) = 0.0508, p = .8227$]. Using a three-way ANOVA [days X condition (Ctrl vs SE) X treatment (Veh vs PLX)] to analyze the weight change over the entire course of the experiment, we found a main effect of days on weight change [$F(20, 900) = 911.1, p < .0001$], indicating that all groups changed weight throughout the experiment. We found a main effect of condition [$F(1, 45) = 23.39, p < .0001$]; the Ctrl groups weighed more throughout the experiment compared to the SE groups as the SE groups changed weight between days one through seven (Table 4). There was no main effect of treatment with PLX3397 [$F(1, 45) = 0.0072, p = .9329$]. We found a significant interaction between days post-SE and condition [$F(20, 900) = 19.41, p < .0001$], where the SE groups had a lower weight compared to the Ctrl groups throughout the experiment. An interaction was not found between days post-SE and treatment [$F(20, 900) = 3.721, p < .0001$], indicating again that inhibition of CSF1R signaling did not affect weight gain across the experiment. There was also no significant interaction between condition and treatment [$F(1, 45) = 0.05693, p = .8125$], meaning that inhibition of CSF1R signaling along with SE did not affect their weight change. The three-way interaction between days post-SE, condition (Ctrl vs SE), and treatment (Veh vs PLX3397) was also not significant [$F(20, 900) = 1.174, p = .2692$]. Taken together, these data support that all the groups gained weight and treatment with PLX3397 in the chow did not affect weight gain.

Treatment with PLX3397 and the Induction of SE does not Alter Locomotion

Starting at 13 days post-SE, animals were put through a series of behavioral tests starting with OF. OF testing allowed for detection of locomotion impairments or anxiety-like behaviors as the rats explored the apparatus (Ennaceur et al., 2006; Feyissa et al., 2017) (Figure 4). The locomotion impairments and anxiety response were analyzed with a two-way ANOVA [condition (Ctrl vs SE) X treatment (Veh vs PLX)]. Average speed (Figure 4A) and total distanced travelled (Figure 4B) were analyzed for detection of locomotion impairments. The anxiety-like behaviors

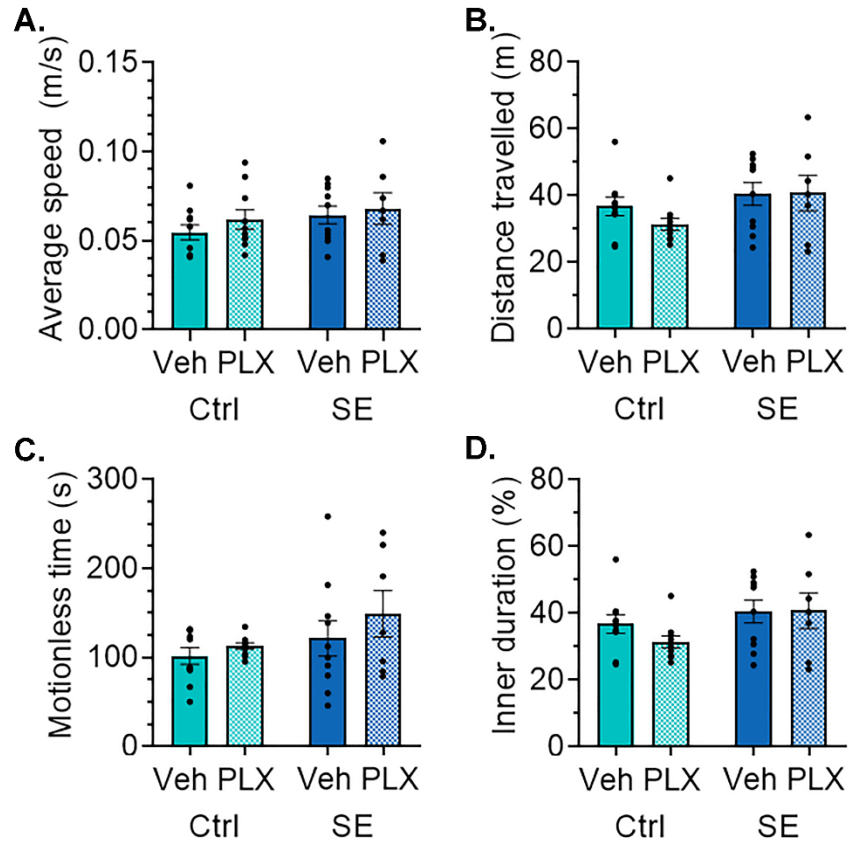


Note. A, Daily weights were recorded. $*p < .05$ by a three-way mixed effects model with Tukey's multiple comparison test. Data shown as mean \pm SEM, Control+Vehicle (Ctrl+Veh), $n = 13$; Ctrl+PLX, $n = 13$; SE+Veh, $n = 14$; SE+PLX, $n = 9$.

Figure 3. Status epilepticus (SE) triggers acute weight loss that is not attenuated with PLX3397 (PLX) treatment.

Table 4. Multiple Comparison Analysis of Weight Change Across Each Day

Days Post-Se	Ctrl+Veh vs. Ctrl+PLX	Ctrl+Veh vs. SE+Veh	Ctrl+PLX vs. SE+PLX	SE+Veh vs. SE+PLX
Day 0	>.9999	.9999	>.9999	>.9999
Day 1	>.9999	<.0001	<.0001	.9978
Day 2	.9771	.0007	.0266	>.9999
Day 3	.9744	.0123	.0851	>.9999
Day 4	.9998	.0211	.2385	>.9999
Day 5	>.9999	.0050	.3942	>.9999
Day 6	>.9999	.0079	.7454	>.9999
Day 7	>.9999	.0337	.6858	>.9999
Day 8	>.9999	.1532	.7365	>.9999
Day 9	>.9999	.4576	.9328	>.9999
Day 10	>.9999	.4303	.8857	>.9999
Day 11	>.9999	.8509	.9294	>.9999
Day 12	>.9999	.8870	.8829	>.9999
Day 13	>.9999	.7460	.9786	>.9999
Day 14	>.9999	.9923	.9925	>.9999
Day 15	>.9999	.9997	.9886	>.9999
Day 16	>.9999	>.9999	.9972	>.9999
Day 17	>.9999	>.9999	.9998	>.9999
Day 18	>.9999	>.9999	>.9999	>.9999
Day 19	>.9999	>.9999	.9997	>.9999
Day 20	>.9999	>.9999	>.9999	>.9999



Note. Rats were habituated to the novel object recognition testing chamber on 13 days post-SE for 10 mins and their average speed (A), total distance travelled (B), time spent motionless (C), and percent of time spent in the inner zone (D) were recorded. Analyzed by a two-way ANOVA with Tukey's multiple comparison test. Data shown as mean \pm SEM, Control+Vehicle (Ctrl+Veh), $n = 10$; Ctrl+PLX, $n = 10$; SE+Veh, $n = 10$; SE+PLX, $n = 7$.

Figure 4. Status epilepticus (SE) or treatment with PLX3397 (PLX) does not alter locomotion during open field (OF) test.

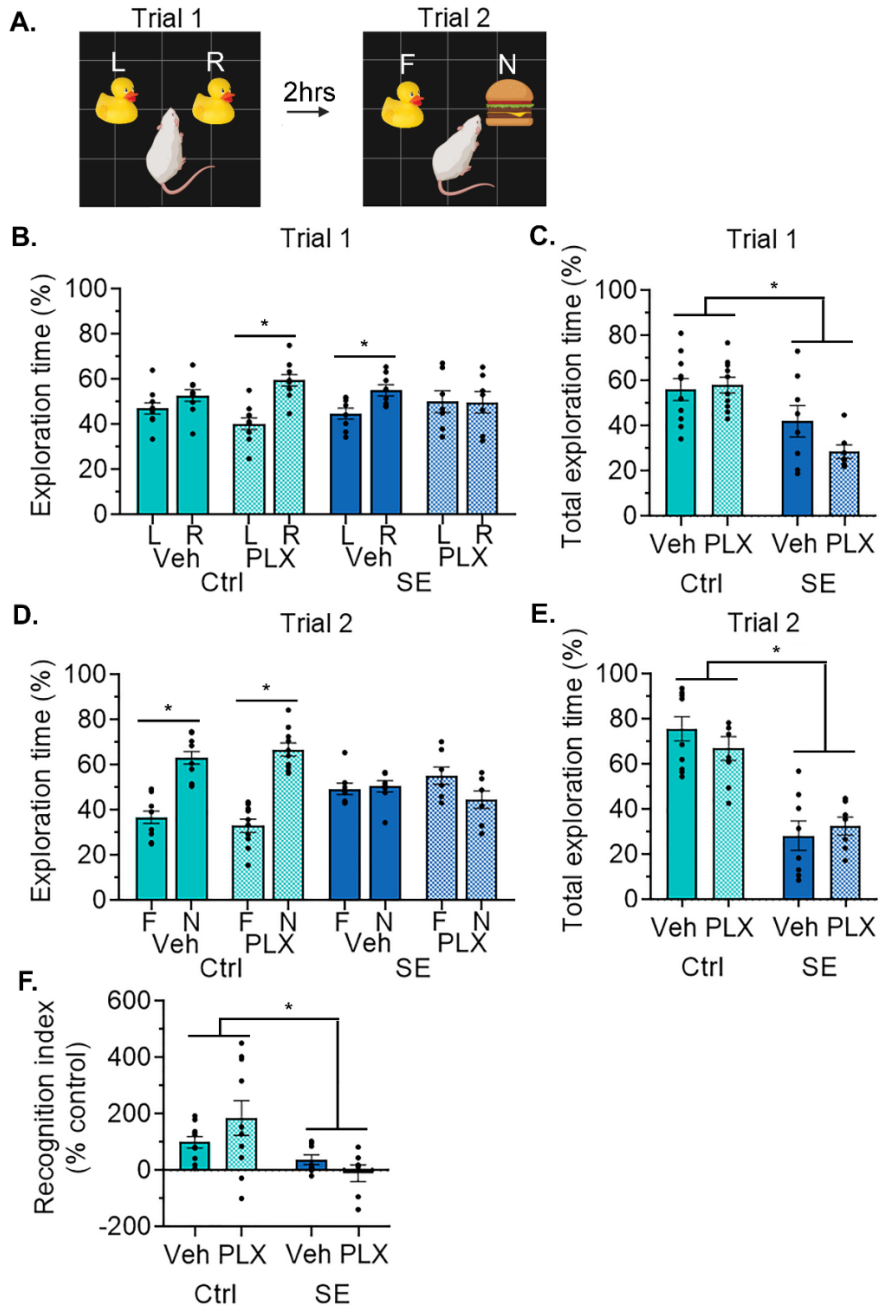
that were analyzed were the time spent motionless (Figure 4C) and percentage of time spent in the inner zone (Figure 4D). We first analyzed the average speed travelled and found that there was not a main effect of condition [$F(1, 33) = 1.054, p = .3121$], indicating that SE did not alter speed (Figure 3A). There was also no main effect of treatment [$F(1, 33) = 0.3384, p = .5647$], meaning that inhibition of CSF1R signaling did not affect speed. We found no significant interaction between the condition and treatment on the average speed the rats travelled while exploring the apparatus [$F(1, 33) = 0.0003, p = .9865$]. When we analyzed total distance the rats travelled, we found it was not altered by condition [$F(1, 33) = 3.964, p = .0548$]; the induction of SE did not alter distance travelled (Figure 3B). We also found that total distance travelled was not altered by treatment [$F(1, 33) = 0.6010, p = .4437$]. There was also no significant interaction between groups [$F(1, 33) = 0.7513, p = .3923$]. Together, these data indicate that locomotion was not impaired by either the induction of SE or treatment with PLX3397.

Furthermore, we analyzed behaviors that have been observed to indicate anxiety-like response. Rats that spend more time motionless rather than exploring the apparatus can indicate a greater anxiety response (Bangasser, 2015; Ennaceur et al., 2006; Feyissa et al., 2017). We analyzed time spent motionless and did not find any main effect of condition [$F(1, 33) = 2.339, p = .1357$], indicating that the induction of SE did not alter the time the rat spent motionless (Figure 4C). We also did not find a significant main effect of treatment with PLX3397 on their time spent motionless [$F(1, 33) = 0.0237, p = .8786$]. There was also no significant interaction between condition and treatment [$F(1, 33) = 0.0549, p = .8163$]. We also measured the time the rats spent in the inner zone versus the outer zone of the apparatus. A highly anxious rat would be expected to spend significantly less time exploring the unprotected center and instead spend more time against the walls in the outer zone compared to a normal rat (Bailey & Crawley, 2009; Bangasser, 2015; Ennaceur et al., 2006). We did not find a main effect of condition on time spent in the inner zone [$F(1, 33) = 3.964, p = .0548$], indicating that the induction of SE did not alter zone preference (Figure 4D). We also did not observe a significant main effect of condition [$F(1, 33) = 0.6010, p = .4437$], meaning inhibition of CSF1R signaling did not alter the time they spent in either area. We did not find an interaction between condition and treatment in the percent of time spent in the inner zone versus the outer zone [$F(1, 33) = 0.7513, p = .3923$]. Taken together, these data indicate the induction of SE and treatment with PLX3397 did not affect anxiety-like behaviors. These data

from OF indicate that the changes from other behavioral tests are not due to locomotion impairments or anxiety-like behaviors.

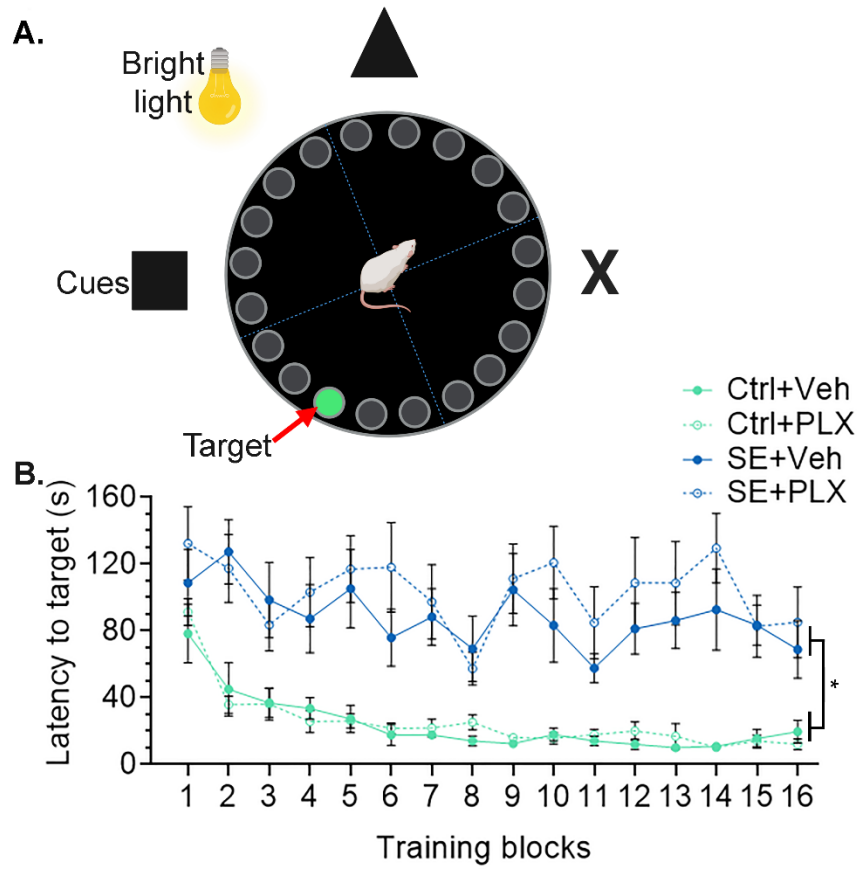
Inhibition of CSF1R Signaling does not Recover the SE-Induced Recognition Memory Deficits

Previous studies following induction of SE have shown recognition and spatial memory deficits (Brewster et al., 2013; Schartz et al., 2018, 2019). To determine if inhibition of microgliosis through CSF1R signaling could recover the SE-induced memory deficits, we used NOR (Figure 5) and BM (Figure 6-9) to test recognition and spatial memory, respectively. Following habituation to the apparatus, NOR testing began at 14 days post-SE. Rats were placed in the same apparatus for familiarization in trial 1 of NOR with two rubber ducks then removed and placed back into the apparatus for trial 2 with one of the rubber ducks replaced with a novel rubber hamburger (Figure 5A). During familiarization, the time the rats spent with each object was recorded and it was anticipated that they would spend an equal time exploring both objects (Antunes & Biala, 2012). As expected, the Ctrl+Veh group spent an equal amount of time with both objects [$t(18) = 1.599, p = .1273$] (Figure 5B). We also found, unexpectedly, a side preference in the SE+Veh [$t(14) = 2.944, p = .0107$], where the SE+Veh group spent more time with the left object. When treated with an inhibitor of CSF1R pathway, the Ctrl group also spent more time with the left object than the right object [$t(16) = 5.155, p < .0001$], while the SE+PLX3397 spent an equal time with both objects [$t(12) = .0228, p = .9822$]. Due to the side preference, objects for trial 2 were counterbalanced to negate for any preference (Hammond et al., 2004). In order to determine if each group spent a similar amount of time with the objects, we measured the percent of total time spent exploring the objects. We found a main effect of condition [$F(1, 31) = 19.94, p < .0001$], indicating the Ctrl rats spent more time with the objects overall compared to the SE animals (Figure 5C). We did not find a main effect of treatment with PLX3397 [$F(1, 31) = 1.369, p = .2510$], meaning that inhibition of CSF1R signaling did not affect time spent with the objects. As expected, we did not find an interaction between condition and treatment [$F(1, 31) = 2.522, p = .1224$]. This means that the Ctrl rats spent overall more time exploring the objects than the SE rats.



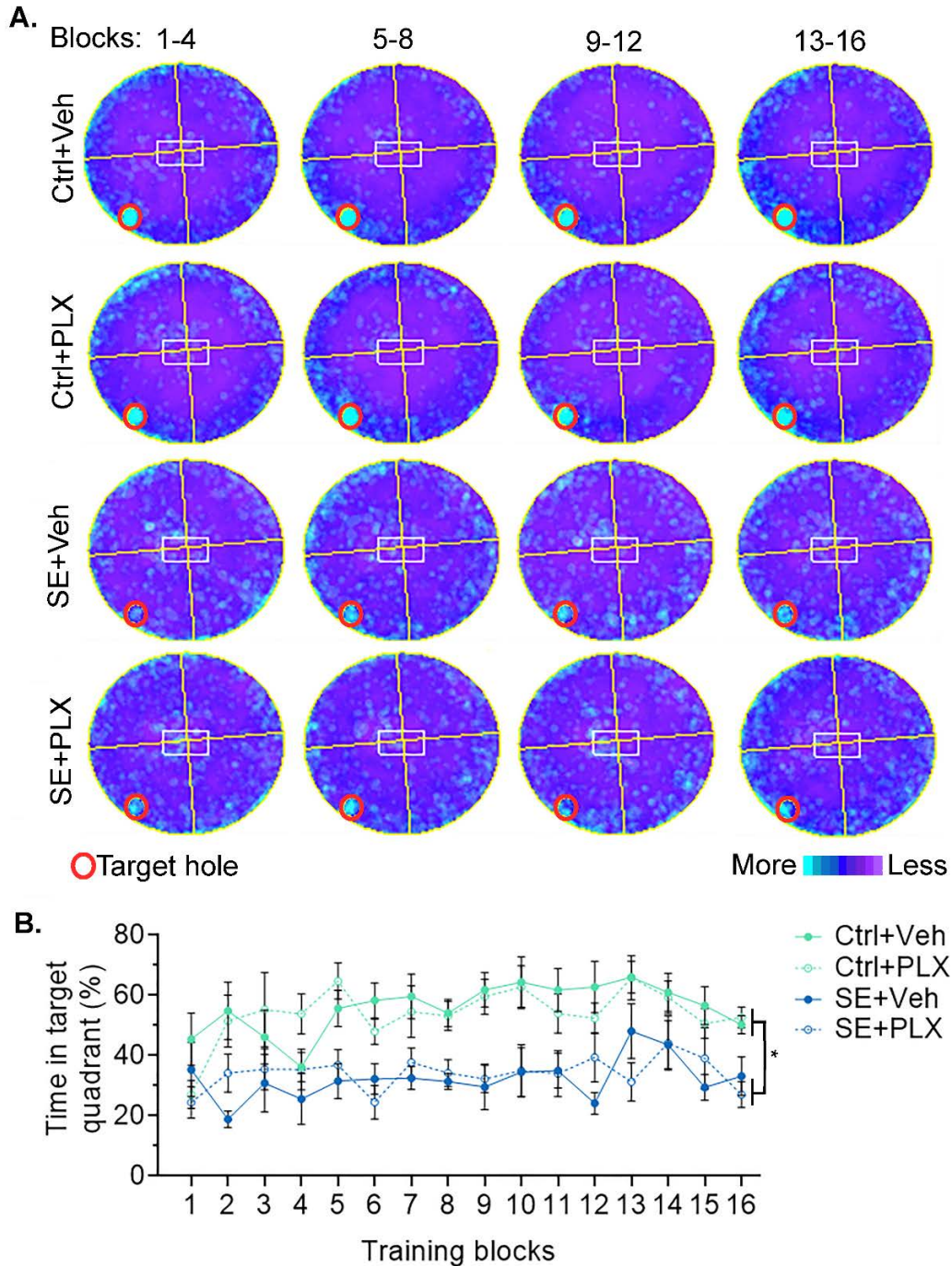
Note. A, Experimental diagram for novel object recognition (NOR) test. B, Rats were familiarized to two identical objects during trial 1, percentage of time spent exploring each object (right, R; left, L) is shown. C, Total time spent exploring each object in trial 1. D, Percentage of time spent exploring the familiar object (F) and the novel object (N) in trial 2 is shown. E, Total time spent exploring each object during trial 2 was recorded. F, A recognition index was calculated based on the familiar object from trial 1 and trial 2. * $p < .05$ by student's t-test for the comparison between (B) L/R and (D) F/N and (C, E, and F) two-way ANOVA with Tukey's multiple comparison test. Data shown as mean \pm SEM, Control+Vehicle (Ctrl+Veh), $n = 10$; Ctrl+PLX, $n = 9$; SE+Veh, $n = 8$; SE+PLX, $n = 7$.

Figure 5. Status epilepticus (SE) results in a deficit in recognition memory which is not recovered by PLX3397 (PLX) treatment.



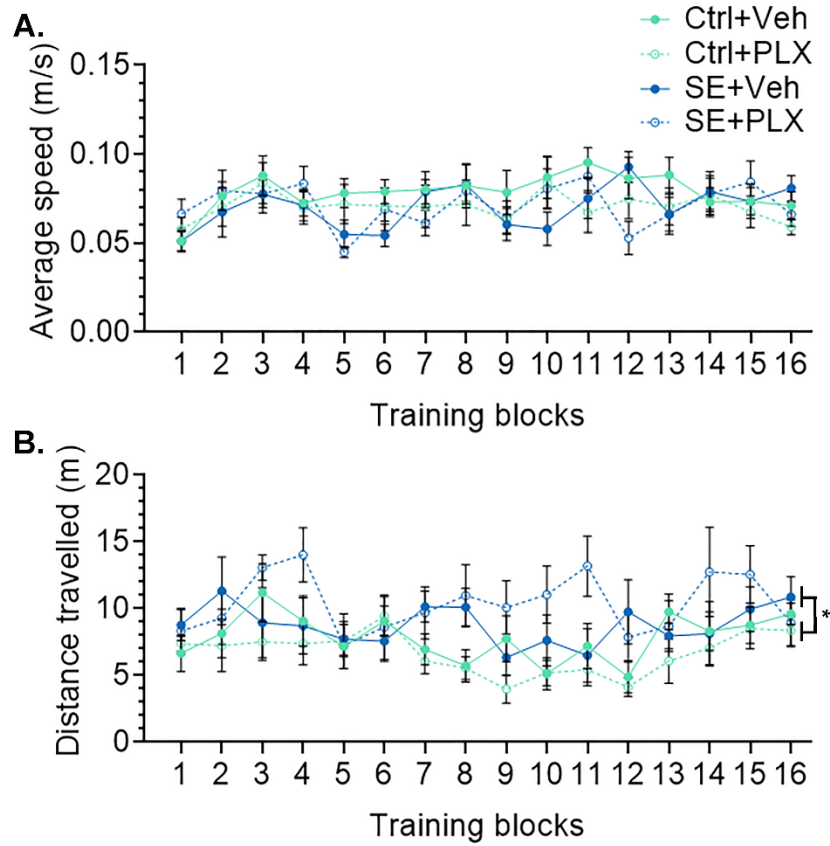
Note. A, Experimental diagram for BM test. B, Latency to first reach target hole. * $p < .05$ by three-way ANOVA with Tukey's multiple comparison. Data shown as mean \pm SEM, Control+Vehicle (Ctrl+Veh), $n = 10$; Ctrl+PLX, $n = 10$; SE+Veh, $n = 10$; SE+PLX, $n = 7$.

Figure 6. Status epilepticus (SE) triggers a decline in hippocampal-dependent spatial learning in Barnes maze (BM) that is not recovered by PLX3397 (PLX).



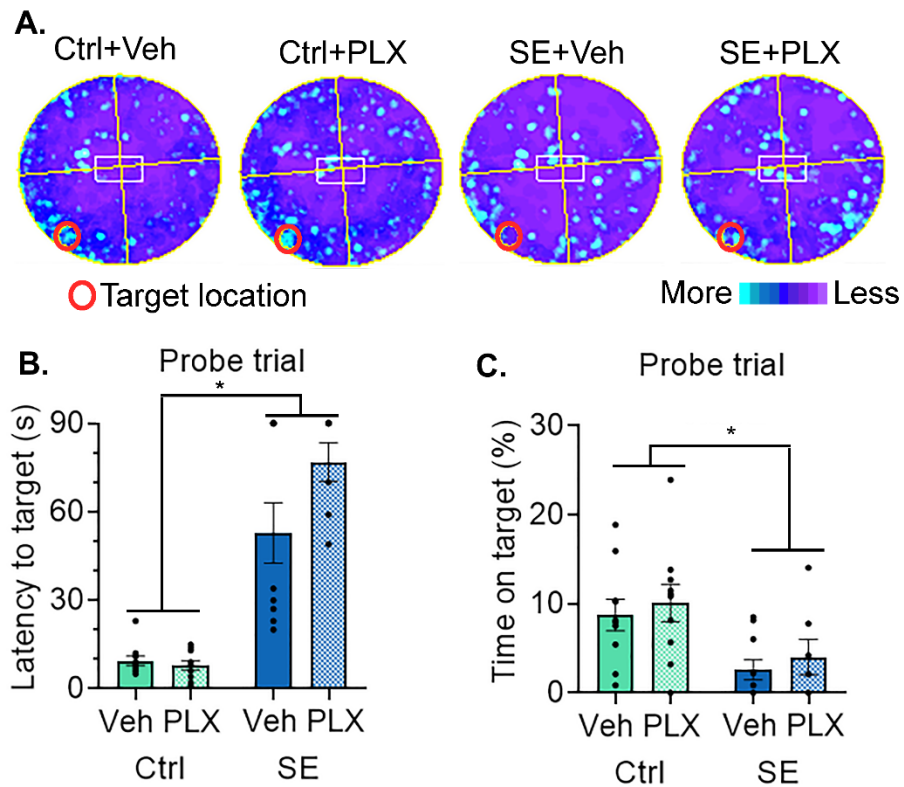
Note. A, Heat maps are shown as average time spent in each location averaged over each training day (4 blocks) with light blue indicating more time spent in a location and purple indicating less. Red circle indicates target hole location on platform. B, Percent of time spent in the quadrant with the target hole. * $p < .05$ by three-way ANOVA with Tukey's multiple comparison. Data shown as mean \pm SEM, Control+Vehicle (Ctrl+Veh), $n = 10$; Ctrl+PLX, $n = 10$; SE+Veh, $n = 10$; SE+PLX, $n = 7$.

Figure 7. Status epilepticus (SE) triggers a decline in time spent in target quadrant in Barnes maze (BM) that is not recovered by PLX3397 (PLX).



Note. A, Average speed travelled by each group recorded for 4 blocks each day for the 4 training. B, Total distanced travelled by each group recorded for 4 blocks each day for the 4 training. * $p < .05$ by three-way ANOVA with Tukey's multiple comparison. Data shown as mean \pm SEM, Control+Vehicle (Ctrl+Veh), $n = 10$; Ctrl+PLX, $n = 10$; SE+Veh, $n = 10$; SE+PLX, $n = 7$.

Figure 8. Status epilepticus (SE) does not alter locomotion during Barnes maze (BM) and this is not affected by PLX3397 (PLX) treatment.



Note. A, Heat maps are shown as the average time spent in each location during the probe trial test with light blue indicating more time spent in a location and purple indicating less. Red circle indicates target location on platform. B, Latency to first reach target location was recorded for the probe trial. C, Percentage of time spent on the target covered hole. * $p < .05$ by two-way ANOVA with Tukey's multiple comparison. Data shown as mean \pm SEM, Control+Vehicle (Ctrl+Veh), $n = 10$; Ctrl+PLX, $n = 10$; SE+Veh, $n = 10$; SE+PLX, $n = 7$.

Figure 9. Status epilepticus (SE) triggers a decline in hippocampal-dependent spatial memory in Barnes maze (BM) that is not recovered by PLX3397 (PLX) treatment.

In order to test the rats' recognition memory, trial 2 occurred two hours following the familiarization trial (Figure 5D-E). When rats encounter a novel object they generally spend more time exploring that object (Antunes & Biala, 2012; Pisula, 2009). Therefore, we expected the Ctrl rats would spend more time with the novel object, while the SE rats will show a deficit. As expected, the Ctrl+Veh group spent significantly more time with the novel object compared to the familiar object [$t(18) = 6.750, p < .0001$], indicating that they remembered that they had previously explored the familiar object (Figure 5D). The SE+Veh group did not spend more time with either object [$t(14) = .3224, p = .7519$] signifying that the group did not remember previously spending time with the familiar object. When treated with PLX3397, the Ctrl group spent more time with the novel object [$t(18) = 8.180, p < .0001$], indicating CSF1R inhibition did not have a negative impact on recognition memory. However, when the SE group was treated with PLX3397, they displayed a similar behavior as the SE+Veh group and spent an equal time with both objects [$t(12) = 1.934, p = .0770$]. Together, these data indicated that the inhibition of CSF1R signaling with PLX3397 did not alter or recover recognition memory. We also analyzed the amount of time in this trial that the rats spent with both objects and found similar results to trial 1. There was a main effect of condition [$F(1, 31) = 54.63, p < .0001$], where the Ctrl groups spent significantly more time with the objects than the SE groups (Figure 5E). There was no significant effect of treatment [$F(1, 31) = 0.1554, p = .6961$] or an interaction between condition and treatment [$F(1, 33) = 1.3830, p = .2490$]. Together these data show that the Ctrl rats spent more time with the novel object and explored both object for longer time than the SE rats.

To further understand the differences in recognition memory, we analyzed the ability of the animals to recognize the familiar object from trial 1 and the same familiar object in trial 2, the recognition index. The recognition index considered the placement of the familiar object in trial 2 and compared it with the same place of the object in trial 1. This was done to negate the side preferences observed in trial 1. As expected, we found a significant main effect of condition [$F(1, 30) = 15.32, p = .0005$], indicating that the Ctrl groups recognized the familiar object while the SE groups did not (Figure 5F). There was no significant effect of treatment [$F(1, 30) = 0.8812, p = .3554$], meaning that CSF1R signaling inhibition did not alter the ability of the rats to recognize the familiar object. There was also no significant interaction between condition and treatment [$F(1, 30) = 5.046, p = .0322$]. These data indicate that the Ctrl groups recognized the familiar object from trial 1 in trial 2 while the SE groups did not, and this was not affected by inhibiting CSF1R.

Taken together, these data showed that the inhibition of CSF1R signaling with PLX3397 treatment did not recover the recognition memory deficit.

Inhibition of CSF1R Signaling does not Recover the SE-Induced Spatial Memory Deficits

Previous studies have shown that two weeks following the induction of SE, deficits in spatial learning and memory are observed (Brewster et al., 2013; Lugo et al., 2012; Nolan et al., 2004; Schartz et al., 2018, 2019). To determine if the inhibition of CSF1R signaling would attenuate the SE-induced spatial learning and memory deficits observed following SE, we used BM. In bright light condition, rats were trained to find the escape box target hole over four training blocks per day for four days using spatial cues on the wall around the maze (Figure 6A). Bright light condition was used as a motivator, as rats prefer the dark and are more active in the night, for the rats to find the escape box (Gawel et al., 2019; Pitts, 2018). The latency to first reach the target hole for each group was recorded and compared for each block (Figure 6B). All rats regardless of group took roughly the same amount of time to find the hole on the first block ($p > .9999$). Using a three-way ANOVA [blocks X condition (Ctrl vs SE) X treatment (Veh vs PLX)], we found a significant main effect of training blocks [$F(15, 528) = 4.485, p < .0001$], with the later training blocks resulting in altered time to reach the hole. We also found a significant main effect of condition [$F(1, 528) = 410.4, p < .0001$], meaning that the Ctrl groups took less time to find the hole compared to the SE groups. There was also a main effect of treatment [$F(1, 528) = 5.408, p = .0204$], indicating that inhibition of CSF1R signaling altered the performance compared to the Veh treated groups. We did not find a significant interaction between training blocks and condition [$F(15, 528) = 1.609, p = .0671$], showing that the performance of the SE groups did not alter across training blocks. There was also no significant interaction between training blocks and treatment [$F(15, 528) = 0.4932, p = .9444$], where inhibiting CSF1R signaling did not alter learning across blocks. We also did not find a significant interaction between condition and treatment [$F(1, 528) = 3.672, p = .0559$], indicating that SE rats treated with PLX3397 did not improve performance over the SE+Veh group. We found no three-way interaction between training blocks, condition, and treatment [$F(15, 528) = 0.4095, p = 0.9765$]. Taken together, this means that the induction of SE produced a deficit in spatial learning compared to the Ctrl groups. This deficit was not recovered by the inhibition of CSF1R signaling the resulting suppression of microgliosis.

We also analyzed the time that the animals spend near the target hole with a spatial pattern of time spent in a location via a heat map (Figure 7A) and time spent in target hole quadrant (Figure 7B). The heat maps were averaged over each training day (four training blocks) for each group. The heat maps indicate more time spent in location (light blue) to less time spent (purple) and the location of the target hole escape box (red circle) (Figure 6A). We observed that the Ctrl groups spent more time over and around the hole compared to the SE groups. We analyzed the percent of time the rats spend in the target hole quadrant and found a significant main effect of training blocks [$F(1, 576) = 2.303, p = .0035$], indicating that the groups altered their time spent in the quadrant over the training blocks (Figure 7B). We also found a main effect of condition [$F(1, 576) = 168.2, p < .0001$], indicating that the Ctrl groups spend more time in the target quadrant compared to SE groups. We did not find a main effect of treatment [$F(1, 528) = 0.0004, p = .9846$], indicating that time spent in the quadrant was not altered by CSF1R signaling inhibition. We found no interaction between training blocks and condition [$F(15, 576) = 0.8028, p = .6751$], meaning time spent in the quadrant did not alter across training blocks due to the induction of SE. Similar findings were found between training blocks and treatment [$F(15, 576) = 1.063, p = .3887$]. We also did not find an interaction between condition and treatment [$F(1, 576) = 0.2791, p = .2791$], indicating that CSF1R inhibition did not alter the SE group's time spent in the target quadrant. We did not find a significant three-way interaction between training blocks, condition, and treatment [$F(15, 576) = 1.155, p = .8435$]. These data indicate that the SE rats spent less time in the target quadrant location compared to the Ctrl rats. This was not altered by inhibition of CSF1R signaling.

To determine if any of these changes were from potential locomotion variations on the BM platform, we used a three-way ANOVA [blocks X condition (Ctrl vs SE) X treatment (Veh vs PLX)] and analyzed the average speed (Figure 8A) and total distance travelled (Figure 8B). We found a main effect of average speed over the training blocks [$F(15, 528) = 1.860, p = .0248$], the average speed changed over training blocks as the animals were repeatedly placed on the platform over the 16 blocks (Figure 8A). We did not find a significant main effect of condition [$F(1, 528) = 2.066, p = .1512$], indicating that SE induction did not alter speed. There was also no significant effect of treatment [$F(1, 528) = 2.508, p = .1138$]. We did not find a significant interaction between training blocks and condition [$F(15, 528) = 0.9409, p = .5181$] or training blocks and treatment [$F(15, 528) = 0.9813, p = .4735$]. There was no significant interaction between condition and treatment [$F(1, 528) = 3.487, p = .0624$], indicating that the SE group was not altered by inhibition

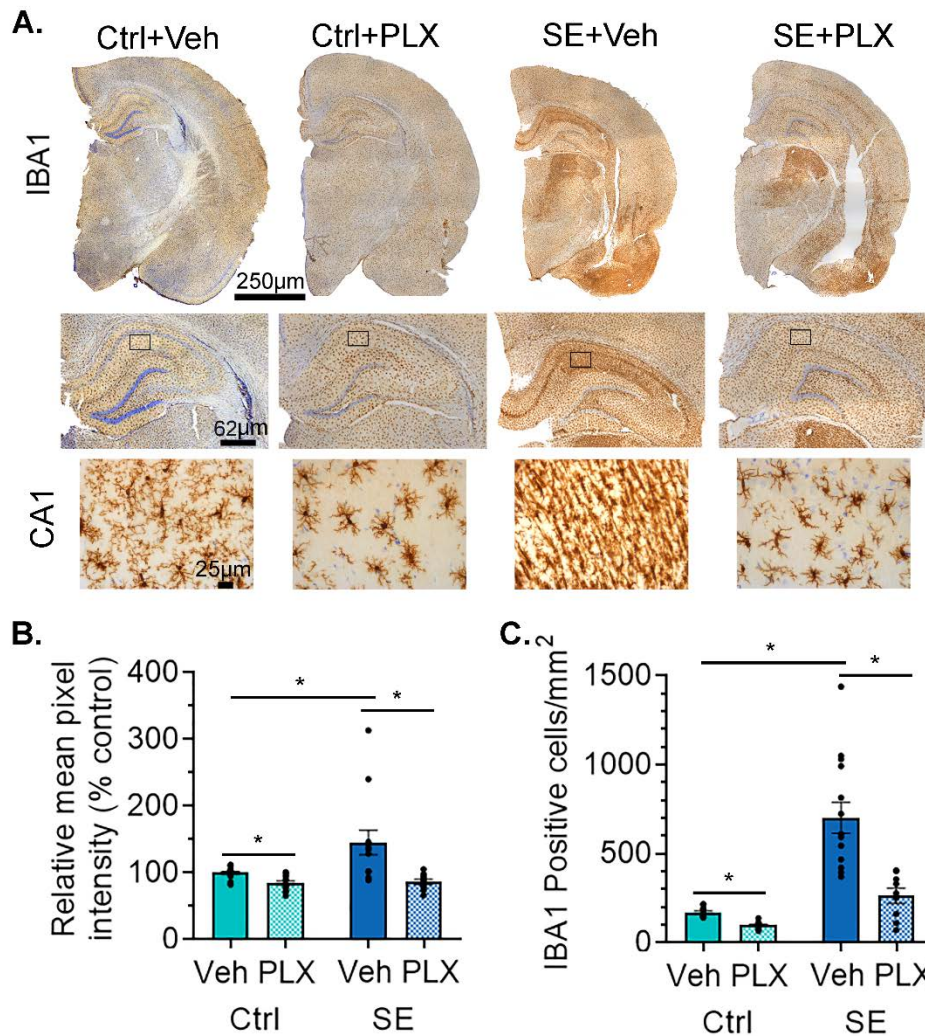
of the CSF1R signaling. We also did not find a significant three-way interaction between training blocks, condition, and treatments [$F(15, 528) = 0.6899, p = .7956$]. These data indicate that rats travelled faster towards the end of the training blocks compared to the beginning, but SE induction and CSF1R signaling inhibition did not alter the average speed. We also analyzed the distance travelled and did not find a main effect of training blocks [$F(15, 528) = 1.642, p = .0590$], indicating that distance travelled did not vary over the training blocks (Figure 8B). However, we found a main effect of distance travelled on condition [$F(1, 528) = 30.97, p < .0001$], showing that the SE rats travelled more than the Ctrl rats, as the Ctrl rats found the hole faster than the SE animals. However, we did not find a main effect of treatment [$F(1, 528) = 0.3047, p = .5812$], indicating that inhibition of CSF1R signaling did not affect the distance travelled. We found no significant interaction between training blocks and condition [$F(15, 528) = 0.6057, p = .8712$] or training blocks and treatment [$F(15, 528) = 0.9817, p = .4731$]. This implies that neither SE induction nor inhibition of CSF1R signaling affected the change in distance travelled over training blocks. We did find a significant main effect of condition and treatment [$F(1, 528) = 10.94, p = .0010$], indicating that SE induction with inhibition of CSF1R signaling did alter distance travelled. There was no significant three-way interaction between training blocks, condition, and treatments [$F(15, 528) = 1.155, p = .3040$]. These data indicate that SE groups travelled further compared to the Ctrl groups, as it took the SE rats longer to find hole. Taken together, these data indicate that locomotion was not impaired by either condition or treatment. Furthermore, we observed that the SE rats travelled more distance while searching for the hole and in total spent less time in the target quadrant when searching for the escape hole. This evidence suggests the possibility that SE rats may not be relying in spatial learning of the cues to navigate to find the target hole and instead searching each time.

Twenty-four hours after the last day of training, the probe trial was performed. The probe trial was used to test the rats' memory of the target hole location without the escape box present (Gawel et al., 2019). We analyzed their memory of the target hole by the time spent in each location (Figure 9A), latency to the target (Figure 9B), and percent of time spent on the target (Figure 9C). The average heat maps for each group were shown for the probe trial with lighter blue visible over the target hole location in the Ctrl groups (Figure 9A). We found a main effect of condition on the latency to find the target during the probe trial [$F(1, 33) = 80.47, p < .0001$], implying that SE groups took more time to find the target location or did not find the target (Figure 9B). However,

there was no effect of treatment [$F(1, 33) = 3.186, p = .0835$] on the latency to find the target hole. This indicates that the inhibition of CSF1R signaling did not alter time to find the target location. There was an interaction between condition and treatment [$F(1, 33) = 4.229, p = .0477$], showing that the SE group treated with the PLX3397 took longer to find the target location. Analyzing the time spent over the target locations, we found that there was a main effect of condition on time spent over the target location [$F(1, 33) = 11.74, p = .0017$], where SE groups spent less time on the target location (Figure 9C). There was no main effect of treatment [$F(1, 33) = 3.186, p = 0.0835$], indicating that inhibition of CSF1R signaling alter the time the rats spent over the target location. We also did not find an interaction between condition and treatment [$F(1, 33) = 0.0005, p = 0.9815$]. Together, these data demonstrate that the Ctrl groups were able to remember the target location compared to the SE groups. This was not affected by inhibiting the CSF1R signaling pathway with PLX3397.

Inhibition of CSF1R Signaling Attenuated the SE-Induced Microgliosis

The SE-induced microgliosis is a hallmark of epileptogenesis and has been thoroughly characterized in experimental models of epilepsy (Abiega et al., 2016; Brewster et al., 2013; Schartz et al., 2016; Shapiro et al., 2008; Sierra et al., 2010; Wyatt-Johnson et al., 2017). We determined the extent to which the inhibition of CSF1R signaling with PLX3397 reduced microgliosis through histological analysis. We investigated IBA1 immunoreactivity in the CA1 region of the hippocampus (Figure 10A) through both densitometry of the immunoreactive signal (Figure 10B) and cell counts (Figure 10C). First, we examined the ability of PLX3397 to reduce the density and number of microglia. We found using a student's t-test that inhibition of CSF1R signaling with PLX3397 reduced both the density of microgliosis and the number of microglia by 60% in Ctrl rats [$t(24) = 3.868, p = .0007$; $t(24) = 8.148, p < .0001$]. We used the reduction from the Ctrl to create a cutoff for the SE+PLX3397 group based on the average number in the SE+Veh group. We analyzed the densitometry of IBA1 in the CA1 region of the hippocampus with a two-way ANOVA. We found a main effect of both condition [$F(1, 45) = 4.526, p = .0389$], indicating that SE groups had higher levels of microgliosis (Figure 10B). We also found a main effect of treatment [$F(1, 45) = 11.21, p = .0017$], implying that groups treated with inhibition of CSF1R signaling had decreased levels of microgliosis. However, we found no interaction between condition and treatment [$F(1, 45) = 3.898, p = .0545$]. The Ctrl+Veh group had a decreased density



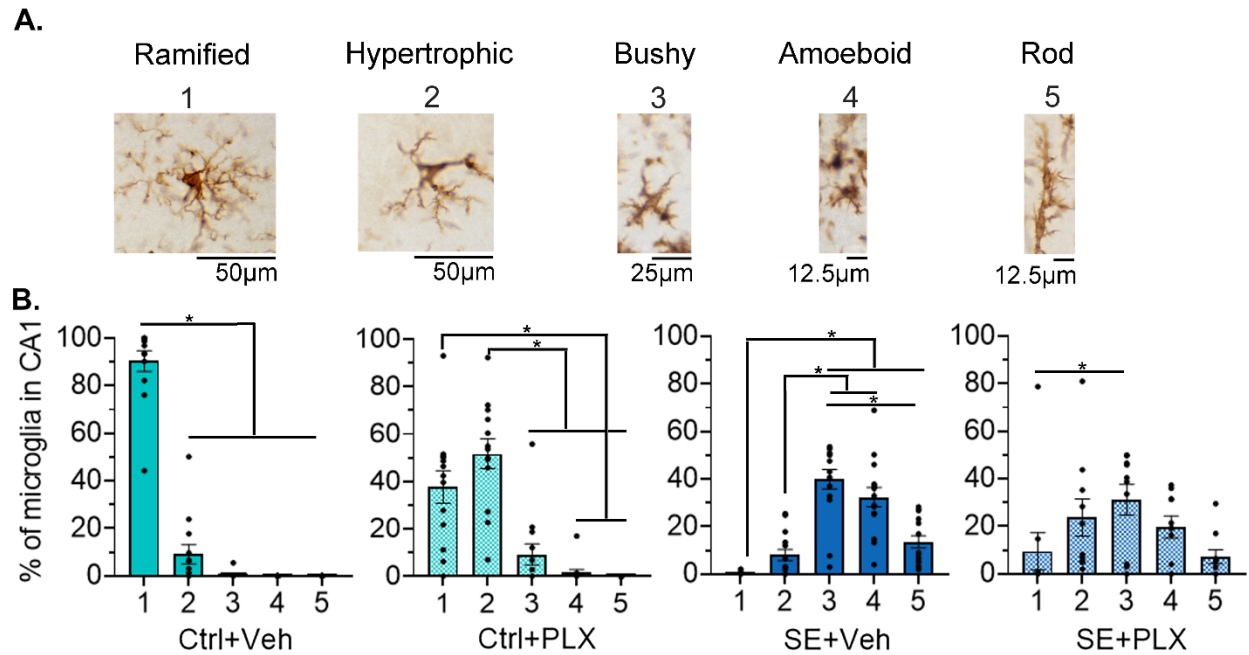
Note. A, Representative IBA1 (brown) and Nissl-stained cellular nuclei (blue) immunostain with 4x images shown on top, 20x images are shown of the hippocampus below, and a corresponding 40x image of the CA1 region of the hippocampus at the bottom. B, Densitometry analysis of IBA1 immunostain in the CA1 region of the hippocampus. C, Cell counts for the number of IBA1 positive cells per mm² in the CA1 region of the hippocampus. **p* < .05 by two-way ANOVA with Tukey's multiple comparison. Data shown as mean±SEM, Control+Vehicle (Ctrl+Veh), *n* = 13; Ctrl+PLX, *n* = 13; SE+Veh, *n* = 14; SE+PLX, *n* = 9.

Figure 10. Status epilepticus (SE) induced hippocampal microgliosis is attenuated by PLX3397 (PLX) treatment.

of microglia compared to SE+Veh group ($p = .0175$). There was no difference between the Ctrl+PLX3397 group and the SE+PLX3397 group ($p = .9996$). We also found that PLX3397 treatment reduced the density of microglia in the SE group compared to the SE+Veh group ($p = .0041$).

In order to fully determine the extent to which we reduced microgliosis, we performed cell counts and found a main effect of condition [$F(1, 45) = 43.22, p < .0001$], where SE groups had higher number of IBA1 positive microglia (Figure 10C). We also found a main effect of treatment [$F(1, 45) = 23.30, p < .0001$], showing that inhibition of CSF1R signaling reduced the number of IBA1 positive microglia. Unlike with densitometry, with a more precise measure of IBA1 cell counts, we found a significant interaction between condition and treatment [$F(1, 45) = 11.96, p = .0012$], indicating that inhibition of CSF1R signaling was able to decrease the microgliosis in both the Ctrl and SE groups. The Ctrl+Veh group had a reduced number of microglia compared to SE+Veh group ($p < .0001$). There was no difference between the Ctrl+PLX3397 group and the SE+PLX3397 group ($p = .1740$). We also found that inhibition of CSF1R signaling reduced the density of microglia in the SE group ($p < .0001$). These data indicate that in both the Ctrl and SE groups in inhibiting CSF1R signaling with PLX3397 resulted in a 60% microglial reduction in the hippocampus.

It is thought that each morphological phenotype of microglia may have a specific biochemical property (Cengiz et al., 2019; Neher & Cunningham, 2019). Although their exact properties are not definitively known, we sought to determine if PLX3397 could be altering the morphology of the remaining microglia thereby suggesting a potential change in function. In order to understand the extent to which the inhibition of CSF1R signaling altered microglial morphological phenotypes, we investigated the percentage of total microglia in each morphological category for each group (Figure 11). We organized the IBA1-labeled microglia into five distinct categories: ramified, hypertrophic, bushy, amoeboid, and rod morphologies (Figure 11A). Due to the non-normally distributed data, the different microglial morphologies were analyzed with Kruskal-Wallis test with Dunn's multiple comparisons.



Note. A, Representative images of the IBA1-labeled (brown) microglia morphology. B, Morphological breakdown of each group, right to left, Control+Vehicle (Ctrl+Veh), Ctrl+PLX, SE+Veh, and SE+PLX, as 1-ramified, 2-hypertrophied, 3-bushy, 4-amoeboid, and 5-rod IBA1 positive cells. $*p < .05$ by Kruskal-Wallis test with Dunn's multiple comparison. Data shown as mean±SEM, Ctrl+Veh, $n = 13$; Ctrl+PLX, $n = 13$; SE+Veh, $n = 14$; SE+PLX, $n = 9$.

Figure 11. Status epilepticus (SE) induced hippocampal microglial morphology is altered by PLX3397 (PLX) treatment

In the Ctrl+Veh group there was a significant difference among the microglial morphologies [$H(5, 65) = 51.07, p < .0001$] (Figure 11B). The Ctrl+Veh group had more microglia with a ramified morphology compared to the other four morphologies (Table 5). The Ctrl+PLX3397 group was also significantly different among all the morphologies [$H(5, 65) = 45.41, p < .0001$]. The Ctrl+PLX3397 group had more ramified and hypertrophic microglial morphologies compared to the bushy, amoeboid, and rod (Table 5). The SE+Veh group was also significantly different across all the morphologies [$H(5, 65) = 53.34, p < .0001$]. With the SE+Veh group having more bushy and amoeboid microglial morphologies compared to ramified and hypertrophic (Table 5). The SE+PLX also had significantly different morphological phenotypes [$H(5, 50) = 13.88, p = .0077$]. The only significant difference found was an increase in microglia with bushy morphology compared to the ramified morphology (Table 5). The total number of microglia in each morphology can be viewed in Table 6. Taken together, the Ctrl+Veh group had increased microglia with ramified shapes while the inhibition of CSF1R signaling increased the number of hypertrophic microglia in the Ctrl+PLX group. The SE+Veh group had more microglia with bushy and amoeboid morphologies while CSF1R inhibition reduced these and had a more evenly distributed morphological phenotype across all five morphological categories. Together these findings suggest that the remaining microglia have distinct morphological phenotypes following inhibition of CSF1R signaling potentially resulting in different functions.

Inhibition of CSF1R Signaling Attenuated the SE-Induced Astrocytic Protein Levels

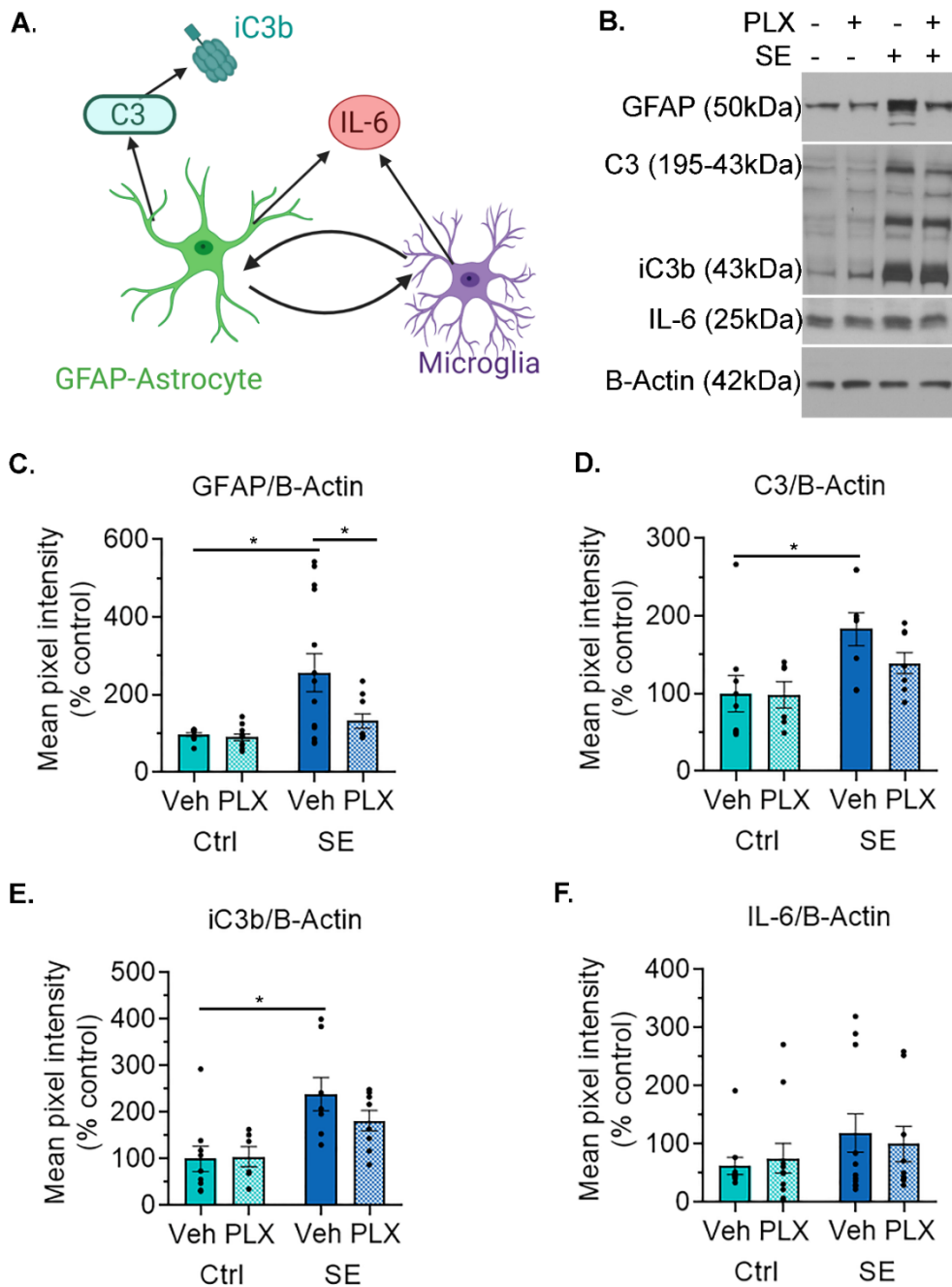
To further understand the effects of CSF1R-mediated suppression of microgliosis we analyzed molecules associated with the crosstalk between microglia and astrocytes, such as C3, iC3b, and IL-6. Astrocytes are labeled with antibodies against GFAP, which is a protein specific to astrocytes. C3/iC3b, is a complement protein that can be produced by astrocytes in response to microglial signals (Lian et al., 2016; Schartz et al., 2018; Wyatt-Johnson & Brewster, 2019) (Figure 12A). Microglia and astrocytes both produce IL-6 with the largest production coming from astrocytes, which aids in microglial response (Batlle et al., 2015; Streit et al., 2000). The increase in astrocytic response, inflammation, and complement activation following the induction of SE has been widely observed (De Sarro et al., 2004; Minami et al., 1991; Schartz et al., 2018; Shapiro et al., 2008). In order to understand the effects of inhibition of microgliosis on astrocytes, C3 and iC3b, and inflammatory response of IL-6, we used western blotting to analyze protein expression

Table 5. Dunn's Multiple Comparison Test for Microglial Morphology for Each Group

Morphology	Ctrl+Veh	Ctrl+PLX	SE+Veh	SE+PLX
1 vs. 2	0.0098	>0.9999	0.4936	0.1035
1 vs. 3	<0.0001	0.1336	<0.0001	0.0128
1 vs. 4	<0.0001	0.0016	<0.0001	0.3705
1 vs. 5	<0.0001	0.0001	0.0096	>0.9999
2 vs. 3	0.4022	0.0034	0.0001	>0.9999
2 vs. 4	0.0906	<0.0001	0.0043	>0.9999
2 vs. 5	0.0906	<0.0001	>0.9999	0.7443
3 vs. 4	>0.9999	>0.9999	>0.9999	>0.9999
3 vs. 5	>0.9999	0.5524	0.0233	0.1467
4 vs. 5	>0.9999	>0.9999	0.2891	>0.9999

Table 6. Microglial Morphological Breakdown of Each Group

	Ctrl+Veh	Ctrl+PLX	SE+Veh	SE+PLX
Total Number	171	99	702	264
Ramified	155	37	1	28
Hypertrophic	16	51	60	69
Bushy	1	9	299	91
Amoeboid	0	1	242	57
Rod	0	0	100	20



Note. A, Diagram of GFAP labeled astrocytes crosstalk with microglia to releasing C3 to be cleaved to iC3b and IL-6. B, Representative western blot of (top to bottom) GFAP, C3, iC3b, and IL-6 and corresponding β -actin. C-F, Mean pixel intensity of GFAP (C), C3 (D), iC3b (E), and IL-6 (F). * $p < .05$ by two-way ANOVA with Tukey's multiple comparison. Data shown as mean \pm SEM, Control+Vehicle (Ctrl+Veh), $n = 9-12$; Ctrl+PLX, $n = 7-13$; SE+Veh, $n = 8-14$; SE+PLX, $n = 8-9$.

Figure 12. Status epilepticus (SE) induced astrogliosis is attenuated with PLX3397 (PLX) treatment.

in the hippocampus (Figure 12). We analyzed the densitometry of the WB with a two-way ANOVA. As expected, there was a main effect of condition on protein levels of GFAP in the hippocampus [$F(1, 41) = 9.921, p = .0030$], indicating that there was an increase in protein level of GFAP in the SE groups compared to the Ctrl groups (Figure 12C). There was also a main effect of treatment [$F(1, 41) = 4.211, p = .0466$], showing that inhibition of CSF1R signaling altered the level of GFAP protein. We did not find a significant interaction between condition and treatment [$F(1, 41) = 3.360, p = .0741$]. The Ctrl+Veh group had significantly reduced levels of GFAP protein compared to SE+Veh group ($p = .0031$). The inhibition of CSF1R signaling did not alter protein levels when comparing the Ctrl+Veh and Ctrl+PLX3397 groups ($p = .9986$). Ctrl+PLX3397 had similar levels of GFAP protein levels compared to the SE+PLX3397 ($p = .8130$). The inhibition of CSF1R signaling also reduced the protein level of GFAP in the SE groups ($p = .0427$). These data show that GFAP was increased after SE-induction but inhibition of CSF1R signaling with PLX3397 reduced the SE-induced increased protein levels.

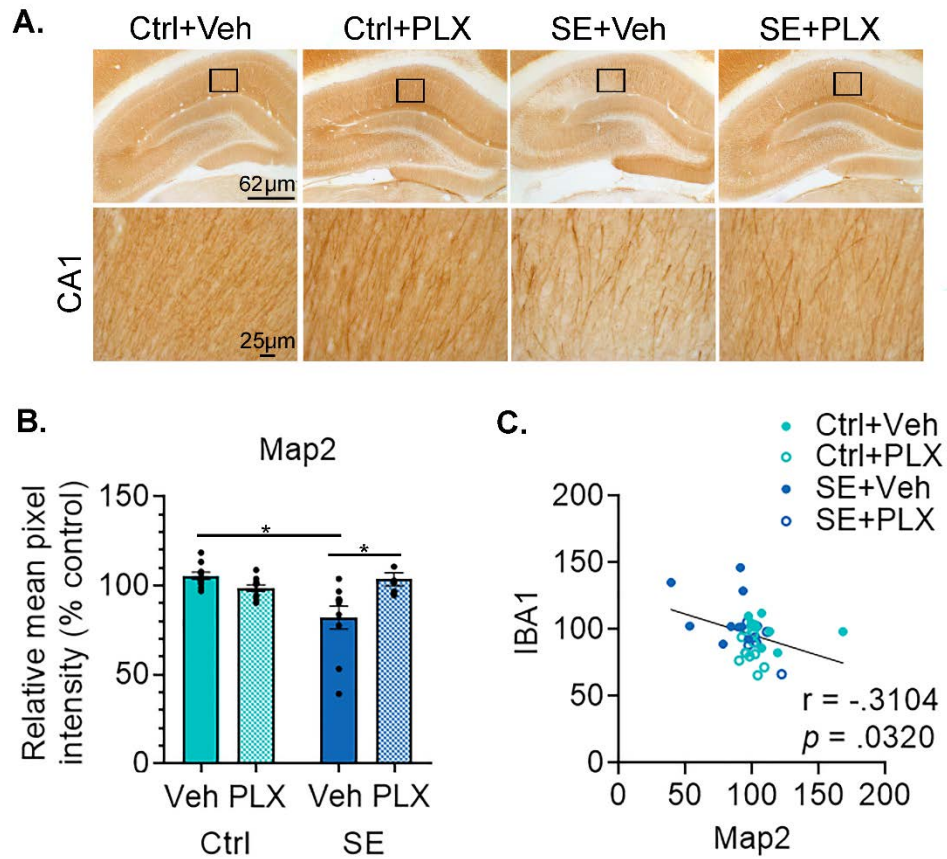
There was a main effect of condition on protein levels of C3 [$F(1, 27) = 9.333, p = .0050$], indicating that there was an increase in protein level of C3 in the SE groups (Figure 12D). There was not a main effect of treatment [$F(1, 27) = 0.1254, p = .2726$], demonstrating that inhibition of the CSF1R pathway did not alter the amount of C3 protein. We also did not find a significant interaction between condition and treatment [$F(1, 27) = 1.1083, p = .3072$]. The Ctrl+Veh group had less C3 protein level compared to the SE+Veh group ($p = .0240$). The treatment with PLX3397 did not alter protein levels in the Ctrl groups ($p > .9999$). There was no change between Ctrl+PLX3397 and SE+PLX3397 protein levels ($p = .5375$). The treatment with PLX3397 also did not reduce the protein level of C3 in the SE groups ($p = .4121$). This indicated that C3 was increased after SE-induction, but those increased levels were not reduced by inhibition of CSF1R signaling. We then analyzed the specific band of C3, iC3b, an “eat me” signal which acts to aid in microglial engulfment of the target cell for phagocytosis (Brown & Neher, 2012; Schafer et al., 2012). There was a main effect of condition on protein levels of iC3b in the hippocampus [$F(1, 27) = 14.44, p = .0008$], indicating that there was an increase in protein level of iC3b in the SE groups (Figure 12E). There was not a main effect of treatment [$F(1, 27) = 0.8435, p = .3665$]. We did not find a significant interaction between condition and treatment [$F(1, 27) = 1.180, p = .2870$]. The Ctrl+Veh group had less iC3b protein level compared to SE+Veh group ($p = .0057$). Inhibition of CSF1R signaling did not alter protein levels in the Ctrl groups ($p = .9994$). There was no change

between Ctrl+PLX3397 and SE+PLX3397 protein levels ($p = .2840$). Inhibition of CSF1R signaling also did not reduce the protein level of iC3b in the SE groups ($p = .4767$). These data imply that iC3b levels were increased following SE-induction but inhibition of CSF1R signaling with PLX3397 does not alter the protein levels of complement C3 and its cleavage product iC3b.

We analyzed the levels of the inflammatory cytokine IL-6, a cytokine that aids in interaction between microglia and astrocytes (Streit et al., 2000). We found there was no main effect of condition on the protein levels of IL-6 in the hippocampus [$F(1, 39) = 3.321$, $p = .0761$] (Figure 12F). There was also no main effect of treatment [$F(1, 39) = 0.0598$, $p = .8081$], indicating that inhibition of CSF1R signaling did not alter levels of IL-6 protein. We did not find a significant interaction between condition and treatment [$F(1, 27) = 0.8853$, $p = .3525$]. The Ctrl+Veh group had no change in protein level compared to SE+Veh group ($p = .1975$). The inhibition of CSF1R signaling did not alter protein levels in the Ctrl groups ($p = .8374$). There was no change between Ctrl+PLX3397 and SE+PLX3397 protein levels ($p = .9303$). Inhibition of CSF1R signaling also did not reduce the protein level of IL-6 in the SE groups ($p = .9599$). This indicated that IL-6 levels were not increased at 20 days post-SE and inhibition of CSF1R signaling did not alter those levels. Taken together, inhibition of CSF1R signaling with PLX3397 treatment reduced astrocytic response but did not alter C3 activation or IL-6.

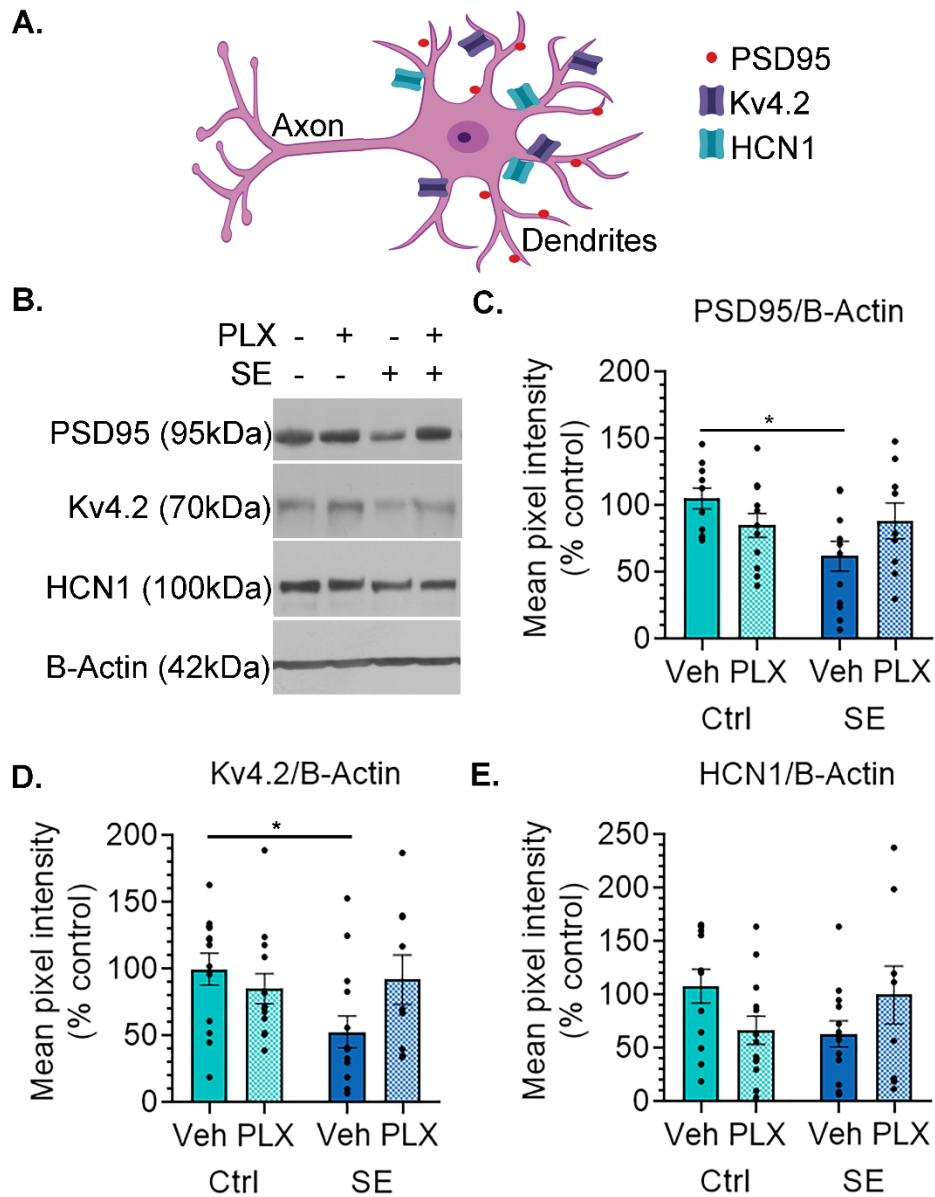
Inhibition of CSF1R Signaling Attenuated the SE-Induced Dendritic Microtubule Decrease

Microglia make direct contacts with synapses and can prune them under physiological and pathological conditions (Hong et al., 2016; Hong & Stevens, 2016; Tremblay, 2011). In both human and experimental epilepsy, microgliosis is found in regions of dendritic instability (Brewster et al., 2013; Dachet et al., 2015; Gross et al., 2016; Schartz et al., 2016; Shapiro et al., 2008; Wyatt et al., 2017). After epileptogenesis, it has been shown that levels of dendritic structural protein Map2 and PSD95 are decreased, alongside Kv4.2 and HCN1 and correlate with high density of microglial cells. Therefore, we determined if inhibiting microgliosis could attenuate the SE-induced hippocampal dendritic structural alterations. We used IHC to determine levels of Map2 (Figure 13) and WB to measure levels of dendritic ion channels, Kv4.2 and HCN1, as well as post synaptic density marker, PSD95 (Figure 14). We analyzed the densitometry of the IHC and WB with a two-way ANOVA. As expected, there was a main effect of condition on Map2 density in the CA1 region of the hippocampus [$F(1, 33) = 5.224$, $p = .0288$], indicating that SE decreased



Note. A, Representative Map2 (brown) immunostain with 20x images shown on top and the corresponding 40x image of the CA1 region of the hippocampus shown below. B, Densitometry analysis of Map2 in the CA1 region of the hippocampus. C, Correlational analysis between the densitometry of Map2 and IBA1 in the CA1 region of the hippocampus. * $p < .05$ by (B) two-way ANOVA with Tukey's multiple comparison and (C) linear regression. Data shown as mean \pm SEM, Control+Vehicle (Ctrl+Veh), $n = 10$; Ctrl+PLX, $n = 10$; SE+Veh, $n = 10$; SE+PLX, $n = 7$.

Figure 13. Status epilepticus (SE) triggers decline in hippocampal Map2 signal that is recovered by PLX3397 (PLX) treatment.



Note. A, Diagram of the location of PSD95 (red), Kv4.2 (purple), and HCN1 (blue) on a neuron. B, Representative western blot of PSD95, Kv4.2, and HCN1, and corresponding β -actin. C-E, Mean pixel intensity of PSD95 (C), Kv4.2 (D), and HCN1 (E). * $p < .05$ by two-way ANOVA with Tukey's multiple comparison. Data shown as mean \pm SEM, Control+Vehicle (Ctrl+Veh), $n = 11-13$; Ctrl+PLX, $n = 12-13$; SE+Veh, $n = 12-14$; SE+PLX, $n = 9$.

Figure 14. Status epilepticus (SE) triggers decline in dendritic markers in the CA1 region of the hippocampus that is not altered by PLX3397 (PLX) treatment

density of Map2 (Figure 13B). There was not a main effect of treatment [$F(1, 27) = 0.6311$, $p = .4326$]. We did find a significant interaction between condition and treatment [$F(1, 33) = 10.41$, $p = .0028$]. The Ctrl+Veh group had higher levels of Map2 density compared to SE+Veh group ($p = .0014$). The inhibition of CSF1R signaling did not alter Map2 density levels in the Ctrl groups ($p = .2873$). Ctrl+PLX3397 showed no change in density of Map2 compared to the SE+PLX3397 ($p = .9200$). The inhibition of CSF1R signaling increased the density of Map2 following SE-induction ($p = .0489$). Together, these show that Map2 density was decreased after SE-induction but inhibition of microgliosis through the CSF1R signaling attenuated this Map2 loss. Previously, we reported a significant correlation between spatial and temporal profile of IBA1-labeled microglia and Map2 (Schartz et al., 2016, 2018). Therefore, we measured the correlation in this study and found similar results. IBA1 density was negatively correlated with Map2 density [$R^2 = .1248$, $F(1, 35) = 4.989$, $p = .0320$] (Figure 13C), indicating that as IBA1 levels were increased, Map2 levels were decreased.

We measured PSD95, Kv4.2, and HCN1 which are typically located on the proximal ends of the CA1 pyramidal neurons (Figure 14A) (Birnbaum et al., 2004; Marcelin et al., 2012). There was no main effect of condition on protein levels of PSD95 in the hippocampus [$F(1, 40) = 3.709$, $p = .0612$], indicating that there was no change in levels of PSD95 in the Ctrl and SE groups (Figure 14C). There was also no main effect of treatment [$F(1, 40) = 0.0861$, $p = .7708$]. We found a significant interaction between condition and treatment [$F(1, 40) = 5.028$, $p = .0306$]. The Ctrl+Veh group had less PSD95 protein level compared to the SE+Veh group ($p = .0213$). Inhibition of CSF1R signaling did not alter protein levels in the Ctrl groups ($p = .4962$). There was no change between Ctrl+PLX3397 and SE+PLX3397 protein levels ($p = .9963$). The inhibition of CSF1R signaling also did not reduce the protein level of PSD95 in the SE groups ($p = .3142$). Together, these show that PSD95 was decreased after SE-induction, but this was not altered by inhibition of CSF1R signaling.

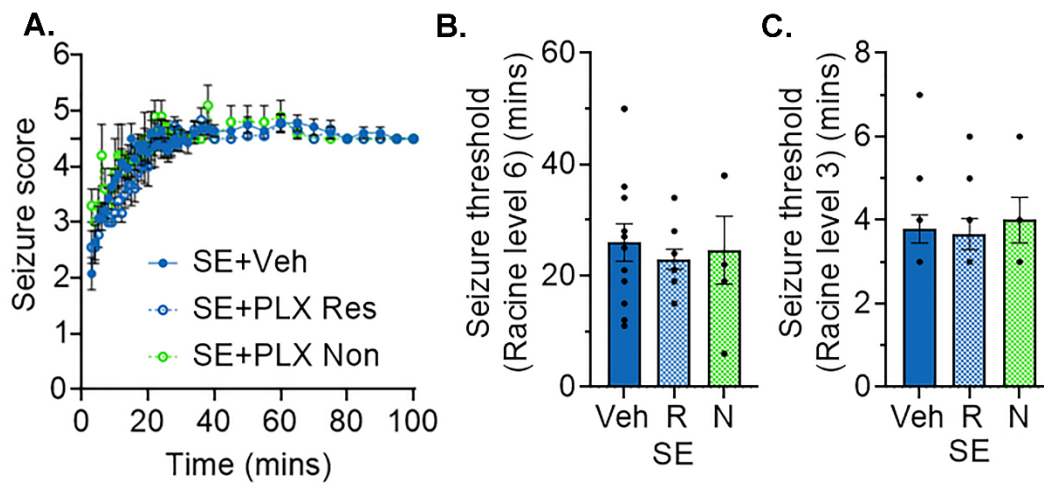
There was no main effect of condition on protein levels of Kv4.2 in the hippocampus [$F(1, 45) = 2.358$, $p = .1317$], indicating that there was no change in protein level of Kv4.2 in the Ctrl and SE groups (Figure 14D). There was also no main effect of treatment [$F(1, 45) = 0.8918$, $p = .3500$]. We found a significant interaction between condition and treatment [$F(1, 45) = 4.225$, $p = .0457$]. The Ctrl+Veh group had less Kv4.2 protein level compared to SE+Veh group ($p = .0459$). The inhibition of CSF1R signaling with PLX3397 did not alter protein levels in the Ctrl groups (p

= .8840). There was no change between Ctrl+PLX3397 and SE+PLX3397 protein levels ($p = .9854$). The inhibition of CSF1R signaling with PLX3397 also did not reduce the protein level of Kv4.2 in the SE groups ($p = .1902$). This indicates that Kv4.2 was decreased after SE-induction but was not altered by inhibition of CSF1R signaling.

When we analyzed HCN1, we found no overall changes. There was no main effect of condition on levels of HCN1 [$F(1, 43) = 0.1182, p = .7327$], demonstrating that there was no change in protein level of HCN1 in the Ctrl and SE groups (Figure 14E). There was also no main effect of treatment [$F(1, 43) = 0.0236, p = .8786$]. We found a significant interaction between condition and treatment [$F(1, 43) = 5.532, p = .0233$]. The Ctrl+Veh group did not have altered level of HCN1 compared to SE+Veh group ($p = .2087$). The inhibition of CSF1R signaling with PLX3397 did not alter protein levels in the Ctrl groups ($p = .2660$). There was no change between Ctrl+PLX3397 and SE+PLX3397 protein levels ($p = .5267$). The inhibition of CSF1R signaling with PLX3397 also did not reduce the protein level of HCN1 in the SE groups ($p = .4487$), indicating that HCN1 was not altered by SE-induction or inhibition of CSF1R signaling. Together, these showed that the SE-induced reduction of PSD95 and Kv4.2 were not recovered by inhibition of CSF1R signaling with PLX3397 but were also not decreased from Ctrl by PLX3397 treatment.

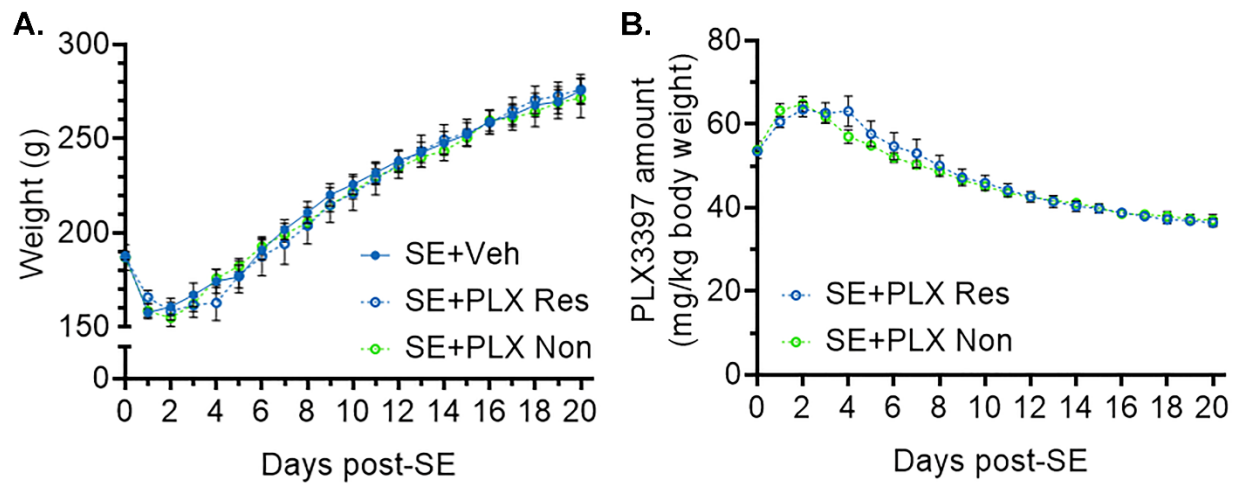
Inhibition of CSF1R Produced a Group of Non-Responders that had no Variation in Weight Change

Few studies have indicated the existence of animals who do not have a reduction in microgliosis following PLX3397 treatment (Spangenberg et al., 2016; Y. Tang et al., 2018), but during our analysis, we found a subset of rats who did not have a reduction in microgliosis at the dose we used in this study. The PLX3397 treated non-responders (Non) were categorized by the rats whose microglia count was higher than the 60% reduction from average number of microglia in the SE+Veh group (Figure 15-18). In order to understand why these non-responders had developed, we analyzed the Racine level and weight changes to determine if SE severity or weight gain had an effect on the drug treatment. We measured the Racine scale with the Kruskal-Wallis test with Dunn's multiple comparison due to the non-normally distributed data. We found that there was a significant difference in Racine scale levels across the three groups the SE+Veh, SE+PLX3397, and SE+PLX3397 Non [$H(3, 150) = 11.98, p = .0025$] (Figure 15A). The SE+PLX3397 Non group was significantly different from both the SE+Veh ($p = .0116$) and



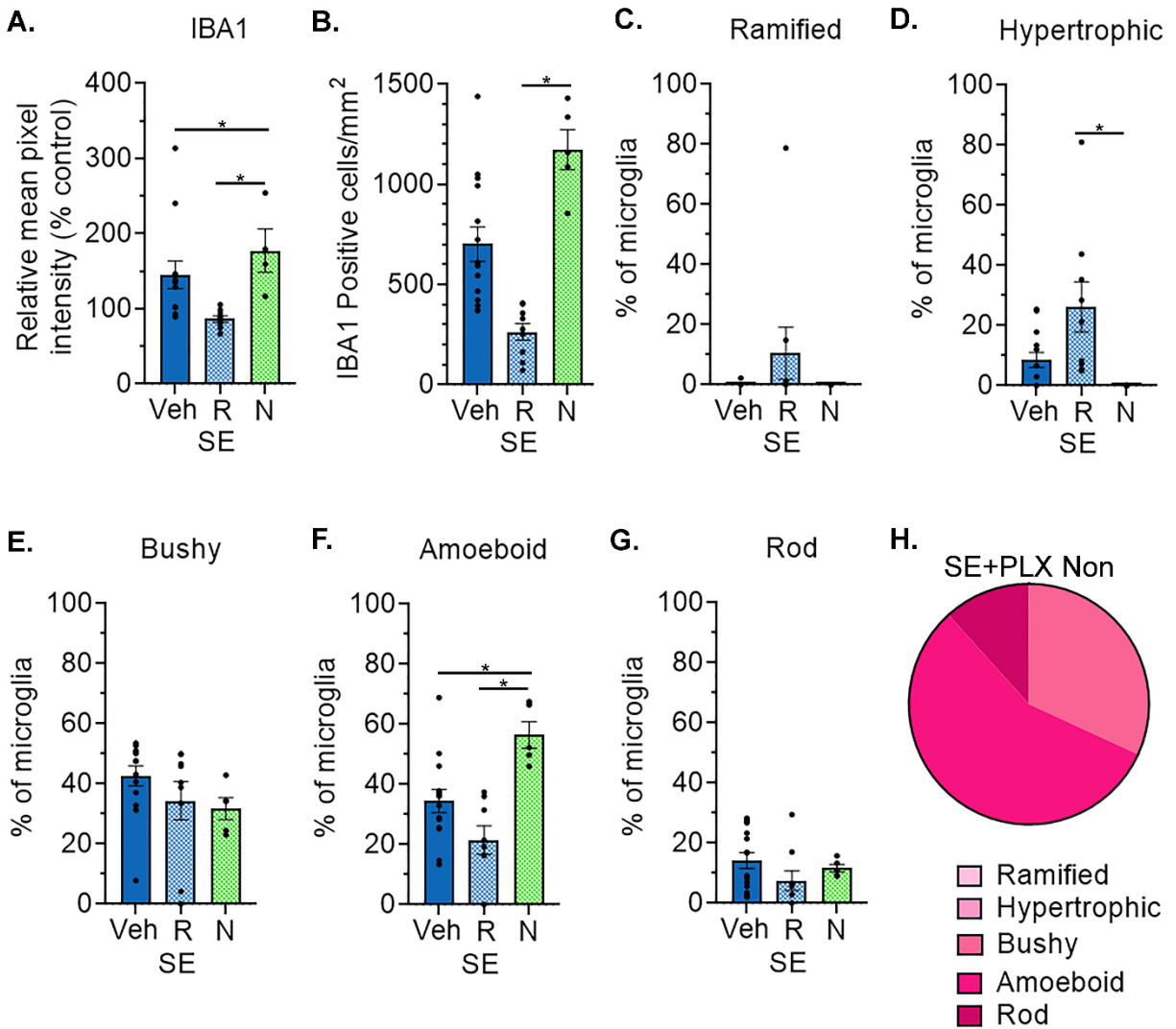
Note. A, Behavioral observation were recorded with the Racine scale. B-C, Time to reach a Racine scale level 3 seizure (B) and 6 SE (C). * $p < .05$ by (A) Kolmogorov-Smirnov test and (B) one-way ANOVA with Dunnett's test. Data shown as mean \pm SEM, SE+Vehicle (Veh), $n = 14$; SE+PLX Responders (Res; R), $n = 9$; SE+PLX Non-responders (Non; N), $n = 5$.

Figure 15. Status epilepticus (SE) induced rats treated with PLX3397 (PLX) that did not have a 60% reduction microgliosis displayed no changes in Racine scale level.



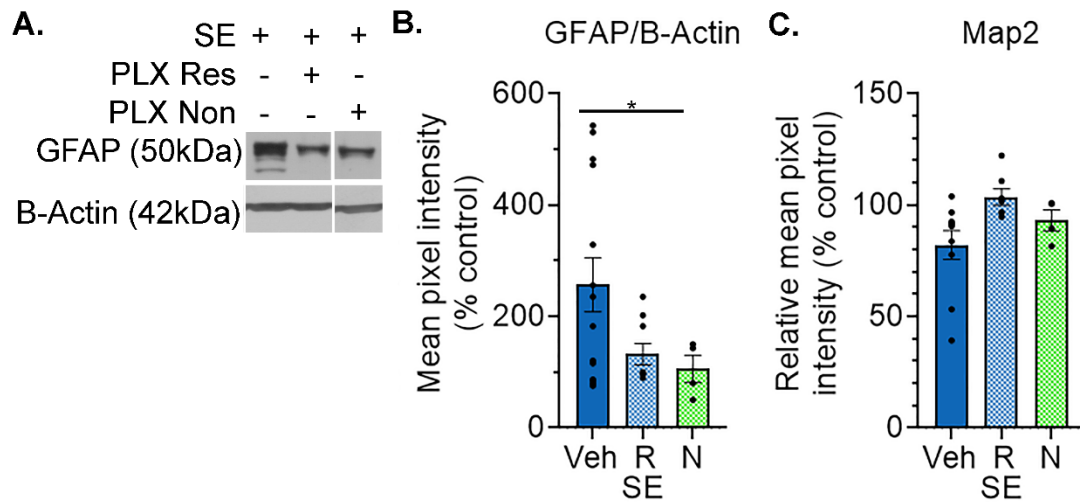
Note. A, Daily weights were recorded. B, The amount of PLX consumed based on an average rat consumption and weight. * $p < 0.05$ by a two-way ANOVA with Dunnett's test. Data shown as mean \pm SEM, SE+Vehicle (Veh), $n = 14$; SE+PLX Responders (Res; R), $n = 9$; SE+PLX Non-responders (Non; N), $n = 5$.

Figure 16. Status epilepticus (SE) induced rats treated with PLX3397 (PLX) that did not have a 60% reduction microgliosis displayed no changes in weight.



Note. A, Densitometry analysis of IBA1 immunostain in the CA1 region of the hippocampus. B, Number of IBA1 positive cells per mm² in the CA1 region of the hippocampus. C-G, Morphological breakdown of each group as ramified (C), hypertrophied (D), bushy (E), amoeboid (F), and rod-shaped (G) IBA1 positive cells. H, Microglial morphological breakdown of SE+PLX Non group is shown as a pie chart. * $p < .05$ by Kruskal-Wallis test with Dunn's test. Data shown as mean \pm SEM, SE+Vehicle (Veh), $n = 14$; SE+PLX Responders (R), $n = 9$; SE+PLX Non-responders (N), $n = 5$.

Figure 17. Status epilepticus (SE) induced rats treated with PLX3397 (PLX) that did not have a 60% reduction in the hippocampal microgliosis displayed increased IBA1 levels and altered morphology.



Note. A, Representative western blots are shown for GFAP and the loading control β -actin. B, Mean pixel intensity of GFAP. C, Densitometry analysis of Map2 in the CA1 region of the hippocampus. * $p < .05$ by one-way ANOVA with Dunnett's test. Data shown as mean \pm SEM, SE+Vehicle (Veh), $n = 14$; SE+PLX Responders (R), $n = 7-9$; SE+PLX Non-responders (N), $n = 3-4$.

Figure 18. Status epilepticus (SE) induced rats treated with PLX3397 (PLX) that did not have a 60% reduction microgliosis still had a reduction in astrocytic protein level GFAP in the CA1 region of the hippocampus.

SE+PLX3397 groups ($p = .0028$). This indicates that the seizure score levels changed across time at a different rate in the non-responders group compared to the other two groups. To further analyze this potential difference, we used a one-way ANOVA to determine if there were any alterations in time to reach a Racine level 3 (Figure 15B) or 6 (Figure 15C). We found no significant effect between the groups of time to reach a level 3 [$F(2, 25) = 0.1228, p = .8850$] or a level 6 [$F(2, 25) = 0.2018, p = .8186$]. Taken together, these data indicate that seizure Racine score was likely not a reason for the non-responder group.

Next, we analyzed the weight change throughout the entire experiment. We also used weight along with the average consumption rate for rats and determined the dose each rat theoretically received throughout the experiment. This was done to determine if dose ranges could be responsible for the non-responder group (National Research Council (US) Subcommittee on Laboratory Animal Nutrition, 1995). We measured weight changes and consumption with a two-way ANOVA with Dunnett's test. When we analyzed the weight changes, we found there was a significant main effect of days post-SE [$F(20, 525) = 82.81, p < .0001$], which was expected as the animals gained weight over time (Figure 16A). There was no main effect of treatment on weight gain [$F(2, 525) = 0.5100, p = .6008$]. The non-responders also showed no significant interaction between days post-SE and treatment on weight change [$F(40, 525) = 0.1679, p > .9999$]. These data indicated that weight gain was likely not a reason for the non-responder group. We also calculated the dose based on rat weight and estimated average consumption and found a significant main effect of days [$F(20, 525) = 41.40, p < .0001$], indicating the dose changes similar to the weight (Figure 16B). There was no main effect of treatment [$F(1, 525) = 0.7064, p = .4014$] nor a significant interaction between days post-SE and treatment [$F(20, 525) = 0.4160, p = .9882$]. The potential dose range of 35-65mg/kg consumed each day by the rats in both groups was likely not the cause of the non-responders.

Inhibition of PLX3397 Produced a Group of Non-Responders that had Increased Microgliosis

To understand the changes that occurred in the animals who did not respond to CSF1R signaling inhibition, we analyzed the properties of microgliosis. These properties included density and number of microglia and morphology of non-responders with a one-way ANOVA compared to the Veh treated SE and the SE+PLX3397 responder groups. The one-way ANOVA revealed an

increase in the density of IBA1 positive cells in the CA1 region of the hippocampus [$F(2, 24) = 4.807, p = .0176$] (Figure 17A). Dunnett's multiple comparison test showed that the non-responders had no change in the density of IBA1 compared to SE+Veh ($p = .4581$). However, the non-responders had increased density of IBA1 compared to PLX3397 responders ($p = .0195$). When we further analyzed the amount of IBA1 levels by counting the number of positive cells in the CA1 region of the hippocampus we found similar results. The one-way ANOVA showed an increase in the number of IBA1 positive cells [$F(2, 24) = 20.40, p < .0001$] (Figure 17B). Comparisons indicated that the non-responders had a higher amount of microglia compared to the Veh treated SE group ($p = .0033$). The non-responders also had a higher amount and density of microgliosis compared to the PLX3397 responder group ($p < .0001$).

We then analyzed the morphologies of the remaining microglia in the non-responders and compared them to the Veh group and the PLX3397 responder group. Due to the non-normally distributed data we used Kruskal-Wallis test with Dunn's multiple comparison. There was no significant across the groups in the ramified morphology [$H(3,28) = 4.056, p = .1316$] (Figure 17C). The comparisons also showed no change in the non-responder group to the SE+Veh ($p > .9999$) and PLX3397 responder groups ($p = .1818$). Analyzing the hypertrophic morphology, there was a significant change across the groups [$H(3,28) = 11.38, p = .0034$], [$F(2, 25) = 5.448, p = .0109$] (Figure 17D). The comparisons revealed that the non-responder's amount of hypertrophic microglia was not different from the SE+Veh group ($p = .1560$). However, there was a decrease between the non-responders group compared to PLX3397 responder group ($p = .0019$).

The Kruskal-Wallis test was not significant among the bushy microglia [$H(3,28) = 5.253, p = .0723$] (Figure 17E). The comparisons of the non-responders to both the SE+Veh ($p = .0642$) and PLX3397 responder groups ($p = .7509$) revealed no significant change. However, there was a significant change across the amoeboid morphology [$H(3,28) = 11.60, p = .0030$] (Figure 17F). The comparisons revealed the non-responders had increases in the amoeboid morphology compared to SE+Veh ($p = .0456$). This increase was also observed in the comparison between the non-responders to PLX3397 responders ($p = .0013$).

There was no significant change among the groups in the rod morphology [$H(3,28) = 3.598, p = .1654$] (Figure 17G). Similarly, the multiple comparisons revealed no change in the non-responders compared to the SE+Veh ($p > .9999$) or PLX3397 responders ($p = .3029$). These data indicated that inhibition of CSF1R signaling with PLX3397 altered the amoeboid morphology.

The morphological average percentage of total microglia of the non-responders was shown as a pie chart (Figure 17H). The percentage and total number of microglia in the PLX3397 non-responders are listed in Table 7. Together these data indicate that PLX3397 treatment had an effect in reducing microgliosis as well as in altering the morphology of remaining microglia.

Table 7. Microglial Morphological Breakdown of the PLX3397 Non-Responders

	Ramified	Hypertrophic	Bushy	Amoeboid	Rod	Total
Percentage	0%	0.04%	32%	56%	12%	100%
Number	0	1	374	663	137	1174

Inhibition of PLX3397 Produced a Group of Non-Responders that had no Recovered GFAP or Map2 Levels

We wanted to understand the effects of CSF1R signaling inhibition in the non-responders. To determine these effects, we analyzed the two proteins that were recovered by inhibition of CSF1R signaling with PLX3397 in the SE condition. Therefore, we analyzed the protein levels of GFAP (Figure 18B) and density of Map2 (Figure 18C) in the non-responders. The one-way ANOVA showed no significant change in protein level of GFAP [$F(2, 24) = 3.148, p = .0611$] (Figure 17B). Likewise, the multiple comparisons revealed that the non-responders had no change in the levels compared to SE+Veh ($p = .1055$) or the PLX3397 responders ($p = .9117$). These data indicate that non-responders had no effect on the levels of GFAP protein. The analysis from the one-way ANOVA of the densitometry of Map2 in the CA1 region of the hippocampus revealed a significant change [$F(2, 18) = 3.772, p = .0428$] (Figure 18C). Dunnett's multiple comparisons test showed that the non-responders had no change in the density compared to SE+Veh ($p = .3911$) or the PLX3397 responders ($p = .4536$). These data indicate that non-responders had no effect on the SE-induced dendritic instability. Together, the proteins shown to be altered with the treatment of the CSF1R inhibitor showed no changes when the microgliosis was not reduced. This suggests that the reduction in microgliosis was the driving factor in the recovery we observed, making it unlikely that the PLX3397 had direct effects on other cell types. Further investigation is required

to understand the remaining population of microglia and how inhibition of CSF1R signaling pathway alters the biochemical properties of these microglia.

DISCUSSION

To identify a disease modifying treatment to cure seizures and cognitive decline in epilepsy is the goal of our research and an utmost concern in epilepsy (Alonso-Vanegas et al., 2013; Demin et al., 2018; Paudel et al., 2018; Vergeer et al., 2019). This is because current ASMs do not alleviate intellectual disabilities in epilepsy, or the associated neuropathology (Brodie et al., 2016; Du et al., 2019; Park & Kwon, 2008; Schmidt, 2011; Thijs et al., 2019; Xia et al., 2017). There is critical need for a novel therapeutic treatment that alters the neuropathology of epilepsy and the associated cognitive deficits. The aims of this study were to determine if inhibition of microgliosis through CSF1R signaling during epileptogenesis could (1) attenuate the cognitive deficits, specifically those in recognition memory and spatial learning and memory and (2) recover dendritic structural stability of hippocampal CA1 neurons. We found (A) CSF1R inhibition did not recover SE-induced weight loss (Figure 2); (B) CSF1R inhibition did not recover the SE-induced recognition or spatial memory (NOR and BM) deficits (Figure 4-8); (C) CSF1R inhibition reduced the density and number of microglia and altered the morphology of the remaining microglia (Figure 9-10); (D) Map2 immunostaining protein levels were recovered with inhibition of microgliosis (Figure 12); (E) a set of rats—non-responders—emerged in the SE group treated with PLX3397 that had higher microgliosis with altered morphology and no recovery of Map2 (Figure 14-17). To our knowledge, this is the first study to show that PLX3397-mediated inhibition of CSF1R signaling reduced microgliosis by 60% in the hippocampus but did not recover recognition or spatial memory deficits or fully recover dendritic stability in the hippocampal CA1 region following pilocarpine induced SE.

The report that SE results in memory deficits, specifically those in recognition and spatial memory have been widely replicated in the epilepsy literature (Brewster et al., 2013; Pearson et al., 2014; Schartz et al., 2018, 2019). Studies have shown that injury to the hippocampus is sufficient to produce a deficit in both recognition and spatial memory (Broadbent et al., 2004; Holley et al., 2018; Sakaguchi & Sakurai, 2020; Z. Tang et al., 2019). Rats that underwent direct injury to the hippocampus performed worse in the NOR task when compared to the non-injured control rats at one, two, three, and four weeks following the injury, but recovered by eight weeks (Broadbent et al., 2010; Cohen & Stackman, 2015). Similar to current literature, our Veh treated SE group displayed cognitive impairments in both NOR and BM at two to three weeks post-SE

compared to the Ctrl group. The Veh treated Ctrl rats were able to recognize the familiar object and were able to navigate to the escape box faster than the Veh treated SE group. However, when analyzing time spent with the objects, we found the SE rats spent significantly less time exploring the objects compared to the controls. Previous studies have shown that normally behaving rats do not experience object fear (Ennaceur et al., 2009). Therefore, one possibility for our observations is that the SE rats may be avoiding the objects due to fear or anxiety of the objects. Although this needs to be investigated in future studies. Taken together, our findings further support that SE promotes cognitive decline that is evident when rats are subjected to NOR and BM tests.

Recognition and spatial memory deficits following SE have been observed to accompany hippocampal injury, including dendritic instability and gliosis (Brewster et al., 2013; Schartz et al., 2018). Dendritic instability has been measured in the CA1 region of the hippocampus with specifically localized ion channels and proteins involved in the structural regulation of microtubules along dendrites (Ballough et al., 1995; Marcelin et al., 2012). The loss of Map2, PSD95, and decline of the ion channels Kv4.2 and HCN1 have been linked to increased seizure susceptibility in epilepsy (Brewster et al., 2005, 2013; Jung et al., 2007; Lugo et al., 2012; Schartz et al., 2016, 2018). In this experiment we observed decreases in Map2, PSD95, and Kv4.2 in our Veh treated SE group compared to our Veh treated Ctrl group, aligning with current literature. However, we did not observe alterations in HCN1 protein levels in the hippocampus. This could be due to the method of detection, as using whole hippocampal homogenates can dilute the effects of a specific region of the hippocampus, which for this study was the CA1 region where HCN1 channels are located. We also did not use synaptosomal preparations which most studies used to measure proteins in low concentrations, similar to HCN1.

The amassing of gliosis and inflammation, including the accumulation of astrogliosis and microgliosis, has been considered a hallmark characterization of temporal lobe epilepsy and has been widely observed throughout the epilepsy literature (Brewster et al., 2013; Datchet et al., 2015; Nirwan et al., 2018; Wirenfeldt et al., 2009; Wyatt-Johnson et al., 2017). Following SE, astrocytes have been shown to be increased at similar timepoints to microgliosis and may also contribute to the CA1 dendritic damage (Brewster et al., 2013; Ravizza & Vezzani, 2006; Schartz et al., 2016; Shapiro et al., 2008). We observed similar results with increases in microgliosis in our Veh treated SE group compared to the Ctrl group. This increase also parallels increases in morphological phenotypes of bushy and amoeboid microglia in the Veh treated SE group compared to the

ramified phenotype observed in the Ctrl rats. We also found increased protein level of GFAP in the Veh treated SE group compared to Ctrl, indicating an increase in astrogliosis. Furthermore, to analyze how we may be modulating this crosstalk between microglia and astrocytes, we measured complement C3 and IL-6, known to be produced by astrocytes and modulate microglia response (Lian et al., 2016). Activation of complement C3 has also been shown previously in correlation with memory decline and deficits (Hernandez et al., 2017; Shi et al., 2015) and we previously have shown an increase in C3 correlates with memory deficits following SE (Schartz et al., 2018). We found that C3 was significantly increased in our Veh treated SE group compared to the Veh treated Ctrl group, similar to our previously findings. We did not, however, find changes in IL-6 protein levels between the SE and Ctrl groups. IL-6 levels are transient and are altered immediately following seizure activity (Rana & Musto, 2018; Schartz et al., 2016; Vezzani et al., 2019). Because latency to last seizure was not determined, our high variance and non-significance could be accounted for by this potential non-uniform latency. Taken together, these data showed that our epileptic group compared to the Ctrl group was able to replicate current pathological findings following SE.

An increasing body of evidence implicates microglia as a crucial response during epileptogenesis (Abiega et al., 2016; Benson et al., 2015; Böttcher et al., 2019; Brewster, 2019; Eyo et al., 2016, 2017; Hiragi et al., 2018), although their response in epilepsy, whether beneficial or detrimental, remains largely under debate. Studies that have altered the mTOR pathway following SE have shown to attenuate memory deficits, recovery dendritic instability, and reduce microgliosis (Brewster et al., 2013; Curatolo, 2015; Mazumder et al., 2017). These studies have specifically focused on the inhibition of mTOR through the reduction of microgliosis, as mTOR in microglia leads to the survival and proliferation of the cell. Although studies have shown that microglial specific mTOR hyperactivation produced a similar phenotype observed in SE animals (Xie et al., 2014; X. Zhao et al., 2018), the exact role of microgliosis remains largely unstudied. For this reason, we evaluated the inhibition of the SE-induced microgliosis through a specific receptor found exclusively on microglia in the brain, CSF1R, with the drug PLX3397 (Butowski et al., 2016; Elmore et al., 2014). The CSF1R signaling pathway allows us to further block upstream from mTOR upstream as well as other signaling molecules to inhibit survival, proliferation, motility, and differentiation (Butowski et al., 2016). The use of drugs targeting the CSF1R pathway have allowed researchers to study the contribution of microgliosis to the

pathophysiology of neurological disorders by blocking the ability of microglia to survive and proliferate.

The use of pharmacological and genetic techniques to manipulate microgliosis implicates microglia as an essential player in the modulation of memory (Dupont & Vercueil, 2015; Neher & Cunningham, 2019; Wyatt-Johnson & Brewster, 2019). However, inhibiting CSF1R signaling following SE in our study did not attenuate hippocampal-dependent recognition or spatial memory deficits (Figure 4-8). The effects of microglial inhibition with a CSF1R inhibitor have been evaluated in several neurological disorders (Acharya et al., 2016; Elmore et al., 2018; Spangenberg et al., 2016). Recent studies have shown that elimination of microglia with a CSF1R inhibitor improved recognition memory with NOR following cranial irradiation (Acharya et al., 2016), improved spatial memory in Morris water maze in aged animals (Elmore et al., 2018), and improved memory in contextual fear condition in a model of AD (Spangenberg et al., 2016). These studies support that inhibition of microgliosis with a CSF1R inhibitor can modulate memory. However, this was not what we observed in our model of epilepsy. This could be due to the nature of epilepsy, where there are spontaneous recurrent seizures producing and exacerbating brain injury. The behavioral performance was measured once spontaneous seizures were evident in the pilocarpine model of SE (Becker, 2018). Since we did not measure seizure frequency or intensity it is possible the inhibition of microgliosis had no effect on the seizures, as previously studies have shown (Brewster et al., 2013; Hiragi et al., 2018). Furthermore, studies have shown a high correlation between memory deficits and seizure frequency with no correlation to the neuropathology (Mazarati, 2008; Zhou et al., 2007), thereby, suggesting that microgliosis may have no impact on behavior but rather seizure severity is the critical factor in behavior. The neuropathological analysis was also only performed in the CA1 region of the hippocampus. When visually observing other regions of the brain we noticed no apparent reduction in the levels of microgliosis in the amygdala or thalamus. Because the thalamus serves as the sensory relay station of the brain it can modulate learning and memory processes (Torricco & Munakomi, 2020), and therefore play a role in the rats' behaviors in NOR and BM tests. We speculate that the non-reduction of microgliosis in the thalamus as well as in other regions of the brain, such as the amygdala, may contribute to the observation that the SE rats treated with SE+PLX3397 did not show improved memory. Together this suggests that PLX3397-mediated inhibition of CSF1R

signaling and the resulting 60% suppression of microgliosis in the CA1 region of the hippocampus is not sufficient to recover or attenuate SE-induced deficits in recognition or spatial memory.

The PLX3397-mediated inhibition of CSF1R signaling reduced the number of IBA1-positive microglial cells by 60% in the CA1 region of the hippocampus in both our Ctrl and SE groups (Figure 7), similar to current literature (Elmore et al., 2014; Srivastava et al., 2018). PLX3397 treatment resulted in a 60% reduction of the CA1 hippocampal microgliosis under non-pathological and pathological conditions. However, we did not fully deplete microgliosis, as we still had 40% of microglia remaining in the CA1 region of the hippocampus and had a subset of SE rats that did not have reduced microgliosis. In a model of AD, treatment with a CSF1R inhibitor reduced microgliosis by 80% in the hippocampus, cortex, and thalamus (Spangenberg et al., 2016), while in healthy aging mice, the reduction in numbers of microglia were close to 99% in the hippocampus, cortex, and thalamus (Elmore et al., 2014; Najafi et al., 2018). Based on our findings and current literature, CSF1R inhibition is effective at reducing the number of microglial cells in non-pathological states but is not entirely efficient in disease states including AD, Parkinson's disease, ischemia, and epilepsy (Schapansky et al., 2015; Spangenberg et al., 2016; Srivastava et al., 2018; Y. Tang et al., 2018). The repeating injury of spontaneous seizures in epilepsy could be a contributing factor driving the lack of apparent effect of PLX3397 in reducing microgliosis in the hippocampus (Reddy & Kuruba, 2013). Together, these data suggest that in pathological states inhibition of CSF1R signaling with PLX3397 is not sufficient to suppress microgliosis throughout the brain. It is possible that activation of other signaling cascades within microglial cells may bypass CSF1R signaling to control their survival and proliferation. It is known if under injury microglia display a complex heterogeneous phenotype of receptors and proteins (Fumagalli et al., 2018). This makes it difficult to determine the exact compensatory mechanism that may be at play. In order to determine this mechanism, we would need a pharmacological or genetic tool that only allowed for specific receptors or proteins to be expressed on microglia at a time. If this existed, we could go through each receptor and determine which receptor or protein may be altered.

However, a caveat to the reduction of microgliosis is the lack of multiple markers to measure the exact microgliosis. The use of one marker, IBA1, for all microglia analysis could mean that CSF1R is just altering that specific protein (IBA) and not the entire microglia. However, other studies have shown inhibition with CSF1R was successful in reducing IBA1 levels alongside levels of CX3CR1 and TMEM119, both of which are expressed by microglia (Elmore et al., 2014;

Spangenberg et al., 2016; Y. Tang et al., 2018). Another limitation of this study is that we were unable to measure the extent at which CSF1R signaling was inhibited by PLX3397. Microglial counts were used as a proxy to measure CSF1R inhibition. This was due to lack of tools available to evaluate CSF1R activation and signaling. It is also possible that the animals' weight gain over the course of the experiment may have altered the efficacy of the drug as the dose per day was not measured by individual weight but by an average of the three weeks. Given this information the rats should still have had a dose between 30mg/kg and 77 mg/kg in which 30mg/kg has still be shown as an effective dose based on previous studies and our preliminary data (Tang et al. 2018; Srivastava et al. 2018).

We are the first study to determine the morphological phenotypes of microglia following PLX3397-mediated inhibition of CSF1R signaling. The remaining microglia displayed altered morphologies with more hypertrophic microglia in the Ctrl and SE treated groups and the non-responders had increased numbers of amoeboid microglia. Current literature suggests that bushy/amoeboid microglia may be reactive and may have a highly phagocytic phenotype characterized by high levels of phagocytic lysosomal markers (Brown & Neher, 2012; Fumagalli et al., 2018; Janda et al., 2018). In contrast, hypertrophic microglia may be closely related to the production of inflammatory cytokines (Fernández-Arjona et al., 2017; Kaur et al., 2014). Without functional or biochemical characterization of these microglia we are unable to draw a conclusion of whether these changes are beneficial or detrimental to the neuropathology or pathophysiology.

To further understand our findings, we analyzed astrocytes and C3 which are highly involved with microglial responses. Studies have shown that astrocytes along with their production of C3 can exert changes on microglial cells and vice versa (Jha et al., 2019; Lévi-Strauss & Mallat, 1987). Therefore, we sought to determine if the inhibition of microgliosis impacted this relationship. We found that SE-induced increases in GFAP protein levels were reduced by inhibition of the CSF1R signaling even without reduction in microgliosis. However, there was no change in GFAP protein levels in the Ctrl groups, indicating that the CSF1R signaling was only being modulated in microglia. The findings that altering CSF1R signaling in microglia reduced astrocytic levels supports the idea that these two cells depend on one another to respond to pathological events (Jha et al., 2019). Reduced astrocytic levels in the non-responders further support that we have altered these microglial cells through the CSF1R inhibition, as we would have expected the levels in the non-responders to be similar to that of the SE+Veh group. However,

exact extent these cells have been altered still requires further investigating. Together, through the inhibition of a single receptor, CSF1R, we were able to alter microglia and effect their relationship with astrocytes. We also sought to determine if a major crosstalk protein, C3, between microglia and astrocytes may be responsible for this altered relationship. C3 has been found to be involved in the regulation of the astrocytic-microglial relationship and reduction in C3 levels have been found to recover cognitive deficits in the mouse model of AD (Lian et al., 2016; Luchena et al., 2018). We found inhibition of CSF1R signaling did not alter protein levels of C3 in the SE group, indicating that we did not suppress C3 activation with microgliosis inhibition or the subsequent reduction in astrocytic levels. Based on our finding and recent studies suggesting that microglia may not modulate memory (Elmore et al., 2014; Neher & Cunningham, 2019; Spangenberg et al., 2016) and decreases in C3 resulting in improved memory outcomes (Carpanini et al., 2019; Morgan, 2018; Shi et al., 2015), our results suggest that the increased levels of C3 may be a potential reason to the recognition and spatial memory deficits observed with the inhibition of CSF1R signaling. Future studies are needed to further evaluate the contribution of C3 to the cognitive deficits following SE.

Cognitive deficits that occur in correlation with SE and epilepsy are often associated with microgliosis and dendritic alterations (Bernard et al., 2004; Brewster et al., 2013; Hall et al., 2015; Holley et al., 2018). Previous studies showed that reduction of microgliosis with rapamycin, attenuated cognitive deficits and dendritic loss in the hippocampus (Brewster et al., 2013; Curatolo, 2015; Nguyen et al., 2015). However, rapamycin inhibits mTOR in both neurons and microglia (Bockaert & Marin, 2015). Here we decreased microgliosis through the inhibition of CSF1R signaling and found a partial recovery of Map2 immunostaining in the CA1 hippocampus with no effect on the SE-induced Kv4.1 change, and cognitive defects. Even though we found a recovery in Map2 in the CA1 region of the hippocampus, this may not be sufficient to modulate memory in this context.

Several factors may contribute to the different outcomes following rapamycin treatment versus PLX3397 treatment, including length of treatment, dose, and administration route. In this study our length of treatment, 20 days, was chosen based on multiple factors including average length of treatment in current PLX3397 literature (Elmore et al., 2018; Spangenberg et al., 2016; Srivastava et al., 2018) as well as the goal of suppressing microgliosis through all events (inflammation, cell loss, and the accumulation of microgliosis) that occurs during epileptogenesis.

However, the studies performed with rapamycin showed discrepancies depending on the length of treatment. Treatment with rapamycin for one to two weeks during epileptogenesis showed a reduction in seizure severity, recovery of learning and memory deficits, and reduced microgliosis in the hippocampus in both rat and mouse models of epilepsy (Zhang et al. 2018; H. Zhao, Zhu, and Huang 2018; Nguyen et al. 2015; Brewster et al. 2013). However, treatment with rapamycin for over one month does not alter seizure severity or the pathology in mice (Buckmaster and Lew 2011; Zeng et al. 2010). Additional studies are required to determine if inhibiting microgliosis at specific times points may be more effective treatment. Treatment with rapamycin required a dose range between 6-10mg/kg given every other day while PLX3397 requires a dose between 30mg/kg-70mg/kg given every day. Treatment with PLX3397 also takes three days to begin reducing microgliosis while rapamycin treatment reduced mTOR signal within 24 hours (Butowski et al., 2016; Elmore et al., 2014; Eshleman et al., 2002; Y. Tang et al., 2018). Furthermore, treatment with rapamycin was given as i.p. injections while PLX3397 was given orally in chow. PLX3397 does not dissolve in solution for i.p. injections without the use of other chemicals, while gastrointestinal absorption has been found to be effective and can reduce stress caused by daily injections (Deutsch-Feldman et al., 2015; Elmore et al., 2014; Y. Tang et al., 2018). However, with PLX3397 treatment in food, we were unable to specifically dose the food each day and instead ended with a range of doses given.

In conclusion, our findings suggest PLX3397-mediated inhibition of CSF1R signaling reduced microgliosis by 60% in the CA1 region of the hippocampus but did not recover recognition or spatial memory deficits or fully recover dendritic stability following pilocarpine induced SE. We also found microglial morphological alterations caused by inhibition of the CSF1R signaling pathway although the specific biochemical or functional changes to microglial cells are not known. This suggests that further investigation is required to determine the disadvantage or advantage of inhibiting microgliosis with PLX3397. Based on our findings we can conclude that microgliosis controlled through the CSF1R signaling pathway may not be contributing factor to the dendritic phenotypes associated with hippocampal CA1 region injury following pilocarpine induced SE. Our findings do not support that PLX3397 may be an efficient treatment for the dendritic pathology or memory deficits that are seen during epileptogenesis in cases of acquired epilepsy.

LIST OF REFERENCES

- Abdelmalik, P. A., Burnham, W. M., & Carlen, P. L. (2005). Increased seizure susceptibility of the hippocampus compared with the neocortex of the immature mouse brain in vitro. *Epilepsia*, *46*(3), 356-366. <https://doi.org/10.1111/j.0013-9580.2005.34204.x>
- Abiega, O., Beccari, S., Diaz-Aparicio, I., Nadjar, A., Layé, S., Leyrolle, Q., Gómez-Nicola, D., Domercq, M., Pérez-Samartín, A., Sánchez-Zafra, V., Paris, I., Valero, J., Savage, J. C., Hui, C.-W., Tremblay, M.-È., Deudero, J. J. P., Brewster, A. L., Anderson, A. E., Zaldumbide, L., . . . Sierra, A. (2016). Neuronal hyperactivity disturbs ATP microgradients, impairs microglial motility, and reduces phagocytic receptor expression triggering apoptosis/microglial phagocytosis uncoupling. *PLoS Biology*, *14*(5), e1002466. <https://doi.org/10.1371/journal.pbio.1002466>
- Acharya, M. M., Green, K. N., Allen, B. D., Najafi, A. R., Syage, A., Minasyan, H., Le, M. T., Kawashita, T., Giedzinski, E., Parihar, V. K., West, B. L., Baulch, J. E., & Limoli, C. L. (2016). Elimination of microglia improves cognitive function following cranial irradiation. *Scientific Reports*, *6*. <https://doi.org/10.1038/srep31545>
- Alonso-Vanegas, M. A., Cisneros-Franco, J. M., Castillo-Montoya, C., Martínez-Rosas, A. R., Gómez-Pérez, M. E., & Rubio-Donnadieu, F. (2013). Self-reported quality of life in pharmaco-resistant temporal lobe epilepsy: Correlation with clinical variables and memory evaluation. *Epileptic Disorders: International Epilepsy Journal with Videotape*, *15*(3), 263-271. <https://doi.org/10.1684/epd.2013.0590>
- Antunes, M., & Biala, G. (2012). The novel object recognition memory: Neurobiology, test procedure, and its modifications. *Cognitive Processing*, *13*(2), 93-110. <https://doi.org/10.1007/s10339-011-0430-z>
- Aronica, E., Boer, K., van Vliet, E. A., Redeker, S., Baayen, J. C., Spliet, W. G. M., van Rijen, P. C., Troost, D., Lopes da Silva, F. H., Wadman, W. J., & Gorter, J. A. (2007). Complement activation in experimental and human temporal lobe epilepsy. *Neurobiology of Disease*, *26*(3), 497-511. <https://doi.org/10.1016/j.nbd.2007.01.015>
- Aronica, E., Ravizza, T., Zurolo, E., & Vezzani, A. (2012). Astrocyte immune responses in epilepsy. *Glia*, *60*(8), 1258-1268. <https://doi.org/10.1002/glia.22312>

- Asadi-Pooya, A. A., Stewart, G. R., Abrams, D. J., & Sharan, A. (2017). Prevalence and incidence of drug-resistant mesial temporal lobe epilepsy in the United States. *World Neurosurgery*, *99*, 662-666. <https://doi.org/10.1016/j.wneu.2016.12.074>
- Bachiller, S., Jiménez-Ferrer, I., Paulus, A., Yang, Y., Swanberg, M., Deierborg, T., & Boza-Serrano, A. (2018). Microglia in neurological diseases: A road map to brain-disease dependent-inflammatory response. *Frontiers in Cellular Neuroscience*, *12*, 488. <https://doi.org/10.3389/fncel.2018.00488>
- Bailey, K. R., & Crawley, J. N. (2009). Anxiety-related behaviors in mice. In J. J. Buccafusco (Ed.), *Methods of behavior analysis in neuroscience* (2nd ed.). Boca Raton, FL: CRC Press/Taylor & Francis. <http://www.ncbi.nlm.nih.gov/books/NBK5221/>
- Ballough, G. P., Martin, L. J., Cann, F. J., Graham, J. S., Smith, C. D., Kling, C. E., Forster, J. S., Phann, S., & Filbert, M. G. (1995). Microtubule-associated protein 2 (MAP-2): A sensitive marker of seizure-related brain damage. *Journal of Neuroscience Methods*, *61*(1-2), 23-32.
- Bangasser, D. (2015). To freeze or not to freeze. *ELife*, *4*. <https://doi.org/10.7554/eLife.13119>
- Barnwell, L. F. S., Lugo, J. N., Lee, W. L., Willis, S. E., Gertz, S. J., Hrachovy, R. A., & Anderson, A. E. (2009). Kv4.2 knockout mice demonstrate increased susceptibility to convulsant stimulation. *Epilepsia*, *50*(7), 1741-1751. <https://doi.org/10.1111/j.1528-1167.2009.02086.x>
- Battle, M., Ferri, L., Andrade, C., Ortega, F.-J., Vidal-Taboada, J. M., Pugliese, M., Mahy, N., & Rodríguez, M. J. (2015). Astroglia-microglia cross talk during neurodegeneration in the rat hippocampus. *BioMed Research International*, *2015*, 102419. <https://doi.org/10.1155/2015/102419>
- Baune, B. T., Konrad, C., Grotegerd, D., Suslow, T., Birosova, E., Ohrmann, P., Bauer, J., Arolt, V., Heindel, W., Domschke, K., Schöning, S., Rauch, A. V., Uhlmann, C., Kugel, H., & Dannlowski, U. (2012). Interleukin-6 gene (IL-6): A possible role in brain morphology in the healthy adult brain. *Journal of Neuroinflammation*, *9*(1), 125. <https://doi.org/10.1186/1742-2094-9-125>
- Beamer, E., Conte, G., & Engel, T. (2019). ATP release during seizures—A critical evaluation of the evidence. *Brain Research Bulletin*, *151*, 65-73. <https://doi.org/10.1016/j.brainresbull.2018.12.021>

- Becker, A. J. (2018). Review: Animal models of acquired epilepsy: Insights into mechanisms of human epileptogenesis. *Neuropathology and Applied Neurobiology*, *44*(1), 112-129. <https://doi.org/10.1111/nan.12451>
- Beckmann, N., Giorgetti, E., Neuhaus, A., Zurbrugg, S., Accart, N., Smith, P., Perdoux, J., Perrot, L., Nash, M., Desrayaud, S., Wipfli, P., Frieauff, W., & Shimshek, D. R. (2018). Brain region-specific enhancement of remyelination and prevention of demyelination by the CSF1R kinase inhibitor BLZ945. *Acta Neuropathologica Communications*, *6*(1), 9. <https://doi.org/10.1186/s40478-018-0510-8>
- Beghi, E. (2019). The epidemiology of epilepsy. *Neuroepidemiology*, 1-7. <https://doi.org/10.1159/000503831>
- Bell, G. S., Neligan, A., & Sander, J. W. (2014). An unknown quantity—The worldwide prevalence of epilepsy. *Epilepsia*, *55*(7), 958-962. <https://doi.org/10.1111/epi.12605>
- Benson, M. J., Manzanero, S., & Borges, K. (2015). Complex alterations in microglial M1/M2 markers during the development of epilepsy in two mouse models. *Epilepsia*, *56*(6), 895-905. <https://doi.org/10.1111/epi.12960>
- Bernard, C., Anderson, A., Becker, A., Poolos, N. P., Beck, H., & Johnston, D. (2004). Acquired dendritic channelopathy in temporal lobe epilepsy. *Science*, *305*(5683), 532-535. <https://doi.org/10.1126/science.1097065>
- Bianchin, M. M., Velasco, T. R., Coimbra, E. R., Gargaro, A. C., Escorsi-Rosset, S. R., Wichert-Ana, L., Terra, V. C., Jr., V. A., Jr., D. A., Santos, A. C. dos, Fernandes, R. M. F., Jr, J. A. A., Jr, C. G. C., Leite, J. P., Takayanagui, O. M., Markowitsch, H. J., & Sakamoto, A. C. (2013). Cognitive and surgical outcome in mesial temporal lobe epilepsy associated with hippocampal sclerosis plus neurocysticercosis: A cohort study. *PLOS ONE*, *8*(4), e60949. <https://doi.org/10.1371/journal.pone.0060949>
- Birnbaum, S. G., Varga, A. W., Yuan, L.-L., Anderson, A. E., Sweatt, J. D., & Schrader, L. A. (2004). Structure and function of Kv4-family transient potassium channels. *Physiological Reviews*, *84*(3), 803-833. <https://doi.org/10.1152/physrev.00039.2003>
- Blackburn, D., Sargsyan, S., Monk, P. N., & Shaw, P. J. (2009). Astrocyte function and role in motor neuron disease: A future therapeutic target? *Glia*, *57*(12), 1251-1264. <https://doi.org/10.1002/glia.20848>

- Blume, W. T. (2010). Focal and generalized: Both here and there. *Epilepsy Currents*, 10(5), 115-117. <https://doi.org/10.1111/j.1535-7511.2010.01375.x>
- Bockaert, J., & Marin, P. (2015). mTOR in brain physiology and pathologies. *Physiological Reviews*, 95(4), 1157-1187. <https://doi.org/10.1152/physrev.00038.2014>
- Boivin, G. P., Bottomley, M. A., Schiml, P. A., Goss, L., & Grobe, N. (2017). Physiologic, behavioral, and histologic responses to various euthanasia methods in C57BL/6NTac male mice. *Journal of the American Association for Laboratory Animal Science: JAALAS*, 56(1), 69-78.
- Bolós, M., Perea, J. R., Terreros-Roncal, J., Pallas-Bazarra, N., Jurado-Arjona, J., Ávila, J., & Llorens-Martín, M. (2018). Absence of microglial CX3CR1 impairs the synaptic integration of adult-born hippocampal granule neurons. *Brain, Behavior, and Immunity*, 68, 76-89. <https://doi.org/10.1016/j.bbi.2017.10.002>
- Böttcher, C., Schlickeiser, S., Sneeboer, M. A. M., Kunkel, D., Knop, A., Paza, E., Fidzinski, P., Kraus, L., Snijders, G. J. L., Kahn, R. S., Schulz, A. R., Mei, H. E., NBB-Psy, Hol, E. M., Siegmund, B., Glauben, R., Spruth, E. J., de Witte, L. D., & Priller, J. (2019). Human microglia regional heterogeneity and phenotypes determined by multiplexed single-cell mass cytometry. *Nature Neuroscience*, 22(1), 78-90. <https://doi.org/10.1038/s41593-018-0290-2>
- Brewster, A. L. (2019). Human microglia seize the chance to be different. *Epilepsy Currents*, 19(3), 190-192. <https://doi.org/10.1177/1535759719843299>
- Brewster, A. L., Lugo, J. N., Patil, V. V., Lee, W. L., Qian, Y., Vanegas, F., & Anderson, A. E. (2013). Rapamycin reverses status epilepticus-induced memory deficits and dendritic damage. *PloS One*, 8(3), e57808. <https://doi.org/10.1371/journal.pone.0057808>
- Brewster, A. L., Bender, R. A., Chen, Y., Dube, C., Eghbal-Ahmadi, M., & Baram, T. Z. (2002). Developmental febrile seizures modulate hippocampal gene expression of hyperpolarization-activated channels in an isoform- and cell-specific manner. *The Journal of Neuroscience*, 22(11), 4591-4599. <https://doi.org/20026437>
- Brewster, A. L., Bernard, J. A., Gall, C. M., & Baram, T. Z. (2005). Formation of heteromeric hyperpolarization-activated cyclic nucleotide-gated (HCN) channels in the hippocampus is regulated by developmental seizures. *Neurobiology of Disease*, 19(1-2), 200-207. <https://doi.org/10.1016/j.nbd.2004.12.015>

- Brites, D., & Vaz, A. R. (2014). Microglia centered pathogenesis in ALS: Insights in cell interconnectivity. *Frontiers in Cellular Neuroscience*, 8, 117. <https://doi.org/10.3389/fncel.2014.00117>
- Broadbent, N. J., Squire, L. R., & Clark, R. E. (2004). Spatial memory, recognition memory, and the hippocampus. *Proceedings of the National Academy of Sciences of the United States of America*, 101(40), 14515-14520. <https://doi.org/10.1073/pnas.0406344101>
- Brodie, M. J., Besag, F., Ettinger, A. B., Mula, M., Gobbi, G., Comai, S., Aldenkamp, A. P., & Steinhoff, B. J. (2016). Epilepsy, antiepileptic drugs, and aggression: An evidence-based review. *Pharmacological Reviews*, 68(3), 563-602. <https://doi.org/10.1124/pr.115.012021>
- Brown, G. C., & Neher, J. J. (2012). Eaten alive! Cell death by primary phagocytosis: “phagoptosis.” *Trends in Biochemical Sciences*, 37(8), 325-332. <https://doi.org/10.1016/j.tibs.2012.05.002>
- Brown, G. C., & Neher, J. J. (2014). Microglial phagocytosis of live neurons. *Nature Reviews Neuroscience*, 15(4), 209-216. <https://doi.org/10.1038/nrn3710>
- Buckmaster, P. S., & Lew, F. H. (2011). Rapamycin suppresses mossy fiber sprouting but not seizure frequency in a mouse model of temporal lobe epilepsy. *The Journal of Neuroscience*, 31(6), 2337-2347. <https://doi.org/10.1523/JNEUROSCI.4852-10.2011>
- Butowski, N., Colman, H., De Groot, J. F., Omuro, A. M., Nayak, L., Wen, P. Y., Cloughesy, T. F., Marimuthu, A., Haidar, S., Perry, A., Huse, J., Phillips, J., West, B. L., Nolop, K. B., Hsu, H. H., Ligon, K. L., Molinaro, A. M., & Prados, M. (2016). Orally administered colony stimulating factor 1 receptor inhibitor PLX3397 in recurrent glioblastoma: An ivy foundation early phase clinical trials consortium phase II study. *Neuro-Oncology*, 18(4), 557-564. <https://doi.org/10.1093/neuonc/nov245>
- Carpanini, S. M., Torvell, M., & Morgan, B. P. (2019). Therapeutic inhibition of the complement system in diseases of the central nervous system. *Frontiers in Immunology*, 10. <https://doi.org/10.3389/fimmu.2019.00362>
- Carpenter, D. C., Hrdina, P. D., & Beaubien, A. R. (1977). Effects of phenobarbital and diazepam on imipramine-induced changes in blood pressure, heart rate and rectal temperature of rats. *Research Communications in Chemical Pathology and Pharmacology*, 18(4), 613-625.

- Casanova, J. R., Nishimura, M., Owens, J. W., & Swann, J. W. (2012). Impact of seizures on developing dendrites: Implications for intellectual developmental disabilities. *Epilepsia*, 53 (Suppl 1), 116-124. <https://doi.org/10.1111/j.1528-1167.2012.03482.x>
- Cengiz, P., Zafer, D., Chandrashekhar, J. H., Chanana, V., Bogost, J., Waldman, A., Novak, B., Kintner, D. B., & Ferrazzano, P. A. (2019). Developmental differences in microglia morphology and gene expression during normal brain development and in response to hypoxia-ischemia. *Neurochemistry International*, 127, 137-147. <https://doi.org/10.1016/j.neuint.2018.12.016>
- Chakir, A., Fabene, P. F., Ouazzani, R., & Bentivoglio, M. (2006). Drug resistance and hippocampal damage after delayed treatment of pilocarpine-induced epilepsy in the rat. *Brain Research Bulletin*, 71(1), 127-138. <https://doi.org/10.1016/j.brainresbull.2006.08.009>
- Chatzikonstantinou, A. (2014). Epilepsy and the hippocampus. *Frontiers of Neurology and Neuroscience*, 34, 121-142. <https://doi.org/10.1159/000356435>
- Chen, W.-F., Chang, H., Huang, L.-T., Lai, M.-C., Yang, C.-H., Wan, T.-H., & Yang, S.-N. (2006). Alterations in long-term seizure susceptibility and the complex of PSD-95 with NMDA receptor from animals previously exposed to perinatal hypoxia. *Epilepsia*, 47(2), 288-296. <https://doi.org/10.1111/j.1528-1167.2006.00420.x>
- Chen, X., Nelson, C. D., Li, X., Winters, C. A., Azzam, R., Sousa, A. A., Leapman, R. D., Gainer, H., Sheng, M., & Reese, T. S. (2011). PSD-95 is required to sustain the molecular organization of the postsynaptic density. *The Journal of Neuroscience*, 31(17), 6329-6338. <https://doi.org/10.1523/JNEUROSCI.5968-10.2011>
- Cherian, A., & Thomas, S. V. (2009). Status epilepticus. *Annals of Indian Academy of Neurology*, 12(3), 140-153. <https://doi.org/10.4103/0972-2327.56312>
- Chu, Y., Jin, X., Parada, I., Pesic, A., Stevens, B., Barres, B., & Prince, D. A. (2010). Enhanced synaptic connectivity and epilepsy in C1q knockout mice. *Proceedings of the National Academy of Sciences of the United States of America*, 107(17), 7975-7980. <https://doi.org/10.1073/pnas.0913449107>
- Chugh, D., & Ekdahl, C. T. (2016). Interactions between microglia and newly formed hippocampal neurons in physiological and seizure-induced inflammatory environment. *Brain Plasticity*, 1(2), 215-221. <https://doi.org/10.3233/BPL-150014>

- Cilio, M. R., Sogawa, Y., Cha, B.-H., Liu, X., Huang, L.-T., & Holmes, G. L. (2003). Long-term effects of status epilepticus in the immature brain are specific for age and model. *Epilepsia*, *44*(4), 518-528. <https://doi.org/10.1046/j.1528-1157.2003.48802.x>
- Codeluppi, S., Fernandez-Zafra, T., Sandor, K., Kjell, J., Liu, Q., Abrams, M., Olson, L., Gray, N. S., Svensson, C. I., & Uhlén, P. (2014). Interleukin-6 secretion by astrocytes is dynamically regulated by PI3K-mTOR-Calcium signaling. *PLOS ONE*, *9*(3), e92649. <https://doi.org/10.1371/journal.pone.0092649>
- Cohen, S. J., & Stackman, R. W. (2015). Assessing rodent hippocampal involvement in the novel object recognition task. A review. *Behavioural Brain Research*, *285*, 105-117. <https://doi.org/10.1016/j.bbr.2014.08.002>
- Cole, A. J., Koh, S., & Zheng, Y. (2002). Are seizures harmful: What can we learn from animal models? *Progress in Brain Research*, *135*, 13-23. [https://doi.org/10.1016/S0079-6123\(02\)35004-0](https://doi.org/10.1016/S0079-6123(02)35004-0)
- Covolan, L., & Mello, L. E. A. M. (2000). Temporal profile of neuronal injury following pilocarpine or kainic acid-induced status epilepticus. *Epilepsy Research*, *39*(2), 133-152. [https://doi.org/10.1016/S0920-1211\(99\)00119-9](https://doi.org/10.1016/S0920-1211(99)00119-9)
- Crino, P. B. (2011). mTOR: A pathogenic signaling pathway in developmental brain malformations. *Trends in Molecular Medicine*, *17*(12), 734-742. <https://doi.org/10.1016/j.molmed.2011.07.008>
- Curatolo, P. (2015). Mechanistic Target of Rapamycin (mTOR) in tuberous sclerosis complex-associated epilepsy. *Pediatric Neurology*, *52*(3), 281-289. <https://doi.org/10.1016/j.pediatrneurol.2014.10.028>
- Curia, G., Longo, D., Biagini, G., Jones, R. S. G., & Avoli, M. (2008). The pilocarpine model of temporal lobe epilepsy. *Journal of Neuroscience Methods*, *172*(2), 143-157. <https://doi.org/10.1016/j.jneumeth.2008.04.019>
- Dachet, F., Bagla, S., Keren-Aviram, G., Morton, A., Balan, K., Saadat, L., Valyi-Nagy, T., Kupsky, W., Song, F., Dratz, E., & Loeb, J. A. (2015). Predicting novel histopathological microlesions in human epileptic brain through transcriptional clustering. *Brain: A Journal of Neurology*, *138*(Pt. 2), 356-370. <https://doi.org/10.1093/brain/awu350>

- D'Adamo, M. C., Catacuzzeno, L., Di Giovanni, G., Franciolini, F., & Pessia, M. (2013). K⁺ channelopathy: Progress in the neurobiology of potassium channels and epilepsy. *Frontiers in Cellular Neuroscience*, *7*. <https://doi.org/10.3389/fncel.2013.00134>
- Dagher, N. N., Najafi, A. R., Kayala, K. M. N., Elmore, M. R. P., White, T. E., Medeiros, R., West, B. L., & Green, K. N. (2015). Colony-stimulating factor 1 receptor inhibition prevents microglial plaque association and improves cognition in 3xTg-AD mice. *Journal of Neuroinflammation*, *12*. <https://doi.org/10.1186/s12974-015-0366-9>
- De Luca, G., Di Giorgio, R. M., Macaione, S., Calpona, P. R., Costantino, S., Di Paola, E. D., De Sarro, A., Ciliberto, G., & De Sarro, G. (2004). Susceptibility to audiogenic seizure and neurotransmitter amino acid levels in different brain areas of IL-6-deficient mice. *Pharmacology, Biochemistry, and Behavior*, *78*(1), 75-81. <https://doi.org/10.1016/j.pbb.2004.02.004>
- De Sarro, G., Russo, E., Ferreri, G., Giuseppe, B., Flocco, M. A., Di Paola, E. D., & De Sarro, A. (2004). Seizure susceptibility to various convulsant stimuli of knockout interleukin-6 mice. *Pharmacology, Biochemistry, and Behavior*, *77*(4), 761-766. <https://doi.org/10.1016/j.pbb.2004.01.012>
- Delint-Ramírez, I., Salcedo-Tello, P., & Bermudez-Rattoni, F. (2008). Spatial memory formation induces recruitment of NMDA receptor and PSD-95 to synaptic lipid rafts. *Journal of Neurochemistry*, *106*(4), 1658-1668. <https://doi.org/10.1111/j.1471-4159.2008.05523.x>
- Demin, K., Berger, J., Holtkamp, M., & Bengner, T. (2018). Are mental distress and cognitive impairment related in temporal lobe epilepsy? *Epilepsy Research*, *146*, 126-131. <https://doi.org/10.1016/j.eplepsyres.2018.07.020>
- Deutsch-Feldman, M., Picetti, R., Seip-Cammack, K., Zhou, Y., & Kreek, M. J. (2015). Effects of handling and vehicle injections on adrenocorticotrophic and corticosterone concentrations in Sprague–Dawley compared with Lewis rats. *Journal of the American Association for Laboratory Animal Science : JAALAS*, *54*(1), 35-39.
- Dong, Y., Li, X., Cheng, J., & Hou, L. (2019). Drug development for Alzheimer's disease: Microglia induced neuroinflammation as a target? *International Journal of Molecular Sciences*, *20*(3). <https://doi.org/10.3390/ijms20030558>

- Du, Y., Lin, J., Shen, J., Ding, S., Ye, M., Wang, L., Wang, Y., Wang, X., Xia, N., Zheng, R., Chen, H., & Xu, H. (2019). Adverse drug reactions associated with six commonly used antiepileptic drugs in southern China from 2003 to 2015. *BMC Pharmacology & Toxicology*, *20*. <https://doi.org/10.1186/s40360-019-0285-y>
- Dupont, S., & Vercueil, L. (2015). Hippocampus: From memory to epilepsy, and back.... *Revue Neurologique*, *171*(3), 203. <https://doi.org/10.1016/j.neurol.2015.03.005>
- Easley-Neal, C., Foreman, O., Sharma, N., Zarrin, A. A., & Weimer, R. M. (2019). CSF1R ligands IL-34 and CSF1 are differentially required for microglia development and maintenance in white and gray matter brain regions. *Frontiers in Immunology*, *10*. <https://doi.org/10.3389/fimmu.2019.02199>
- El-Gamal, M. I., Al-Ameen, S. K., Al-Koumi, D. M., Hamad, M. G., Jalal, N. A., & Oh, C.-H. (2018). Recent advances of Colony-Stimulating Factor-1 Receptor (CSF-1R) kinase and its inhibitors. *Journal of Medicinal Chemistry*, *61*(13) 5450-5466. <https://doi.org/10.1021/acs.jmedchem.7b00873>
- Elmore, M. R. P., Hohsfield, L. A., Kramár, E. A., Soreq, L., Lee, R. J., Pham, S. T., Najafi, A. R., Spangenberg, E. E., Wood, M. A., West, B. L., & Green, K. N. (2018). Replacement of microglia in the aged brain reverses cognitive, synaptic, and neuronal deficits in mice. *Aging Cell*, *17*, e12832. <https://doi.org/10.1111/accel.12832>
- Elmore, M. R. P., Lee, R. J., West, B. L., & Green, K. N. (2015). Characterizing newly repopulated microglia in the adult mouse: Impacts on animal behavior, cell morphology, and neuroinflammation. *PloS One*, *10*(4), e0122912. <https://doi.org/10.1371/journal.pone.0122912>
- Elmore, M. R. P., Najafi, A. R., Koike, M. A., Dagher, N. N., Spangenberg, E. E., Rice, R. A., Kitazawa, M., Matusow, B., Nguyen, H., West, B. L., & Green, K. N. (2014). Colony-stimulating factor 1 receptor signaling is necessary for microglia viability, unmasking a microglia progenitor cell in the adult brain. *Neuron*, *82*(2), 380-397. <https://doi.org/10.1016/j.neuron.2014.02.040>
- England, M. J., Liverman, C. T., Schultz, A. M., & Strawbridge, L. M. (2012). Epilepsy across the spectrum: Promoting health and understanding. A summary of the Institute of Medicine report. *Epilepsy & Behavior: E&B*, *25*(2), 266-276. <https://doi.org/10.1016/j.yebeh.2012.06.016>

- Ennaceur, A., Michalikova, S., & Chazot, P. L. (2006). Models of anxiety: Responses of rats to novelty in an open space and an enclosed space. *Behavioural Brain Research*, *171*(1), 26-49. <https://doi.org/10.1016/j.bbr.2006.03.016>
- Ennaceur, A., Michalikova, S., & Chazot, P. L. (2009). Do rats really express neophobia towards novel objects? Experimental evidence from exposure to novelty and to an object recognition task in an open space and an enclosed space. *Behavioural Brain Research*, *197*(2), 417-434. <https://doi.org/10.1016/j.bbr.2008.10.007>
- Erblich, B., Zhu, L., Etgen, A. M., Dobrenis, K., & Pollard, J. W. (2011). Absence of colony stimulation factor-1 receptor results in loss of microglia, disrupted brain development and olfactory deficits. *PloS One*, *6*(10), e26317. <https://doi.org/10.1371/journal.pone.0026317>
- Erta, M., Quintana, A., & Hidalgo, J. (2012). Interleukin-6, a major cytokine in the central nervous system. *International Journal of Biological Sciences*, *8*(9), 1254-1266. <https://doi.org/10.7150/ijbs.4679>
- Eshleman, J. S., Carlson, B. L., Mladek, A. C., Kastner, B. D., Shide, K. L., & Sarkaria, J. N. (2002). Inhibition of the mammalian target of rapamycin sensitizes U87 xenografts to fractionated radiation therapy. *Cancer Research*, *62*(24), 7291-7297.
- Eyo, U. B., Murugan, M., & Wu, L.-J. (2017). Microglia-neuron communication in epilepsy. *Glia*, *65*(1), 5-18. <https://doi.org/10.1002/glia.23006>
- Eyo, U. B., Peng, J., Murugan, M., Mo, M., Lalani, A., Xie, P., Xu, P., Margolis, D. J., & Wu, L.-J. (2016). Regulation of physical microglia-neuron interactions by fractalkine signaling after status epilepticus. *ENeuro*, *3*(6). <https://doi.org/10.1523/ENEURO.0209-16.2016>
- Eyo, U. B., Peng, J., Swiatkowski, P., Mukherjee, A., Bispo, A., & Wu, L.-J. (2014). Neuronal hyperactivity recruits microglial processes via neuronal NMDA receptors and microglial P2Y12 receptors after status epilepticus. *The Journal of Neuroscience*, *34*(32), 10528-10540. <https://doi.org/10.1523/JNEUROSCI.0416-14.2014>
- Eyo, U. B., & Wu, L.-J. (2013). Bidirectional microglia-neuron communication in the healthy brain. *Neural Plasticity*, *2013*, 456857. <https://doi.org/10.1155/2013/456857>
- Eyo, U. B., & Wu, L.-J. (2019). Microglia: Lifelong patrolling immune cells of the brain. *Progress in Neurobiology*, *179*, 101614. <https://doi.org/10.1016/j.pneurobio.2019.04.003>

- Faria, L. C., Gu, F., Parada, I., Barres, B., Luo, Z. D., & Prince, D. A. (2017). Epileptiform activity and behavioral arrests in mice overexpressing the calcium channel subunit $\alpha 2\delta$ -1. *Neurobiology of Disease*, *102*, 70-80. <https://doi.org/10.1016/j.nbd.2017.01.009>
- Feng, L., Shu, Y., Wu, Q., Liu, T., Long, H., Yang, H., Li, Y., & Xiao, B. (2017). EphA4 may contribute to microvessel remodeling in the hippocampal CA1 and CA3 areas in a mouse model of temporal lobe epilepsy. *Molecular Medicine Reports*, *15*(1), 37-46. <https://doi.org/10.3892/mmr.2016.6017>
- Feng, L., Murugan, M., Bosco, D. B., Liu, Y., Peng, J., Worrell, G. A., Wang, H.-L., Ta, L. E., Richardson, J. R., Shen, Y., & Wu, L.-J. (2019). Microglial proliferation and monocyte infiltration contribute to microgliosis following status epilepticus. *Glia*, *67*(8), 1434-1448. <https://doi.org/10.1002/glia.23616>
- Fernández-Arjona, M. del M., Grondona, J. M., Granados-Durán, P., Fernández-Llebrez, P., & López-Ávalos, M. D. (2017). Microglia morphological categorization in a rat model of neuroinflammation by hierarchical cluster and principal components analysis. *Frontiers in Cellular Neuroscience*, *11*. <https://doi.org/10.3389/fncel.2017.00235>
- Feyissa, D. D., Aher, Y. D., Engidawork, E., Höger, H., Lubec, G., & Korz, V. (2017). Individual differences in male rats in a behavioral test battery: A multivariate statistical approach. *Frontiers in Behavioral Neuroscience*, *11*. <https://doi.org/10.3389/fnbeh.2017.00026>
- Filipello, F., Morini, R., Corradini, I., Zerbi, V., Canzi, A., Michalski, B., Erreni, M., Markicevic, M., Starvaggi-Cucuzza, C., Otero, K., Piccio, L., Cignarella, F., Perrucci, F., Tamborini, M., Genua, M., Rajendran, L., Menna, E., Vetrano, S., Fahnestock, M., . . . Matteoli, M. (2018). The Microglial Innate Immune Receptor TREM2 Is Required for Synapse Elimination and Normal Brain Connectivity. *Immunity*, *48*(5), 979-991.e8. <https://doi.org/10.1016/j.immuni.2018.04.016>
- Fischer, K. E., Gelfond, J. A. L., Soto, V. Y., Han, C., Someya, S., Richardson, A., & Austad, S. N. (2015). Health effects of long-term rapamycin treatment: The impact on mouse health of enteric rapamycin treatment from four months of age throughout life. *PLOS ONE*, *10*(5), e0126644. <https://doi.org/10.1371/journal.pone.0126644>
- Frankel, W. N. (2009). Genetics of complex neurological disease: Challenges and opportunities for modeling epilepsy in mice and rats. *Trends in Genetics*, *25*(8), 361-367. <https://doi.org/10.1016/j.tig.2009.07.001>

- Frigerio, F., Flynn, C., Han, Y., Lyman, K., Lugo, J. N., Ravizza, T., Ghestem, A., Pitsch, J., Becker, A., Anderson, A. E., Vezzani, A., Chetkovich, D., & Bernard, C. (2018). Neuroinflammation alters integrative properties of rat hippocampal pyramidal cells. *Molecular Neurobiology*, *55*(9), 7500-7511. <https://doi.org/10.1007/s12035-018-0915-1>
- Fuhrmann, M., Bittner, T., Jung, C. K. E., Burgold, S., Page, R. M., Mitteregger, G., Haass, C., LaFerla, F. M., Kretschmar, H., & Herms, J. (2010). Microglial Cx3cr1 knockout prevents neuron loss in a mouse model of Alzheimer's disease. *Nature Neuroscience*, *13*(4), 411-413. <https://doi.org/10.1038/nn.2511>
- Fumagalli, M., Lombardi, M., Gressens, P., & Verderio, C. (2018). How to reprogram microglia toward beneficial functions. *Glia*, *66*(12), 2531-2549. <https://doi.org/10.1002/glia.23484>
- Gawel, K., Gibula, E., Marszalek-Grabska, M., Filarowska, J., & Kotlinska, J. H. (2019). Assessment of spatial learning and memory in the Barnes maze task in rodents—Methodological consideration. *Naunyn-Schmiedeberg's Archives of Pharmacology*, *392*(1), 1-18. <https://doi.org/10.1007/s00210-018-1589-y>
- Giovagnoli, A. R., & Avanzini, G. (1999). Learning and memory impairment in patients with temporal lobe epilepsy: Relation to the presence, type, and location of brain lesion. *Epilepsia*, *40*(7), 904-911. <https://doi.org/10.1111/j.1528-1157.1999.tb00797.x>
- Glenn, J. A., Booth, P. L., & Thomas, W. E. (1991). Pinocytotic activity in ramified microglia. *Neuroscience Letters*, *123*(1), 27-31. [https://doi.org/10.1016/0304-3940\(91\)90150-r](https://doi.org/10.1016/0304-3940(91)90150-r)
- Glien, M., Brandt, C., Potschka, H., & Löscher, W. (2002). Effects of the novel antiepileptic drug levetiracetam on spontaneous recurrent seizures in the rat pilocarpine model of temporal lobe epilepsy. *Epilepsia*, *43*(4), 350-357. <https://doi.org/10.1046/j.1528-1157.2002.18101.x>
- Glushakov, A. V., Glushakova, O. Y., Doré, S., Carney, P. R., & Hayes, R. L. (2016). Animal models of posttraumatic seizures and epilepsy. *Methods in Molecular Biology*, *1462*, 481-519. https://doi.org/10.1007/978-1-4939-3816-2_27
- Goffin, K., Nissinen, J., Van Laere, K., & Pitkänen, A. (2007). Cyclicity of spontaneous recurrent seizures in pilocarpine model of temporal lobe epilepsy in rat. *Experimental Neurology*, *205*(2), 501-505. <https://doi.org/10.1016/j.expneurol.2007.03.008>

- Golarai, G., Greenwood, A. C., Feeney, D. M., & Connor, J. A. (2001). Physiological and structural evidence for hippocampal involvement in persistent seizure susceptibility after traumatic brain injury. *The Journal of Neuroscience*, *21*(21), 8523-8537.
- Gomes-Leal, W. (2019). Why microglia kill neurons after neural disorders? The friendly fire hypothesis. *Neural Regeneration Research*, *14*(9), 1499–1502. <https://doi.org/10.4103/1673-5374.255359>
- Gosselin, D., Skola, D., Coufal, N. G., Holtman, I. R., Schlachetzki, J. C. M., Sajti, E., Jaeger, B. N., O'Connor, C., Fitzpatrick, C., Pasillas, M. P., Pena, M., Adair, A., Gonda, D. D., Levy, M. L., Ransohoff, R. M., Gage, F. H., & Glass, C. K. (2017). An environment-dependent transcriptional network specifies human microglia identity. *Science*, *356*(6344). <https://doi.org/10.1126/science.aal3222>
- Grayson, B., Leger, M., Piercy, C., Adamson, L., Harte, M., & Neill, J. C. (2015). Assessment of disease-related cognitive impairments using the novel object recognition (NOR) task in rodents. *Behavioural Brain Research*, *285*, 176-193. <https://doi.org/10.1016/j.bbr.2014.10.025>
- Greene, D. L., Kosenko, A., & Hoshi, N. (2018). Attenuating M-current suppression in vivo by a mutant *Kcnq2* gene knock-in reduces seizure burden and prevents status epilepticus-induced neuronal death and epileptogenesis. *Epilepsia*, *59*(10), 1908-1918. <https://doi.org/10.1111/epi.14541>
- Greenlund, S. F., Croft, J. B., & Kobau, R. (2017). Epilepsy by the numbers: Epilepsy deaths by age, race/ethnicity, and gender in the United States significantly increased from 2005 to 2014. *Epilepsy & Behavior*, *69*, 28-30. <https://doi.org/10.1016/j.yebeh.2017.01.016>
- Griffiths, M., Neal, J. W., & Gasque, P. (2007). Innate immunity and protective neuroinflammation: New emphasis on the role of neuroimmune regulatory proteins. *International Review of Neurobiology*, *82*, 29-55. [https://doi.org/10.1016/S0074-7742\(07\)82002-2](https://doi.org/10.1016/S0074-7742(07)82002-2)
- Gross, C., Yao, X., Engel, T., Tiwari, D., Xing, L., Rowley, S., Danielson, S. W., Thomas, K. T., Jimenez-Mateos, E. M., Schroeder, L. M., Pun, R. Y. K., Danzer, S. C., Henshall, D. C., & Bassell, G. J. (2016). MicroRNA-mediated downregulation of the potassium channel Kv4.2 contributes to seizure onset. *Cell Reports*, *17*(1), 37-45. <https://doi.org/10.1016/j.celrep.2016.08.074>

- Guadagno, J., Xu, X., Karajgikar, M., Brown, A., & Cregan, S. P. (2013). Microglia-derived TNF α induces apoptosis in neural precursor cells via transcriptional activation of the Bcl-2 family member Puma. *Cell Death & Disease*, 4, e538. <https://doi.org/10.1038/cddis.2013.59>
- Hall, A. M., Throesch, B. T., Buckingham, S. C., Markwardt, S. J., Peng, Y., Wang, Q., Hoffman, D. A., & Roberson, E. D. (2015). Tau-Dependent Kv4.2 depletion and dendritic hyperexcitability in a mouse model of Alzheimer's disease. *The Journal of Neuroscience*, 35(15), 6221-6230. <https://doi.org/10.1523/JNEUROSCI.2552-14.2015>
- Hammond, R. S., Tull, L. E., & Stackman, R. W. (2004). On the delay-dependent involvement of the hippocampus in object recognition memory. *Neurobiology of Learning and Memory*, 82(1), 26-34. <https://doi.org/10.1016/j.nlm.2004.03.005>
- Han, J., Harris, R. A., & Zhang, X.-M. (2017). An updated assessment of microglia depletion: Current concepts and future directions. *Molecular Brain*, 10(1), 25. <https://doi.org/10.1186/s13041-017-0307-x>
- Harrison, J. K., Jiang, Y., Chen, S., Xia, Y., Maciejewski, D., McNamara, R. K., Streit, W. J., Salafranca, M. N., Adhikari, S., Thompson, D. A., Botti, P., Bacon, K. B., & Feng, L. (1998). Role for neuronally derived fractalkine in mediating interactions between neurons and CX3CR1-expressing microglia. *Proceedings of the National Academy of Sciences of the United States of America*, 95(18), 10896-10901. <https://doi.org/10.1073/pnas.95.18.10896>
- Hasegawa, S., Yamaguchi, M., Nagao, H., Mishina, M., & Mori, K. (2007). Enhanced cell-to-cell contacts between activated microglia and pyramidal cell dendrites following kainic acid-induced neurotoxicity in the hippocampus. *Journal of Neuroimmunology*, 186(1-2), 75-85. <https://doi.org/10.1016/j.jneuroim.2007.03.005>
- Heindl, S., Gesierich, B., Benakis, C., Llovera, G., Duering, M., & Liesz, A. (2018). Automated morphological analysis of microglia after stroke. *Frontiers in Cellular Neuroscience*, 12, 106. <https://doi.org/10.3389/fncel.2018.00106>
- Herfel, T. (2018, July 10). *Custom PLX3397 rat diets* [Personal communication].

- Hernandez, M. X., Jiang, S., Cole, T. A., Chu, S.-H., Fonseca, M. I., Fang, M. J., Hohsfield, L. A., Torres, M. D., Green, K. N., Wetsel, R. A., Mortazavi, A., & Tenner, A. J. (2017). Prevention of C5aR1 signaling delays microglial inflammatory polarization, favors clearance pathways and suppresses cognitive loss. *Molecular Neurodegeneration*, *12*. <https://doi.org/10.1186/s13024-017-0210-z>
- Hickman, S. E., Allison, E. K., & El Khoury, J. (2008). Microglial dysfunction and defective beta-amyloid clearance pathways in aging Alzheimer's disease mice. *The Journal of Neuroscience*, *28*(33), 8354-8360. <https://doi.org/10.1523/JNEUROSCI.0616-08.2008>
- Hiragi, T., Ikegaya, Y., & Koyama, R. (2018). Microglia after seizures and in epilepsy. *Cells*, *7*(4). <https://doi.org/10.3390/cells7040026>
- Hocker. (2015). Status Epilepticus. *Continuum (Minneapolis, Minn.)*, *21*(5 Neurocritical Care), 1362–1383. <https://doi.org/10.1212/CON.0000000000000225>
- Holley, A. J., Hodges, S. L., Nolan, S. O., Binder, M., Okoh, J. T., Ackerman, K., Tomac, L. A., & Lugo, J. N. (2018). A single seizure selectively impairs hippocampal-dependent memory and is associated with alterations in PI3K/Akt/mTOR and FMRP signaling. *Epilepsia Open*, *3*(4), 511-523. <https://doi.org/10.1002/epi4.12273>
- Holtman, I. R., Raj, D. D., Miller, J. A., Schaafsma, W., Yin, Z., Brouwer, N., Wes, P. D., Möller, T., Orre, M., Kamphuis, W., Hol, E. M., Boddeke, E. W. G. M., & Eggen, B. J. L. (2015). Induction of a common microglia gene expression signature by aging and neurodegenerative conditions: A co-expression meta-analysis. *Acta Neuropathologica Communications*, *3*, 31. <https://doi.org/10.1186/s40478-015-0203-5>
- Hong, S., Dissing-Olesen, L., & Stevens, B. (2016). New insights on the role of microglia in synaptic pruning in health and disease. *Current Opinion in Neurobiology*, *36*, 128-134. <https://doi.org/10.1016/j.conb.2015.12.004>
- Hong, S., & Stevens, B. (2016). Microglia: Phagocytosing to clear, sculpt, and eliminate. *Developmental Cell*, *38*(2), 126-128. <https://doi.org/10.1016/j.devcel.2016.07.006>
- Hong, Y., Deng, N., Jin, H.-N., Xuan, Z.-Z., Qian, Y.-X., Wu, Z., & Xie, W. (2018). Saikosaponin A modulates remodeling of Kv4.2-mediated A-type voltage-gated potassium currents in rat chronic temporal lobe epilepsy. *Drug Design, Development and Therapy*, *12*, 2945-2958. <https://doi.org/10.2147/DDDT.S166408>

- Hwang, J.-Y., Aromolaran, K. A., & Zukin, R. S. (2013). Epigenetic mechanisms in stroke and epilepsy. *Neuropsychopharmacology*, *38*(1), 167-182. <https://doi.org/10.1038/npp.2012.134>
- Iacobas, D. A., Iacobas, S., Nebieridze, N., Velíšek, L., & Velíšková, J. (2018). Estrogen protects neurotransmission transcriptome during status epilepticus. *Frontiers in Neuroscience*, *12*, 332. <https://doi.org/10.3389/fnins.2018.00332>
- Imai, Y., & Kohsaka, S. (2002). Intracellular signaling in M-CSF-induced microglia activation: Role of Iba1. *Glia*, *40*(2), 164-174. <https://doi.org/10.1002/glia.10149>
- Jäkel, S., & Dimou, L. (2017). Glial cells and their function in the adult brain: A journey through the history of their ablation. *Frontiers in Cellular Neuroscience*, *11*. <https://doi.org/10.3389/fncel.2017.00024>
- Janda, E., Boi, L., & Carta, A. R. (2018). Microglial phagocytosis and its regulation: A therapeutic target in Parkinson's disease? *Frontiers in Molecular Neuroscience*, *11*. <https://doi.org/10.3389/fnmol.2018.00144>
- Jessberger, S., & Parent, J. M. (2015). Epilepsy and adult neurogenesis. *Cold Spring Harbor Perspectives in Biology*, *7*(12). <https://doi.org/10.1101/cshperspect.a020677>
- Jha, M. K., Jo, M., Kim, J.-H., & Suk, K. (2019). Microglia-astrocyte crosstalk: An intimate molecular conversation. *The Neuroscientist*, *25*(3), 227-240. <https://doi.org/10.1177/1073858418783959>
- Jin, W.-N., Shi, S. X.-Y., Li, Z., Li, M., Wood, K., Gonzales, R. J., & Liu, Q. (2017). Depletion of microglia exacerbates postischemic inflammation and brain injury. *Journal of Cerebral Blood Flow and Metabolism*, *37*(6), 2224-2236. <https://doi.org/10.1177/0271678X17694185>
- Jung, S., Jones, T. D., Lugo, J. N., Sheerin, A. H., Miller, J. W., D'Ambrosio, R., Anderson, A. E., & Poolos, N. P. (2007). Progressive dendritic HCN channelopathy during epileptogenesis in the rat pilocarpine model of epilepsy. *The Journal of Neuroscience*, *27*(47), 13012-13021. <https://doi.org/10.1523/JNEUROSCI.3605-07.2007>
- Kandratavicius, L., Balista, P. A., Lopes-Aguiar, C., Ruggiero, R. N., Umeoka, E. H., Garcia-Cairasco, N., Bueno-Junior, L. S., & Leite, J. P. (2014). Animal models of epilepsy: Use and limitations. *Neuropsychiatric Disease and Treatment*, *10*, 1693-1705. <https://doi.org/10.2147/NDT.S50371>

- Kaur, C., Sivakumar, V., Zou, Z., & Ling, E.-A. (2014). Microglia-derived proinflammatory cytokines tumor necrosis factor-alpha and interleukin-1beta induce Purkinje neuronal apoptosis via their receptors in hypoxic neonatal rat brain. *Brain Structure & Function*, 219(1), 151-170. <https://doi.org/10.1007/s00429-012-0491-5>
- Keith, D., & El-Husseini, A. (2008). Excitation control: Balancing PSD-95 function at the synapse. *Frontiers in Molecular Neuroscience*, 1. <https://doi.org/10.3389/neuro.02.004.2008>
- Kettenmann, H., Hanisch, U.-K., Noda, M., & Verkhratsky, A. (2011). Physiology of microglia. *Physiological Reviews*, 91(2), 461-553. <https://doi.org/10.1152/physrev.00011.2010>
- Kierdorf, K., Erny, D., Goldmann, T., Sander, V., Schulz, C., Perdiguero, E. G., Wieghofer, P., Heinrich, A., Riemke, P., Hölscher, C., Müller, D. N., Luckow, B., Brocker, T., Debowski, K., Fritz, G., Opdenakker, G., Diefenbach, A., Biber, K., Heikenwalder, M., . . . Prinz, M. (2013). Microglia emerge from erythromyeloid precursors via Pu.1- and Irf8-dependent pathways. *Nature Neuroscience*, 16(3), 273-280. <https://doi.org/10.1038/nn.3318>
- Kosonowska, E., Janeczko, K., & Setkowicz, Z. (2015). Inflammation induced at different developmental stages affects differently the range of microglial reactivity and the course of seizures evoked in the adult rat. *Epilepsy & Behavior*, 49, 66-70. <https://doi.org/10.1016/j.yebeh.2015.04.063>
- Kwan, P., Arzimanoglou, A., Berg, A. T., Brodie, M. J., Allen Hauser, W., Mathern, G., Moshé, S. L., Perucca, E., Wiebe, S., & French, J. (2010). Definition of drug resistant epilepsy: Consensus proposal by the ad hoc task force of the ILAE Commission on Therapeutic Strategies. *Epilepsia*, 51(6), 1069-1077. <https://doi.org/10.1111/j.1528-1167.2009.02397.x>
- Lalancette-Hébert, M., Gowing, G., Simard, A., Weng, Y. C., & Kriz, J. (2007). Selective ablation of proliferating microglial cells exacerbates ischemic injury in the brain. *The Journal of Neuroscience*, 27(10), 2596-2605. <https://doi.org/10.1523/JNEUROSCI.5360-06.2007>
- Langfitt, J., & Wiebe, S. (2002). Cost-effectiveness of epilepsy therapy: How should treatment effects be measured? *Epilepsia*, 43(Suppl 4), 17-24. <https://doi.org/10.1046/j.1528-1157.43.s.4.4.x>
- Leal, M. C., Casabona, J. C., Puntel, M., & Pitossi, F. (2013). Interleukin-1 β and tumor necrosis factor- α : Reliable targets for protective therapies in Parkinson's Disease? *Frontiers in Cellular Neuroscience*, 7. <https://doi.org/10.3389/fncel.2013.00053>

- Lehmann, T.-N., Gabriel, S., Eilers, A., Njunting, M., Kovacs, R., Schulze, K., Lanksch, W. R., & Heinemann, U. (2001). Fluorescent tracer in pilocarpine-treated rats shows widespread aberrant hippocampal neuronal connectivity. *European Journal of Neuroscience*, *14*(1), 83-95. <https://doi.org/10.1046/j.0953-816x.2001.01632.x>
- Lerche, H., Shah, M., Beck, H., Noebels, J., Johnston, D., & Vincent, A. (2013). Ion channels in genetic and acquired forms of epilepsy. *The Journal of Physiology*, *591*(Pt 4), 753-764. <https://doi.org/10.1113/jphysiol.2012.240606>
- Lévesque, M., Avoli, M., & Bernard, C. (2016). Animal models of temporal lobe epilepsy following systemic chemoconvulsant administration. *Journal of Neuroscience Methods*, *260*, 45-52. <https://doi.org/10.1016/j.jneumeth.2015.03.009>
- Lévi-Strauss, M., & Mallat, M. (1987). Primary cultures of murine astrocytes produce C3 and factor B, two components of the alternative pathway of complement activation. *Journal of Immunology*, *139*(7), 2361-2366.
- Li, J., Kim, J. S., Abejuela, V. A., Lamano, J. B., Klein, N. J., & Christian, C. A. (2016). Disrupted female estrous cyclicity in the intrahippocampal kainic acid mouse model of temporal lobe epilepsy. *Epilepsia Open*, *2*(1), 39-47. <https://doi.org/10.1002/epi4.12026>
- Li, J., Robare, J. A., Gao, L., Ghane, M. A., Flaws, J. A., Nelson, M. E., & Christian, C. A. (2018). Dynamic and sex-specific changes in gonadotropin-releasing hormone neuron activity and excitability in a mouse model of temporal lobe epilepsy. *ENeuro*, *5*(5). <https://doi.org/10.1523/ENEURO.0273-18.2018>
- Li, J., Chen, K., Zhu, L., & Pollard, J. W. (2006). Conditional deletion of the colony stimulating factor-1 receptor (c-fms proto-oncogene) in mice. *Genesis*, *44*(7), 328-335. <https://doi.org/10.1002/dvg.20219>
- Li, M., Li, Z., Ren, H., Jin, W.-N., Wood, K., Liu, Q., Sheth, K. N., & Shi, F.-D. (2017). Colony stimulating factor 1 receptor inhibition eliminates microglia and attenuates brain injury after intracerebral hemorrhage. *Journal of Cerebral Blood Flow and Metabolism*, *37*(7), 2383-2395. <https://doi.org/10.1177/0271678X16666551>

- Li, Q., Cheng, Z., Zhou, L., Darmanis, S., Neff, N. F., Okamoto, J., Gulati, G., Bennett, M. L., Sun, L. O., Clarke, L. E., Marschallinger, J., Yu, G., Quake, S. R., Wyss-Coray, T., & Barres, B. A. (2019). Developmental heterogeneity of microglia and brain myeloid cells revealed by deep single-cell RNA sequencing. *Neuron*, *101*(2), 207-223.e10. <https://doi.org/10.1016/j.neuron.2018.12.006>
- Lian, H., Litvinchuk, A., Chiang, A. C.-A., Aithmitti, N., Jankowsky, J. L., & Zheng, H. (2016). Astrocyte-microglia cross talk through complement activation modulates amyloid pathology in mouse models of Alzheimer's disease. *The Journal of Neuroscience*, *36*(2), 577-589. <https://doi.org/10.1523/JNEUROSCI.2117-15.2016>
- Loewen, J. L., Barker-Haliski, M. L., Dahle, E. J., White, H. S., & Wilcox, K. S. (2016). Neuronal injury, gliosis, and glial proliferation in two models of temporal lobe epilepsy. *Journal of Neuropathology and Experimental Neurology*, *75*(4), 366-378. <https://doi.org/10.1093/jnen/nlw008>
- Long, J. M., Kalehua, A. N., Muth, N. J., Calhoun, M. E., Jucker, M., Hengemihle, J. M., Ingram, D. K., & Mouton, P. R. (1998). Stereological analysis of astrocyte and microglia in aging mouse hippocampus. *Neurobiology of Aging*, *19*(5), 497-503.
- Long, J. M., Kalehua, A. N., Muth, N. J., Hengemihle, J. M., Jucker, M., Calhoun, M. E., Ingram, D. K., & Mouton, P. R. (1998). Stereological estimation of total microglia number in mouse hippocampus. *Journal of Neuroscience Methods*, *84*(1-2), 101-108.
- Lopes, A. F., Monteiro, J. P., Fonseca, M. J., Robalo, C., & Simões, M. R. (2014). Memory functioning in children with epilepsy: Frontal lobe epilepsy, childhood absence epilepsy, and benign epilepsy with centrotemporal spikes. *Behavioural Neurology*, *2014*, 218637. <https://doi.org/10.1155/2014/218637>
- Löscher, W. (2011). Critical review of current animal models of seizures and epilepsy used in the discovery and development of new antiepileptic drugs. *Seizure*, *20*(5), 359-368. <https://doi.org/10.1016/j.seizure.2011.01.003>
- Losi, G., Cammarota, M., & Carmignoto, G. (2012). The role of astroglia in the epileptic brain. *Frontiers in Pharmacology*, *3*. <https://doi.org/10.3389/fphar.2012.00132>

- Lossius, M. I., Hessen, E., Mowinckel, P., Stavem, K., Erikssen, J., Gulbrandsen, P., & Gjerstad, L. (2008). Consequences of antiepileptic drug withdrawal: A randomized, double-blind study (Akershus Study). *Epilepsia*, *49*(3), 455-463. <https://doi.org/10.1111/j.1528-1167.2007.01323.x>
- Low, D., & Ginhoux, F. (2018). Recent advances in the understanding of microglial development and homeostasis. *Cellular Immunology*, *330*, 68-78. <https://doi.org/10.1016/j.cellimm.2018.01.004>
- Luchena, C., Zuazo-Ibarra, J., Alberdi, E., Matute, C., & Capetillo-Zarate, E. (2018). Contribution of neurons and glial cells to complement-mediated synapse removal during development, aging and in Alzheimer's disease. *Mediators of Inflammation*; Hindawi. <https://doi.org/10.1155/2018/2530414>
- Lugo, J. N., Brewster, A. L., Spencer, C. M., & Anderson, A. E. (2012). Kv4.2 knockout mice have hippocampal-dependent learning and memory deficits. *Learning & Memory*, *19*(5), 182-189. <https://doi.org/10.1101/lm.023614.111>
- Ma, Y., Ramachandran, A., Ford, N., Parada, I., & Prince, D. A. (2013). Remodeling of dendrites and spines in the C1q knockout model of genetic epilepsy. *Epilepsia*, *54*(7), 1232-1239. <https://doi.org/10.1111/epi.12195>
- Manno, I., Macchi, F., Caleo, M., & Bozzi, Y. (2011). Environmental enrichment reduces spontaneous seizures in the Q54 transgenic mouse model of temporal lobe epilepsy. *Epilepsia*, *52*(9), e113-e117. <https://doi.org/10.1111/j.1528-1167.2011.03166.x>
- Marcelin, B., Lugo, J. N., Brewster, A. L., Liu, Z., Lewis, A. S., McClelland, S., Chetkovich, D. M., Baram, T. Z., Anderson, A. E., Becker, A., Esclapez, M., & Bernard, C. (2012). Differential dorso-ventral distributions of Kv4.2 and HCN proteins confer distinct integrative properties to hippocampal CA1 pyramidal cell distal dendrites. *The Journal of Biological Chemistry*, *287*(21), 17656-17661. <https://doi.org/10.1074/jbc.C112.367110>
- Marini, C., Porro, A., Rastetter, A., Dalle, C., Rivolta, I., Bauer, D., Oegema, R., Nava, C., Parrini, E., Mei, D., Mercer, C., Dhamija, R., Chambers, C., Coubes, C., Thévenon, J., Kuentz, P., Julia, S., Pasquier, L., Dubourg, C., . . . Depienne, C. (2018). HCN1 mutation spectrum: From neonatal epileptic encephalopathy to benign generalized epilepsy and beyond. *Brain: A Journal of Neurology*, *141*(11), 3160-3178. <https://doi.org/10.1093/brain/awy263>

- Mattison, H. A., Nie, H., Gao, H., Zhou, H., Hong, J.-S., & Zhang, J. (2013). Suppressed pro-inflammatory response of microglia in CX3CR1 knockout mice. *Journal of Neuroimmunology*, 257(1–2), 110-115. <https://doi.org/10.1016/j.jneuroim.2013.02.008>
- Mazarati, A. (2008). Epilepsy and forgetfulness: One impairment, multiple mechanisms. *Epilepsy Currents*, 8(1), 25-26. <https://doi.org/10.1111/j.1535-7511.2007.00224.x>
- Mazumder, A. G., Sharma, P., Patial, V., & Singh, D. (2017). Ginkgo biloba L. attenuates spontaneous recurrent seizures and associated neurological conditions in lithium-pilocarpine rat model of temporal lobe epilepsy through inhibition of mammalian target of rapamycin pathway hyperactivation. *Journal of Ethnopharmacology*, 204, 8-17. <https://doi.org/10.1016/j.jep.2017.03.060>
- McEwen, B. S. (1994). Corticosteroids and hippocampal plasticity. *Annals of the New York Academy of Sciences*, 746, 134–142; discussion 142-144, 178-179.
- Meador, K. J., Baker, G., Cohen, M. J., Gaily, E., & Westerveld, M. (2007). Cognitive/behavioral teratogenic effects of antiepileptic drugs. *Epilepsy & Behavior*, 11(3), 292-302. <https://doi.org/10.1016/j.yebeh.2007.08.009>
- Medvedeva, Y. V., Ji, S. G., Yin, H. Z., & Weiss, J. H. (2017). Differential vulnerability of CA1 versus CA3 pyramidal neurons after ischemia: Possible relationship to sources of Zn²⁺ accumulation and its entry into and prolonged effects on mitochondria. *The Journal of Neuroscience*, 37(3), 726-737. <https://doi.org/10.1523/JNEUROSCI.3270-16.2016>
- Memarian, N., Thompson, P. M., Engel, J., & Staba, R. J. (2013). Quantitative analysis of structural neuroimaging of mesial temporal lobe epilepsy. *Imaging in Medicine*, 5(3). <https://doi.org/10.2217/iim.13.28>
- Ménard, C., Pfau, M. L., Hodes, G. E., & Russo, S. J. (2017). Immune and neuroendocrine mechanisms of stress vulnerability and resilience. *Neuropsychopharmacology*, 42(1), 62-80. <https://doi.org/10.1038/npp.2016.90>
- Meucci, O., Fatatis, A., Simen, A. A., & Miller, R. J. (2000). Expression of CX3CR1 chemokine receptors on neurons and their role in neuronal survival. *Proceedings of the National Academy of Sciences of the United States of America*, 97(14), 8075–8080. <https://doi.org/10.1073/pnas.090017497>

- Minami, M., Kuraishi, Y., & Satoh, M. (1991). Effects of kainic acid on messenger RNA levels of IL-1 beta, IL-6, TNF alpha and LIF in the rat brain. *Biochemical and Biophysical Research Communications*, *176*(2), 593-598. [https://doi.org/10.1016/s0006-291x\(05\)80225-6](https://doi.org/10.1016/s0006-291x(05)80225-6)
- Morgan, B. P. (2018). Complement in the pathogenesis of Alzheimer's disease. *Seminars in Immunopathology*, *40*(1), 113-124. <https://doi.org/10.1007/s00281-017-0662-9>
- Morimoto, K., Fahnestock, M., & Racine, R. J. (2004). Kindling and status epilepticus models of epilepsy: Rewiring the brain. *Progress in Neurobiology*, *73*(1), 1-60. <https://doi.org/10.1016/j.pneurobio.2004.03.009>
- Morin-Brureau, M., Milior, G., Royer, J., Chali, F., LeDuigou, C., Savary, E., Blugeon, C., Jourden, L., Akbar, D., Dupont, S., Navarro, V., Baulac, M., Bielle, F., Mathon, B., Clemenceau, S., & Miles, R. (2018). Microglial phenotypes in the human epileptic temporal lobe. *Brain*, *141*(12), 3343–3360. <https://doi.org/10.1093/brain/awy276>
- Najafi, A. R., Crapser, J., Jiang, S., Ng, W., Mortazavi, A., West, B. L., & Green, K. N. (2018). A limited capacity for microglial repopulation in the adult brain. *Glia*, *66*(11), 2385-2396. <https://doi.org/10.1002/glia.23477>
- National Research Council (US) Subcommittee on Laboratory Animal Nutrition. (1995). *Nutrient requirements of laboratory animals: Fourth revised edition, 1995*. Washington, DC: National Academies Press (US). <http://www.ncbi.nlm.nih.gov/books/NBK231927/>
- Naydenov, K., Petkov, Y., Manchev, I., Chengeliyska, V., & Komsiyiska, D. (2019). Comorbidity of epilepsy and mental disorders. *Trakia Journal of Sciences*, *17*, 4.
- Neher, J. J., & Cunningham, C. (2019). Priming microglia for innate immune memory in the brain. *Trends in Immunology*, *40*(4), 358-374. <https://doi.org/10.1016/j.it.2019.02.001>
- Neniskyte, U., Vilalta, A., & Brown, G. C. (2014). Tumour necrosis factor alpha-induced neuronal loss is mediated by microglial phagocytosis. *Febs Letters*, *588*(17), 2952-2956. <https://doi.org/10.1016/j.febslet.2014.05.046>
- Nguyen, L. H., Brewster, A. L., Clark, M. E., Regnier-Golanov, A., Sunnen, C. N., Patil, V. V., D'Arcangelo, G., & Anderson, A. E. (2015). MTOR inhibition suppresses established epilepsy in a mouse model of cortical dysplasia. *Epilepsia*, *56*(4), 636-646. <https://doi.org/10.1111/epi.12946>

- Nguyen, L. H., Mahadeo, T., & Bordey, A. (2019). MTOR hyperactivity levels influence the severity of epilepsy and associated neuropathology in an experimental model of tuberous sclerosis complex and focal cortical dysplasia. *Journal of Neuroscience*, *39*(14), 2762-2773. <https://doi.org/10.1523/JNEUROSCI.2260-18.2019>
- Nirwan, N., Vyas, P., & Vohora, D. (2018). Animal models of status epilepticus and temporal lobe epilepsy: A narrative review. *Reviews in the Neurosciences*, *29*(7), 757-770. <https://doi.org/10.1515/revneuro-2017-0086>
- Nolan, M. F., Malleret, G., Dudman, J. T., Buhl, D. L., Santoro, B., Gibbs, E., Vronskaya, S., Buzsáki, G., Siegelbaum, S. A., Kandel, E. R., & Morozov, A. (2004). A behavioral role for dendritic integration: HCN1 channels constrain spatial memory and plasticity at inputs to distal dendrites of CA1 pyramidal neurons. *Cell*, *119*(5), 719-732. <https://doi.org/10.1016/j.cell.2004.11.020>
- Nouha, F., Sawsan, D., Salma, S., Olfa, H., Hanen, H. K., Mariem, D., & Chokri, M. (2018). Cognitive impairment in patients with temporal lobe epilepsy. *Journal of Neuropsychiatry*, *2*(2), 5. <https://doi.org/10.21767/2471-8548.10009>
- Ohgomori, T., & Jinno, S. (2019). The expression of keratan sulfate reveals a unique subset of microglia in the mouse hippocampus after pilocarpine-induced status epilepticus. *The Journal of Comparative Neurology*, *528*, 18-35. <https://doi.org/10.1002/cne.24734>
- Ohsawa, K., Imai, Y., Sasaki, Y., & Kohsaka, S. (2004). Microglia/macrophage-specific protein Iba1 binds to fimbrin and enhances its actin-bundling activity. *Journal of Neurochemistry*, *88*(4), 844-856. <https://doi.org/10.1046/j.1471-4159.2003.02213.x>
- Oosterhof, N., Chang, I. J., Karimiani, E. G., Kuil, L. E., Jensen, D. M., Daza, R., Young, E., Astle, L., van der Linde, H. C., Shivaram, G. M., Demmers, J., Latimer, C. S., Keene, C. D., Loter, E., Maroofian, R., van Ham, T. J., Hevner, R. F., & Bennett, J. T. (2019). Homozygous mutations in CSF1R cause a pediatric-onset leukoencephalopathy and can result in congenital absence of microglia. *The American Journal of Human Genetics*, *104*(5), 936-947. <https://doi.org/10.1016/j.ajhg.2019.03.010>
- Ozanne, A., Graneheim, U. H., Ekstedt, G., & Malmgren, K. (2016). Patients' expectations and experiences of epilepsy surgery—A population-based long-term qualitative study. *Epilepsia*, *57*(4), 605-611. <https://doi.org/10.1111/epi.13333>

- Pack, A. M. (2019). Epilepsy overview and revised classification of seizures and epilepsies. *Continuum*, 25(2), 306-321. <https://doi.org/10.1212/CON.0000000000000707>
- Panayiotopoulos, C. P. (2005). *Clinical aspects of the diagnosis of epileptic seizures and epileptic syndromes*. Oxfordshire, United Kingdom: Bladon Medical Publishing. <https://www.ncbi.nlm.nih.gov/books/NBK2609/>
- Paolicelli, R. C., Bolasco, G., Pagani, F., Maggi, L., Scianni, M., Panzanelli, P., Giustetto, M., Ferreira, T. A., Guiducci, E., Dumas, L., Ragozzino, D., & Gross, C. T. (2011). Synaptic pruning by microglia is necessary for normal brain development. *Science*, 333(6048), 1456-1458. <https://doi.org/10.1126/science.1202529>
- Park, S.-P., & Kwon, S.-H. (2008). Cognitive Effects of Antiepileptic Drugs. *Journal of Clinical Neurology*, 4(3), 99-106. <https://doi.org/10.3988/jcn.2008.4.3.99>
- Patel, D. C., Tewari, B. P., Chaunsali, L., & Sontheimer, H. (2019). Neuron–glia interactions in the pathophysiology of epilepsy. *Nature Reviews Neuroscience*, 20(5), 282-297. <https://doi.org/10.1038/s41583-019-0126-4>
- Paudel, Y. N., Shaikh, M. F., Shah, S., Kumari, Y., & Othman, I. (2018). Role of inflammation in epilepsy and neurobehavioral comorbidities: Implication for therapy. *European Journal of Pharmacology*, 837, 145-155. <https://doi.org/10.1016/j.ejphar.2018.08.020>
- Pearson, J. N., Schulz, K. M., & Patel, M. (2014). Specific alterations in the performance of learning and memory tasks in models of chemoconvulsant-induced status epilepticus. *Epilepsy Research*, 108(6), 1032-1040. <https://doi.org/10.1016/j.eplepsyres.2014.04.003>
- Perez-Pouchoulen, M., VanRyzin, J. W., & McCarthy, M. M. (2015). Morphological and phagocytic profile of microglia in the developing rat cerebellum. *ENeuro*, 2(4). <https://doi.org/10.1523/ENEURO.0036-15.2015>
- Pichler, M., & Hocker, S. (2017). Management of status epilepticus. *Handbook of Clinical Neurology*, 140, 131-151. <https://doi.org/10.1016/B978-0-444-63600-3.00009-X>
- Pisula, W. (2009). *Curiosity and information seeking in animal and human behavior*. Boca Raton, FL: Brown Walker Press.
- Pitts, M. W. (2018). Barnes maze procedure for spatial learning and memory in mice. *Bio-Protocol*, 8(5). <https://doi.org/10.21769/bioprotoc.2744>
- Poolos, N. P., & Johnston, D. (2012). Dendritic ion channelopathy in acquired epilepsy. *Epilepsia*, 53(Suppl 9), 32-40. <https://doi.org/10.1111/epi.12033>

- Priel, M. R., & Albuquerque, E. X. (2002). Short-term effects of pilocarpine on rat hippocampal neurons in culture. *Epilepsia*, 43(s5), 40-46. <https://doi.org/10.1046/j.1528-1157.43.s.5.18.x>
- Purves, D., Augustine, G. J., Fitzpatrick, D., Katz, L. C., LaMantia, A.-S., McNamara, J. O., & Williams, S. M. (2001). Neuroglial Cells. In *Neuroscience* (2nd ed.). Sunderland, MA: Sinauer Associates. <https://www.ncbi.nlm.nih.gov/books/NBK10869/>
- Racine, R. J. (1972). Modification of seizure activity by electrical stimulation: II. Motor seizure. *Electroencephalography and Clinical Neurophysiology*, 32(3), 281-294. [https://doi.org/10.1016/0013-4694\(72\)90177-0](https://doi.org/10.1016/0013-4694(72)90177-0)
- Rana, A., & Musto, A. E. (2018). The role of inflammation in the development of epilepsy. *Journal of Neuroinflammation*, 15(1), 144. <https://doi.org/10.1186/s12974-018-1192-7>
- Ravizza, T., & Vezzani, A. (2006). Status epilepticus induces time-dependent neuronal and astrocytic expression of interleukin-1 receptor type I in the rat limbic system. *Neuroscience*, 137(1), 301-308. <https://doi.org/10.1016/j.neuroscience.2005.07.063>
- Reddy, D. S., & Kuruba, R. (2013). Experimental models of status epilepticus and neuronal injury for evaluation of therapeutic interventions. *International Journal of Molecular Sciences*, 14(9), 18284-18318. <https://doi.org/10.3390/ijms140918284>
- Reddy, S. D., Younus, I., Sridhar, V., & Reddy, D. S. (2019). Neuroimaging biomarkers of experimental epileptogenesis and refractory epilepsy. *International Journal of Molecular Sciences*, 20(1). <https://doi.org/10.3390/ijms20010220>
- Renner, U. D., Oertel, R., & Kirch, W. (2005). Pharmacokinetics and pharmacodynamics in clinical use of scopolamine. *Therapeutic Drug Monitoring*, 27(5), 655-665.
- Rojas, A., Ganesh, T., Manji, Z., O'Neill, T., & Dingledine, R. (2016). Inhibition of the prostaglandin E2 receptor EP2 prevents status epilepticus-induced deficits in the novel object recognition task in rats. *Neuropharmacology*, 110(Pt. A), 419-430. <https://doi.org/10.1016/j.neuropharm.2016.07.028>
- Sadasivan, S., Zanin, M., O'Brien, K., Schultz-Cherry, S., & Smeyne, R. J. (2015). Induction of microglia activation after infection with the non-neurotropic A/CA/04/2009 H1N1 influenza virus. *PLoS One*, 10(4), e0124047. <https://doi.org/10.1371/journal.pone.0124047>

- Sakaguchi, Y., & Sakurai, Y. (2020). Left-right functional difference of the rat dorsal hippocampus for short-term memory and long-term memory. *Behavioural Brain Research*, 382, 112478. <https://doi.org/10.1016/j.bbr.2020.112478>
- Salomon, J. A., Vos, T., Hogan, D. R., Gagnon, M., Naghavi, M., Mokdad, A., Begum, N., Shah, R., Karyana, M., Kosen, S., Farje, M. R., Moncada, G., Dutta, A., Sazawal, S., Dyer, A., Seiler, J., Aboyans, V., Baker, L., Baxter, A., . . . Murray, C. J. (2012). Common values in assessing health outcomes from disease and injury: Disability weights measurement study for the Global Burden of Disease Study 2010. *The Lancet*, 380(9859), 2129-2143. [https://doi.org/10.1016/S0140-6736\(12\)61680-8](https://doi.org/10.1016/S0140-6736(12)61680-8)
- Sanchez, J. M. S., DePaula-Silva, A. B., Doty, D. J., Truong, A., Libbey, J. E., & Fujinami, R. S. (2019). Microglial cell depletion is fatal with low level picornavirus infection of the central nervous system. *Journal of NeuroVirology*, 25(3), 415-421. <https://doi.org/10.1007/s13365-019-00740-3>
- Santamarina, E., Gonzalez, M., Toledo, M., Sueiras, M., Guzman, L., Rodríguez, N., Quintana, M., Mazuela, G., & Salas-Puig, X. (2015). Prognosis of status epilepticus (SE): Relationship between SE duration and subsequent development of epilepsy. *Epilepsy & Behavior*, 49, 138-140. <https://doi.org/10.1016/j.yebeh.2015.04.059>
- Saxena, S., & Li, S. (2017). Defeating epilepsy: A global public health commitment. *Epilepsia Open*, 2(2), 153-155. <https://doi.org/10.1002/epi4.12010>
- Schafer, D. P., Lehrman, E. K., Kautzman, A. G., Koyama, R., Mardinly, A. R., Yamasaki, R., Ransohoff, R. M., Greenberg, M. E., Barres, B. A., & Stevens, B. (2012). Microglia sculpt postnatal neural circuits in an activity and complement-dependent manner. *Neuron*, 74(4), 691-705. <https://doi.org/10.1016/j.neuron.2012.03.026>
- Schapansky, J., Nardozzi, J. D., & LaVoie, M. J. (2015). The complex relationships between microglia, alpha-synuclein, and LRRK2 in Parkinson's disease. *Neuroscience*, 302, 74-88. <https://doi.org/10.1016/j.neuroscience.2014.09.049>
- Scharfman, H. E. (2007). The neurobiology of epilepsy. *Current Neurology and Neuroscience Reports*, 7(4), 348-354. <https://doi.org/10.1007/s11910-007-0053-z>

- Schartz, N. D., Herr, S. A., Madsen, L., Butts, S. J., Torres, C., Mendez, L. B., & Brewster, A. L. (2016). Spatiotemporal profile of Map2 and microglial changes in the hippocampal CA1 region following pilocarpine-induced status epilepticus. *Scientific Reports*, *6*, 24988. <https://doi.org/10.1038/srep24988>
- Schartz, N. D., Sommer, A. L., Colin, S. A., Mendez, L. B., & Brewster, A. L. (2019). Early treatment with C1 esterase inhibitor improves weight but not memory deficits in a rat model of status epilepticus. *Physiology & Behavior*, *212*, 112705. <https://doi.org/10.1016/j.physbeh.2019.112705>
- Schartz, N. D., Wyatt-Johnson, S. K., Price, L. R., Colin, S. A., & Brewster, A. L. (2018). Status epilepticus triggers long-lasting activation of complement C1q-C3 signaling in the hippocampus that correlates with seizure frequency in experimental epilepsy. *Neurobiology of Disease*, *109*(Pt. A), 163-173. <https://doi.org/10.1016/j.nbd.2017.10.012>
- Schiller, Y. (2009). Seizure relapse and development of drug resistance following long-term seizure remission. *Archives of Neurology*, *66*(10), 1233-1239. <https://doi.org/10.1001/archneurol.2009.211>
- Schmidt, D. (2011). AED discontinuation may be dangerous for seizure-free patients. *Journal of Neural Transmission*, *118*(2), 183-186. <https://doi.org/10.1007/s00702-010-0527-z>
- Seidenberg, M., Pulsipher, D. T., & Hermann, B. (2009). Association of epilepsy and comorbid conditions. *Future Neurology*, *4*(5), 663-668. <https://doi.org/10.2217/fnl.09.32>
- Seinfeld, S., Goodkin, H. P., & Shinnar, S. (2016). Status epilepticus. *Cold Spring Harbor Perspectives in Medicine*, *6*(3), a022830. <https://doi.org/10.1101/cshperspect.a022830>
- Semah, F., Picot, M. C., Adam, C., Broglin, D., Arzimanoglou, A., Bazin, B., Cavalcanti, D., & Baulac, M. (1998). Is the underlying cause of epilepsy a major prognostic factor for recurrence? *Neurology*, *51*(5), 1256-1262. <https://doi.org/10.1212/wnl.51.5.1256>
- Serrano-Castro, P. J., Payan-Ortiz, M., Quiroga-Subirana, P., Fernandez-Perez, J., & Parron-Carreño, T. (2012). Predictive model for refractoriness in temporal lobe epilepsy based on clinical and diagnostic test data. *Epilepsy Research*, *101*(1-2), 113-121. <https://doi.org/10.1016/j.eplepsyres.2012.03.009>

- Shackleton, D. P., Westendorp, R. G. J., Trenité, D. G. A. K.-N., & Vandenbroucke, J. P. (1999). Mortality in patients with epilepsy: 40 years of follow up in a Dutch cohort study. *Journal of Neurology, Neurosurgery & Psychiatry*, 66(5), 636-640. <https://doi.org/10.1136/jnnp.66.5.636>
- Shapiro, L. A., Wang, L., & Ribak, C. E. (2008). Rapid astrocyte and microglial activation following pilocarpine-induced seizures in rats. *Epilepsia*, 49(Suppl 2), 33-41. <https://doi.org/10.1111/j.1528-1167.2008.01491.x>
- Sharma, A. K., Reams, R. Y., Jordan, W. H., Miller, M. A., Thacker, H. L., & Snyder, P. W. (2007). Mesial temporal lobe epilepsy: Pathogenesis, induced rodent models and lesions. *Toxicologic Pathology*, 35(7), 984-999. <https://doi.org/10.1080/01926230701748305>
- Sharma, S., Puttachary, S., Thippeswamy, A., Kanthasamy, A. G., & Thippeswamy, T. (2018). Status epilepticus: Behavioral and electroencephalography seizure correlates in kainate experimental models. *Frontiers in Neurology*, 9. <https://doi.org/10.3389/fneur.2018.00007>
- Shen, Y., Qin, H., Chen, J., Mou, L., He, Y., Yan, Y., Zhou, H., Lv, Y., Chen, Z., Wang, J., & Zhou, Y.-D. (2016). Postnatal activation of TLR4 in astrocytes promotes excitatory synaptogenesis in hippocampal neurons. *The Journal of Cell Biology*, 215(5), 719-734. <https://doi.org/10.1083/jcb.201605046>
- Sheng, M., & Kim, E. (2011). The postsynaptic organization of synapses. *Cold Spring Harbor Perspectives in Biology*, 3(12). <https://doi.org/10.1101/cshperspect.a005678>
- Sheridan, G. K., & Murphy, K. J. (2013). Neuron–glia crosstalk in health and disease: Fractalkine and CX3CR1 take centre stage. *Open Biology*, 3(12). <https://doi.org/10.1098/rsob.130181>
- Shi, Q., Colodner, K. J., Matousek, S. B., Merry, K., Hong, S., Kenison, J. E., Frost, J. L., Le, K. X., Li, S., Dodart, J.-C., Caldarone, B. J., Stevens, B., & Lemere, C. A. (2015). Complement C3-deficient mice fail to display age-related hippocampal decline. *The Journal of Neuroscience*, 35(38), 13029-13042. <https://doi.org/10.1523/JNEUROSCI.1698-15.2015>
- Sierra, A., Abiega, O., Shahraz, A., & Neumann, H. (2013). Janus-faced microglia: Beneficial and detrimental consequences of microglial phagocytosis. *Frontiers in Cellular Neuroscience*, 7, 6. <https://doi.org/10.3389/fncel.2013.00006>

- Sierra, A., Encinas, J. M., Deudero, J. J. P., Chancey, J. H., Enikolopov, G., Overstreet-Wadiche, L. S., Tsirka, S. E., & Maletic-Savatic, M. (2010). Microglia shape adult hippocampal neurogenesis through apoptosis-coupled phagocytosis. *Cell Stem Cell*, 7(4), 483-495. <https://doi.org/10.1016/j.stem.2010.08.014>
- Silva-Alves, M. S., Secolin, R., Carvalho, B. S., Yasuda, C. L., Bilevicius, E., Alvim, M. K. M., Santos, R. O., Maurer-Morelli, C. V., Cendes, F., & Lopes-Cendes, I. (2017). A prediction algorithm for drug response in patients with mesial temporal lobe epilepsy based on clinical and genetic information. *PloS One*, 12(1), e0169214. <https://doi.org/10.1371/journal.pone.0169214>
- Siman, R., Cocca, R., & Dong, Y. (2015). The mTOR inhibitor rapamycin mitigates perforant pathway neurodegeneration and synapse loss in a mouse model of early-stage Alzheimer-type tauopathy. *PloS One*, 10(11), e0142340. <https://doi.org/10.1371/journal.pone.0142340>
- Smith, G. D., Gao, N., & Lugo, J. N. (2017). Kv4.2 knockout mice display learning and memory deficits in the Lashley maze. *F1000Research*, 5:2456. <https://doi.org/10.12688/f1000research.9664.2>
- Soulé, J., Penke, Z., Kanhema, T., Alme, M. N., Laroche, S., & Bramham, C. R. (2008). Object-place recognition learning triggers rapid induction of plasticity-related immediate early genes and synaptic proteins in the rat dentate gyrus. *Neural Plasticity*, 2008. <https://doi.org/10.1155/2008/269097>
- Spangenberg, E. E., Lee, R. J., Najafi, A. R., Rice, R. A., Elmore, M. R. P., Blurton-Jones, M., West, B. L., & Green, K. N. (2016). Eliminating microglia in Alzheimer's mice prevents neuronal loss without modulating amyloid- β pathology. *Brain: A Journal of Neurology*, 139(Pt 4), 1265-1281. <https://doi.org/10.1093/brain/aww016>
- Srivastava, P. K., van Eyll, J., Godard, P., Mazzuferi, M., Delahaye-Duriez, A., Steenwinckel, J. V., Gressens, P., Danis, B., Vandenplas, C., Foerch, P., Leclercq, K., Mairet-Coello, G., Cardenas, A., Vanclef, F., Laaniste, L., Niespodziany, I., Keaney, J., Gasser, J., Gillet, G., . . . Johnson, M. R. (2018). A systems-level framework for drug discovery identifies Csf1R as an anti-epileptic drug target. *Nature Communications*, 9(1), 3561. <https://doi.org/10.1038/s41467-018-06008-4>

- Stanley, E. R., & Chitu, V. (2014). CSF-1 receptor signaling in myeloid cells. *Cold Spring Harbor Perspectives in Biology*, 6(6). <https://doi.org/10.1101/cshperspect.a021857>
- Steiger, B. K., & Jokeit, H. (2017). Why epilepsy challenges social life. *Seizure*, 44, 194-198. <https://doi.org/10.1016/j.seizure.2016.09.008>
- Stevens, B., Allen, N. J., Vazquez, L. E., Howell, G. R., Christopherson, K. S., Nouri, N., Micheva, K. D., Mehalow, A. K., Huberman, A. D., Stafford, B., Sher, A., Litke, A. M., Lambris, J. D., Smith, S. J., John, S. W. M., & Barres, B. A. (2007). The classical complement cascade mediates CNS synapse elimination. *Cell*, 131(6), 1164-1178. <https://doi.org/10.1016/j.cell.2007.10.036>
- Stratoulas, V., Venero, J. L., Tremblay, M.-È., & Joseph, B. (2019). Microglial subtypes: Diversity within the microglial community. *The EMBO Journal*, 38(17), e101997. <https://doi.org/10.15252/emj.2019101997>
- Streit, W. J., Hurley, S. D., McGraw, T. S., & Semple-Rowland, S. L. (2000). Comparative evaluation of cytokine profiles and reactive gliosis supports a critical role for interleukin-6 in neuron-glia signaling during regeneration. *Journal of Neuroscience Research*, 61(1), 10-20. [https://doi.org/10.1002/1097-4547\(20000701\)61:1<10::AID-JNR2>3.0.CO;2-E](https://doi.org/10.1002/1097-4547(20000701)61:1<10::AID-JNR2>3.0.CO;2-E)
- Sun, Q.-J., Duan, R.-S., Wang, A.-H., Shang, W., Zhang, T., Zhang, X.-Q., & Chi, Z.-F. (2009). Alterations of NR2B and PSD-95 expression in hippocampus of kainic acid-exposed rats with behavioural deficits. *Behavioural Brain Research*, 201(2), 292-299. <https://doi.org/10.1016/j.bbr.2009.02.027>
- Swann, J. W., Al-Noori, S., Jiang, M., & Lee, C. L. (2000). Spine loss and other dendritic abnormalities in epilepsy. *Hippocampus*, 10(5), 617-625. [https://doi.org/10.1002/1098-1063\(2000\)10:5<617::AID-HIPO13>3.0.CO;2-R](https://doi.org/10.1002/1098-1063(2000)10:5<617::AID-HIPO13>3.0.CO;2-R)
- Szalay, G., Martinecz, B., Lénárt, N., Környei, Z., Orsolits, B., Judák, L., Császár, E., Fekete, R., West, B. L., Katona, G., Rózsa, B., & Dénes, Á. (2016). Microglia protect against brain injury and their selective elimination dysregulates neuronal network activity after stroke. *Nature Communications*, 7, 11499. <https://doi.org/10.1038/ncomms11499>
- Talati, R., Scholle, J. M., Phung, O. J., Baker, W. L., Baker, E. L., Ashaye, A., Kluger, J., Quercia, R., Mather, J., Giovenale, S., Coleman, C. I., & White, C. M. (2011, December). *Effectiveness and safety of antiepileptic medications in patients with epilepsy* [Text]. <https://www.ncbi.nlm.nih.gov/books/NBK83926/table/introduction.t4/>

- Tam, W. Y., & Ma, C. H. E. (2014). Bipolar/rod-shaped microglia are proliferating microglia with distinct M1/M2 phenotypes. *Scientific Reports*, *4*. <https://doi.org/10.1038/srep07279>
- Tan, M., & Tan, U. (2001). Sex difference in susceptibility to epileptic seizures in rats: Importance of estrous cycle. *The International Journal of Neuroscience*, *108*(3-4), 175-191.
- Tang, C.-M., & Thompson, S. M. (2012). Perturbations of dendritic excitability in epilepsy. In J. L. Noebels, M. Avoli, M. A. Rogawski, R. W. Olsen, & A. V. Delgado-Escueta (Eds.), *Jasper's basic mechanisms of the epilepsies* (4th ed.). Bethesda, MD: National Center for Biotechnology Information (US). <http://www.ncbi.nlm.nih.gov/books/NBK98167/>
- Tang, Y., Liu, L., Xu, D., Zhang, W., Zhang, Y., Zhou, J., & Huang, W. (2018). Interaction between astrocytic colony stimulating factor and its receptor on microglia mediates central sensitization and behavioral hypersensitivity in chronic post ischemic pain model. *Brain, Behavior, and Immunity*, *68*, 248-260. <https://doi.org/10.1016/j.bbi.2017.10.023>
- Tang, Z., Cheng, S., Sun, Y., Zhang, Y., Xiang, X., Ouyang, Z., Zhu, X., Wang, B., & Hei, M. (2019). Early TLR4 inhibition reduces hippocampal injury at puberty in a rat model of neonatal hypoxic-ischemic brain damage via regulation of neuroimmunity and synaptic plasticity. *Experimental Neurology*, *321*, 113039. <https://doi.org/10.1016/j.expneurol.2019.113039>
- Tap, W. D., Wainberg, Z. A., Anthony, S. P., Ibrahim, P. N., Zhang, C., Healey, J. H., Chmielowski, B., Staddon, A. P., Cohn, A. L., Shapiro, G. I., Keedy, V. L., Singh, A. S., Puzanov, I., Kwak, E. L., Wagner, A. J., Von Hoff, D. D., Weiss, G. J., Ramanathan, R. K., Zhang, J., . . . Bollag, G. (2015). Structure-guided blockade of CSF1R kinase in tenosynovial giant-cell tumor. *The New England Journal of Medicine*, *373*(5), 428-437. <https://doi.org/10.1056/NEJMoa1411366>
- Tatum, W. O. (2012). Mesial temporal lobe epilepsy. *Journal of Clinical Neurophysiology*, *29*(5), 356-365. <https://doi.org/10.1097/WNP.0b013e31826b3ab7>
- Taylor, S. E., Morganti-Kossmann, C., Lifshitz, J., & Ziebell, J. M. (2014). Rod microglia: A morphological definition. *PloS One*, *9*(5), e97096. <https://doi.org/10.1371/journal.pone.0097096>
- Thijs, R. D., Surges, R., O'Brien, T. J., & Sander, J. W. (2019). Epilepsy in adults. *The Lancet*, *393*(10172), 689-701. [https://doi.org/10.1016/S0140-6736\(18\)32596-0](https://doi.org/10.1016/S0140-6736(18)32596-0)

- Tian, N., Boring, M., Kobau, R., Zack, M. M., & Croft, J. B. (2018). Active epilepsy and seizure control in adults—United States, 2013 and 2015. *Morbidity and Mortality Weekly Report*, 67(15), 437-442. <https://doi.org/10.15585/mmwr.mm6715a1>
- Timmerman, R., Burm, S. M., & Bajramovic, J. J. (2018). An overview of in vitro methods to study microglia. *Frontiers in Cellular Neuroscience*, 12:242. <https://doi.org/10.3389/fncel.2018.00242>
- Torres-Platas, S. G., Comeau, S., Rachalski, A., Bo, G. D., Cruceanu, C., Turecki, G., Giros, B., & Mechawar, N. (2014). Morphometric characterization of microglial phenotypes in human cerebral cortex. *Journal of Neuroinflammation*, 11, 12. <https://doi.org/10.1186/1742-2094-11-12>
- Torrico, T. J., & Munakomi, S. (2020). Neuroanatomy, Thalamus. In *StatPearls*. StatPearls Publishing. <http://www.ncbi.nlm.nih.gov/books/NBK542184/>
- Tremblay, M.-È. (2011). The role of microglia at synapses in the healthy CNS: Novel insights from recent imaging studies. *Neuron Glia Biology*, 7(1), 67-76. <https://doi.org/10.1017/S1740925X12000038>
- Tremblay, M.-È., Lowery, R. L., & Majewska, A. K. (2010). Microglial interactions with synapses are modulated by visual experience. *PLoS Biology*, 8(11), e1000527. <https://doi.org/10.1371/journal.pbio.1000527>
- Tyler, B., Wadsworth, S., Recinos, V., Mehta, V., Vellimana, A., Li, K., Rosenblatt, J., Do, H., Gallia, G. L., Siu, I.-M., Wicks, R. T., Rudek, M. A., Zhao, M., & Brem, H. (2011). Local delivery of rapamycin: A toxicity and efficacy study in an experimental malignant glioma model in rats. *Neuro-Oncology*, 13(7), 700-709. <https://doi.org/10.1093/neuonc/nor050>
- Ulland, T. K., Wang, Y., & Colonna, M. (2015). Regulation of microglial survival and proliferation in health and diseases. *Seminars in Immunology*, 27(6), 410-415. <https://doi.org/10.1016/j.smim.2016.03.011>
- Vallières, L., Campbell, I. L., Gage, F. H., & Sawchenko, P. E. (2002). Reduced hippocampal neurogenesis in adult transgenic mice with chronic astrocytic production of interleukin-6. *The Journal of Neuroscience*, 22(2), 486-492.
- Vargas-Sánchez, K., Mogilevskaya, M., Rodríguez-Pérez, J., Rubiano, M. G., Javela, J. J., & González-Reyes, R. E. (2018). Astroglial role in the pathophysiology of status epilepticus: An overview. *Oncotarget*, 9(42), 26954-26976. <https://doi.org/10.18632/oncotarget.25485>

- Vasek, M. J., Garber, C., Dorsey, D., Durrant, D. M., Bollman, B., Soung, A., Yu, J., Perez-Torres, C., Frouin, A., Wilton, D. K., Funk, K., DeMasters, B. K., Jiang, X., Bowen, J. R., Mennerick, S., Robinson, J. K., Garbow, J. R., Tyler, K. L., Suthar, M. S., . . . Klein, R. S. (2016). A complement-microglial axis drives synapse loss during virus-induced memory impairment. *Nature*, *534*(7608), 538-543. <https://doi.org/10.1038/nature18283>
- Vasile, F., Dossi, E., & Rouach, N. (2017). Human astrocytes: Structure and functions in the healthy brain. *Brain Structure & Function*, *222*(5), 2017-2029. <https://doi.org/10.1007/s00429-017-1383-5>
- Vergeer, M., de Ranitz-Greven, W. L., Neary, M. P., Ionescu-Ittu, R., Emond, B., Sheng Duh, M., Jansen, F., & Zonnenberg, B. A. (2019). Epilepsy, impaired functioning, and quality of life in patients with tuberous sclerosis complex. *Epilepsia Open*, *4*(4), 581-592. <https://doi.org/10.1002/epi4.12365>
- Vezzani, A., Balosso, S., & Ravizza, T. (2019). Neuroinflammatory pathways as treatment targets and biomarkers in epilepsy. *Nature Reviews. Neurology*, *15*(8), 459-472. <https://doi.org/10.1038/s41582-019-0217-x>
- Vincent, P., & Mulle, C. (2009). Kainate receptors in epilepsy and excitotoxicity. *Neuroscience*, *158*(1), 309-323. <https://doi.org/10.1016/j.neuroscience.2008.02.066>
- Voltzenlogel, V., Hirsch, E., Vignal, J.-P., Valton, L., & Manning, L. (2015). Preserved anterograde and remote memory in drug-responsive temporal lobe epileptic patients. *Epilepsy Research*, *115*, 126-132. <https://doi.org/10.1016/j.eplesyres.2015.06.006>
- Wang, D. D., Englot, D. J., Garcia, P. A., Lawton, M. T., & Young, W. L. (2012). Minocycline- and tetracycline-class antibiotics are protective against partial seizures in vivo. *Epilepsy & Behavior*, *24*(3), 314-318. <https://doi.org/10.1016/j.yebeh.2012.03.035>
- Weinhard, L., di Bartolomei, G., Bolasco, G., Machado, P., Schieber, N. L., Neniskyte, U., Exiga, M., Vadasiute, A., Raggioli, A., Schertel, A., Schwab, Y., & Gross, C. T. (2018). Microglia remodel synapses by presynaptic trogocytosis and spine head filopodia induction. *Nature Communications*, *9*. <https://doi.org/10.1038/s41467-018-03566-5>

- Wesolowski, R., Sharma, N., Reebel, L., Rodal, M. B., Peck, A., West, B. L., Marimuthu, A., Severson, P., Karlin, D. A., Dowlati, A., Le, M. H., Coussens, L. M., & Rugo, H. S. (2019). Phase Ib study of the combination of pexidartinib (PLX3397), a CSF-1R inhibitor, and paclitaxel in patients with advanced solid tumors. *Therapeutic Advances in Medical Oncology*, *11*. <https://doi.org/10.1177/1758835919854238>
- Wiebe, S. (2000). Epidemiology of temporal lobe epilepsy. *Canadian Journal of Neurological Sciences*, *27*(S1), S6-S10. <https://doi.org/10.1017/S0317167100000561>
- Wiebe, S., Blume, W. T., Girvin, J. P., Eliasziw, M., & Effectiveness and Efficiency of Surgery for Temporal Lobe Epilepsy Study Group. (2001). A randomized, controlled trial of surgery for temporal-lobe epilepsy. *The New England Journal of Medicine*, *345*(5), 311-318. <https://doi.org/10.1056/NEJM200108023450501>
- Wiebe, S., Eliasziw, M., & Matijevec, S. (2001). Changes in quality of life in epilepsy: How large must they be to be real? *Epilepsia*, *42*(1), 113-118. <https://doi.org/10.1046/j.1528-1157.2001.081425.x>
- Wilcox, K. S., & Vezzani, A. (2014). Does brain inflammation mediate pathological outcomes in epilepsy? *Advances in Experimental Medicine and Biology*, *813*, 169-183. https://doi.org/10.1007/978-94-017-8914-1_14
- Wirenfeldt, M., Clare, R., Tung, S., Bottini, A., Mathern, G. W., & Vinters, H. V. (2009). Increased activation of Iba1+ microglia in pediatric epilepsy patients with Rasmussen's encephalitis compared with cortical dysplasia and tuberous sclerosis complex. *Neurobiology of Disease*, *34*(3), 432-440. <https://doi.org/10.1016/j.nbd.2009.02.015>
- Wolf, S. A., Boddeke, H. W. G. M., & Kettenmann, H. (2017). Microglia in physiology and disease. *Annual Review of Physiology*, *79*, 619-643. <https://doi.org/10.1146/annurev-physiol-022516-034406>
- Wolfart, J., & Laker, D. (2015). Homeostasis or channelopathy? Acquired cell type-specific ion channel changes in temporal lobe epilepsy and their antiepileptic potential. *Frontiers in Physiology*, *6*. <https://doi.org/10.3389/fphys.2015.00168>
- Wong, M. (2008). Stabilizing dendritic structure as a novel therapeutic approach for epilepsy. *Expert Review of Neurotherapeutics*, *8*(6), 907-915. <https://doi.org/10.1586/14737175.8.6.907>

- Wong, M., & Guo, D. (2013). Dendritic spine pathology in epilepsy: Cause or consequence? *Neuroscience*, *251*, 141-150. <https://doi.org/10.1016/j.neuroscience.2012.03.048>
- Wu, C.-L., Huang, L.-T., Liou, C.-W., Wang, T.-J., Tung, Y.-R., Hsu, H.-Y., & Lai, M.-C. (2001). Lithium-pilocarpine-induced status epilepticus in immature rats result in long-term deficits in spatial learning and hippocampal cell loss. *Neuroscience Letters*, *312*(2), 113-117. [https://doi.org/10.1016/S0304-3940\(01\)02202-9](https://doi.org/10.1016/S0304-3940(01)02202-9)
- Wyatt, S. K., Witt, T., Barbaro, N. M., Cohen-Gadol, A. A., & Brewster, A. L. (2017). Enhanced classical complement pathway activation and altered phagocytosis signaling molecules in human epilepsy. *Experimental Neurology*, *295*, 184-193. <https://doi.org/10.1016/j.expneurol.2017.06.009>
- Wyatt-Johnson, S. K., & Brewster, A. L. (2019). Emerging roles for microglial phagocytic signaling in epilepsy. *Epilepsy Currents*, *15*(3), 153-157. <https://doi.org/10.1177/1535759719890336>
- Wyatt-Johnson, S. K., Herr, S. A., & Brewster, A. L. (2017). Status epilepticus triggers time-dependent alterations in microglia abundance and morphological phenotypes in the hippocampus. *Frontiers in Neurology*, *8*, 700. <https://doi.org/10.3389/fneur.2017.00700>
- Wylie, T., Sandhu, D. S., Goyal, A., & Murr, N. (2020). Status Epilepticus. In *StatPearls*. StatPearls Publishing. <http://www.ncbi.nlm.nih.gov/books/NBK430686/>
- Wyneken, U., Marengo, J.-J., Villanueva, S., Soto, D., Sandoval, R., Gundelfinger, E. D., & Orrego, F. (2003). Epilepsy-induced changes in signaling systems of human and rat postsynaptic densities. *Epilepsia*, *44*(2), 243-246. <https://doi.org/10.1046/j.1528-1157.2003.17602.x>
- Xia, L., Ou, S., & Pan, S. (2017). Initial response to antiepileptic drugs in patients with newly diagnosed epilepsy as a predictor of long-term outcome. *Frontiers in Neurology*, *8*. <https://doi.org/10.3389/fneur.2017.00658>
- Xie, L., Sun, F., Wang, J., Mao, X., Xie, L., Yang, S.-H., Su, D.-M., Simpkins, J. W., Greenberg, D. A., & Jin, K. (2014). mTOR signaling inhibition modulates macrophage/microglia-mediated neuroinflammation and secondary injury via regulatory T cells after focal ischemia. *Journal of Immunology*, *192*(12), 6009-6019. <https://doi.org/10.4049/jimmunol.1303492>

- Ying, Z., Bingaman, W., & Najm, I. M. (2004). Increased numbers of coassembled PSD-95 to NMDA-receptor subunits NR2B and NR1 in human epileptic cortical dysplasia. *Epilepsia*, 45(4), 314-321. <https://doi.org/10.1111/j.0013-9580.2004.37703.x>
- Zeng, L.-H., McDaniel, S., Rensing, N. R., & Wong, M. (2010). Regulation of cell death and epileptogenesis by the mammalian target of rapamycin (mTOR): A double-edged sword? *Cell Cycle*, 9(12), 2281-2285. <https://doi.org/10.4161/cc.9.12.11866>
- Zeng, L.-H., Rensing, N. R., & Wong, M. (2009). The Mammalian Target of Rapamycin (mTOR) signaling pathway mediates epileptogenesis in a model of temporal lobe epilepsy. *The Journal of Neuroscience*, 29(21), 6964-6972. <https://doi.org/10.1523/JNEUROSCI.0066-09.2009>
- Zhang, B., Gaiteri, C., Bodea, L.-G., Wang, Z., McElwee, J., Podtelezchnikov, A. A., Zhang, C., Xie, T., Tran, L., Dobrin, R., Fluder, E., Clurman, B., Melquist, S., Narayanan, M., Suver, C., Shah, H., Mahajan, M., Gillis, T., Mysore, J., . . . Emilsson, V. (2013). Integrated systems approach identifies genetic nodes and networks in late-onset Alzheimer's disease. *Cell*, 153(3), 707-720. <https://doi.org/10.1016/j.cell.2013.03.030>
- Zhang, B., Zou, J., Han, L., Beeler, B., Friedman, J. L., Griffin, E., Piao, Y.-S., Rensing, N. R., & Wong, M. (2018). The specificity and role of microglia in epileptogenesis in mouse models of tuberous sclerosis complex. *Epilepsia*, 59(9), 1796-1806. <https://doi.org/10.1111/epi.14526>
- Zhang, C., G.-E., Yang, Q., Lu, Q.-C., Li, S.-T., & Ju, G. (2010). Time-dependent changes in learning ability and induction of long-term potentiation in the lithium–pilocarpine-induced epileptic mouse model. *Epilepsy & Behavior*, 17(4), 448-454. <https://doi.org/10.1016/j.yebeh.2010.02.008>
- Zhao, H., Zhu, C., & Huang, D. (2018). Microglial activation: An important process in the onset of epilepsy. *American Journal of Translational Research*, 10(9), 2877-2889.
- Zhao, X., Liao, Y., Morgan, S., Mathur, R., Feustel, P., Mazurkiewicz, J., Qian, J., Chang, J., Mathern, G. W., Adamo, M. A., Ritaccio, A. L., Gruenthal, M., Zhu, X., & Huang, Y. (2018). Noninflammatory changes of microglia are sufficient to cause epilepsy. *Cell Reports*, 22(8), 2080-2093. <https://doi.org/10.1016/j.celrep.2018.02.004>

- Zhou, J.-L., Shatskikh, T. N., Liu, X., & Holmes, G. L. (2007). Impaired single cell firing and long-term potentiation parallels memory impairment following recurrent seizures. *The European Journal of Neuroscience*, 25(12), 3667-3677. <https://doi.org/10.1111/j.1460-9568.2007.05598.x>
- Ziebell, J. M., Taylor, S. E., Cao, T., Harrison, J. L., & Lifshitz, J. (2012). Rod microglia: Elongation, alignment, and coupling to form trains across the somatosensory cortex after experimental diffuse brain injury. *Journal of Neuroinflammation*, 9, 247. <https://doi.org/10.1186/1742-2094-9-247>